SUPPORTING INFORMATION

BEATING HETEROGENEITY OF SINGLE-SITE CATALYSTS: MGO-SUPPORTED IRIDIUM COMPLEXES

Adam S. Hoffman[1,2†], Louise M. Debefve[1†], Shengjie Zhang[3], Jorge E. Perez-Aguilar[1], Edward T. Conley[1,4], Kimberly R. Justl[1,4], Ilke Arslan[5,6], David A. Dixon[3], & Bruce C. Gates[1*]

[1]Department of Chemical Engineering, University of California—Davis, Davis, California, 95616, USA
[2]Present address: Stanford Synchrotron Radiation Lightsource, SLAC National Accelerator Laboratory, Menlo Park, California, 94025, USA
[3]Department of Chemistry, The University of Alabama, Tuscaloosa, Alabama, 35487, USA
[4]Department of Materials Science and Engineering, University of California—Davis, Davis, California, 95616, USA
[5]Fundamental and Computational Sciences Directorate, Institute for Integrated Catalysis and Environmental Molecular Science Laboratory, Pacific Northwest National Laboratory, P O Box 999, Richland, Washington, 99352, USA
[6]Present address: Center for Nanoscale Materials, Argonne National Laboratory, Lemont, IL, 60439, USA
[†]These authors contributed equally to this work.
[*]Corresponding Author - E-mail: bcgates@ucdavis.edu

Detailed experimental results

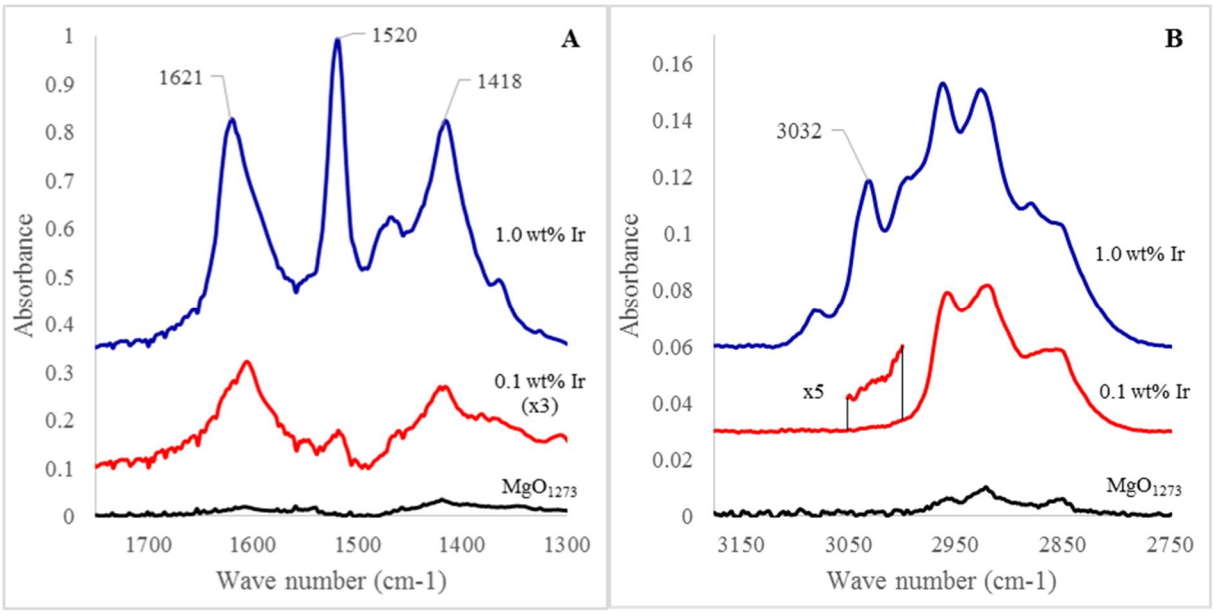

Figure S1. IR spectra characterizing species formed from the reaction of $Ir(C_2H_4)_2(acac)$ with MgO that had been treated at 1273 K. (A) C=O stretching region characterizing the residual (acac) ligands on the MgO support; (B) C–H stretching region characterizing the C_2H_4 ligands. Spectra were recorded with sample in flowing helium at room temperature and atmospheric pressure. The iridium loadings were 1.0 wt% (blue, top) and 0.1 wt% (red, middle). The spectrum of the MgO support is that of the initial form (black, bottom).

Table S1: Orientations of particles imaged by STEM

Wt% Ir in sample made from $Ir(C_2H_4)_2$ on MgO	Total number of images recorded for sample	Number of images showing particle in [100]	Number of images showing particle in [111]	number of images showing particle in [110]
1	17	4	1	0
0.1	33	0	1	1 (a particle)
0.05	47	5	6	0
0.01	30	8	1	1 (a defect area)

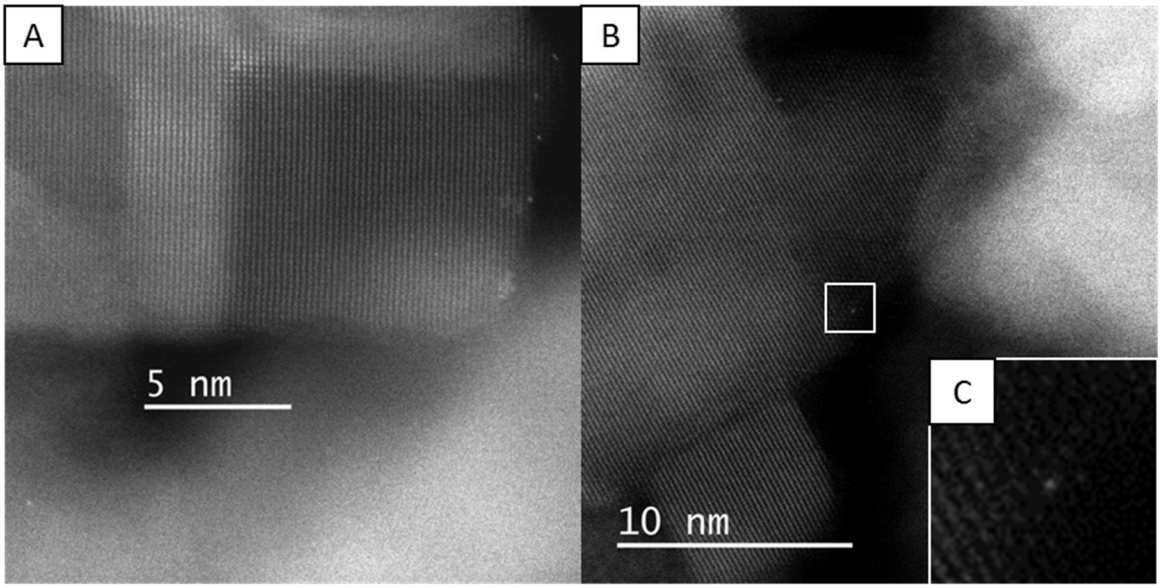

Figure S2: STEM images of sample containing 0.01 wt% Ir made from $Ir(C_2H_4)_2$ on MgO. (A) particle in the (100) orientation with Ir located on the adjacent defect area; (B) particle in an unidentified orientation with one Ir atom located on a defect area which exposes the (110) face; (C) zoom-in on one of the Ir atoms.

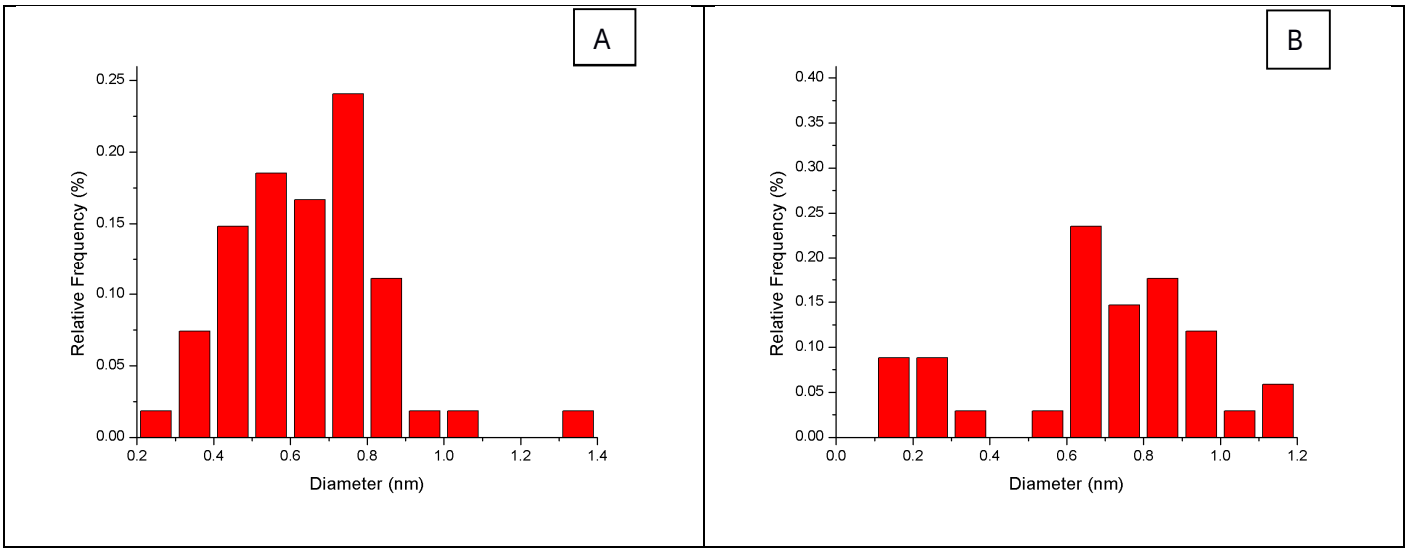

Figure S3. Size distribution plots corresponding to the MgO-supported Ir complexes at various loadings after exposure to flowing H_2 at 573 K. (A) 1 wt% Ir. (B) 0.1 wt% Ir.

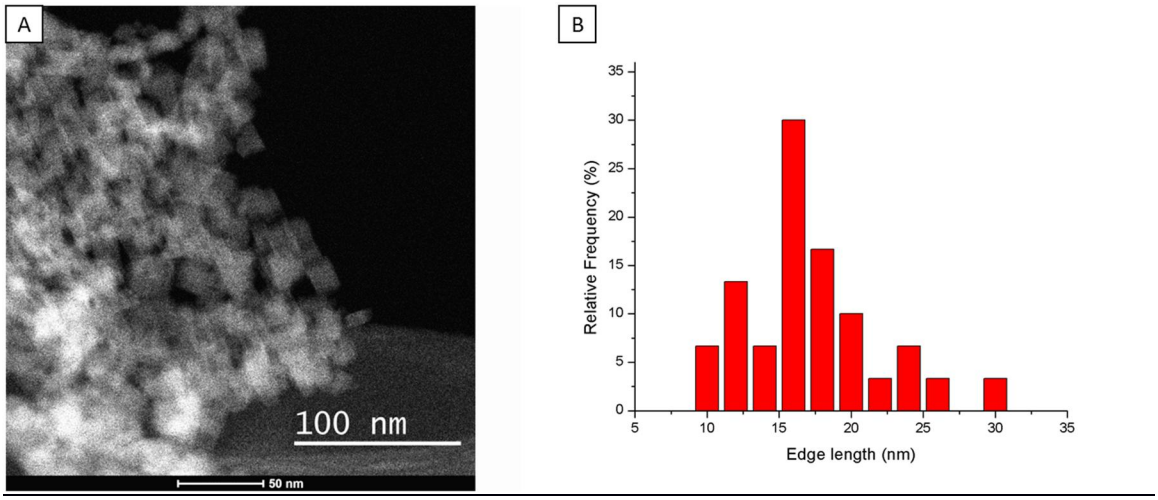

Figure S4. (A) STEM image of MgO treated at 1273 K; (B) distribution of edge lengths of MgO crystallites as determined from STEM images.

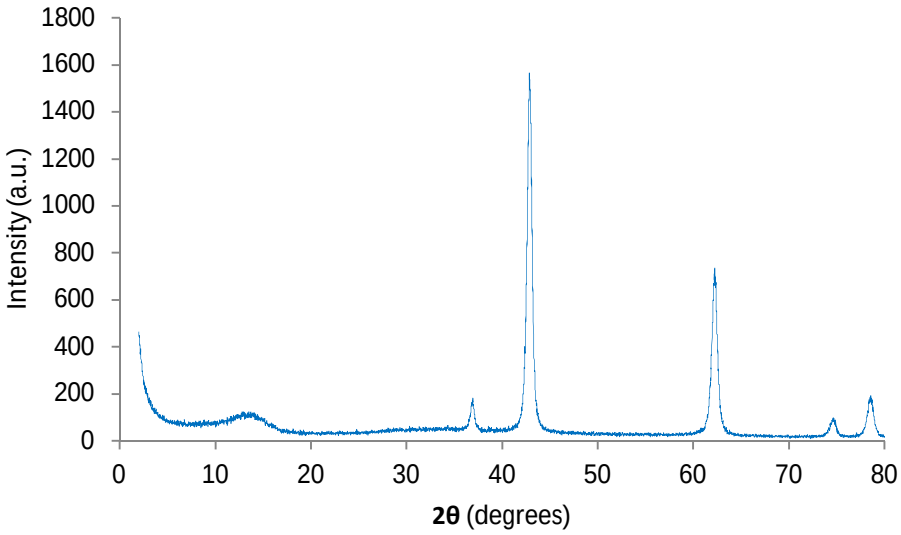

Figure S5: XRD pattern characterizing the pretreated MgO.

Details of analysis of microscopy data

Population of defect areas

In the samples with low Ir loadings, there is little evidence of Ir on the (100) face, but there are also several images showing the (100) face with no Ir at all. Figure S2A is an image of MgO showing the (100) face. There is no Ir on terrace sites. The right side of the MgO particle is not smooth, and there is what we suggest to be a defect on the right side. On this defect, there are several Ir atoms, and there are Ir atoms on the edge of the particle next to it. Similar statements pertain about Fig S2B. The main terrace of the particle does not incorporate any iridium. It is in an unidentifiable orientation. There is a large defect area on the right, where the sides seem to be polished, exposing the (110) face. There are 2 Ir atoms located in this defect area. These observations are consistent with the inference that iridium populates defect sites before the rest of the surface.

Edge lengths

Thirty particle edges of single particles dangling over vacuum were measured.

Cluster size distribution

For each sample, the intensity plot of at least 30 clusters (IrMgO1 n = 54; IrMgO2 n = 34) was obtained in digital micrographs. The spectra were exported to Origin where they were

background subtracted. The peaks were fitted as Gaussians and the full width at half maximum was measured and recorded as the diameter.

Details of EXAFS data analysis characterizing samples containing 0.05 and 0.01 wt% Ir, respectively, following treatment in H_2

Samples with the lowest Ir loadings, 0.05 and 0.01 wt%: Following exposure to H_2 the samples were characterized by the lack of a detectable Ir–Ir contribution (Table 1), and correspondingly single-site Ir was observed by STEM imaging (Figure 3G-H). Within the error of the EXAFS analysis, 20%, there was no change with Ir loading in the coordination of the Ir atom to the support; the Ir–O coordination number was 3.0 ± 0.1, all consistent with the stability of the tripodal Ir complex.

There is evidence of a change in the Ir–C coordination number, at a bonding distance, from 4 to 3, for the sample containing 0.05 wt% Ir as a result of the exposure to H_2 (Table 1). The decrease in the Ir–C contribution is inferred to have occurred as a fraction of the ethylene ligands were converted to ethyl ligands by reaction with H_2. Within error, there was no change in the Ir–C coordination characterizing the sample containing 0.01 wt% Ir (Table 1). STEM images show that the Ir atoms were located near edges and corners, consistent with what was observed for the initially prepared samples (Figure 3B-D).

EXAFS Data Analysis:

MgO-supported $Ir(C_2H_4)_2$; as made; 1.0 wt% Ir:

Notation (in part): Subscripts: Sup, refers to an atom identified to be belonging to the support; L refers to the long absorber–backscatter contribution involving an atom in the support, and short refers to the short absorber–backscatter contribution involving an atom in the support.

Table S2. EXAFS models representing the data at the Ir L_{III} edge characterizing MgO-supported complexes formed by adsorption of $Ir(C_2H_4)_2(acac)$ on MgO treated at 1273 K to give an Ir loading of 1.0 wt%. Values of the wave vector *k* ranged from 3.85 to 11.45 Å; error = 0.00087; *Denotes best-fit model; [a]notation: *N*, coordination number; *R*, distance between absorber and backscatterer atoms; σ^2, Debye-Waller/disorder term; ΔE_0, inner potential correction. Subscripts: *Sup*, refers to an atom identified to be belonging to the support; *L*, refers to the long absorber–backscatterer contribution involving an atom in the support.

Model	Shell	N^a	$10^3 \times \sigma^2$ (Å^2)[a]	R (Å) [a]	ΔE_0 (eV) [a]	Goodness of Fit
1*	$Ir–O_{Sup}$	2.4	2.4	1.94	-11.8	3.39
	Ir–C	4.0	1.7	2.07	0.7	
	$Ir–Mg_{Sup}$	1.1	4.6	3.10	-13.3	
	$Ir\text{-}O_{SupL}$	2.8	1.1	3.62	2.7	
2	$Ir\text{-}O_{Sup}$	1.9	5.5	1.92	-10.0	5.81
	Ir-C	4.0	4.2	2.06	0.0	
	$Ir\text{-}Mg_{Sup}$	1.1	4.9	3.07	-11.7	
	$Ir\text{-}O_{SupL}$	2.9	2.2	3.60	3.3	
3	$Ir\text{-}O_{Sup}$	1.9	1.3	1.92	-11.2	2.72
	Ir-C	4.0	1.7	2.05	2.8	
	$Ir\text{-}Mg_{Sup}$	1.8	0.1	3.08	-4.1	
	Ir-Ir	1.7	3.4	2.83	-30	

Model 1:

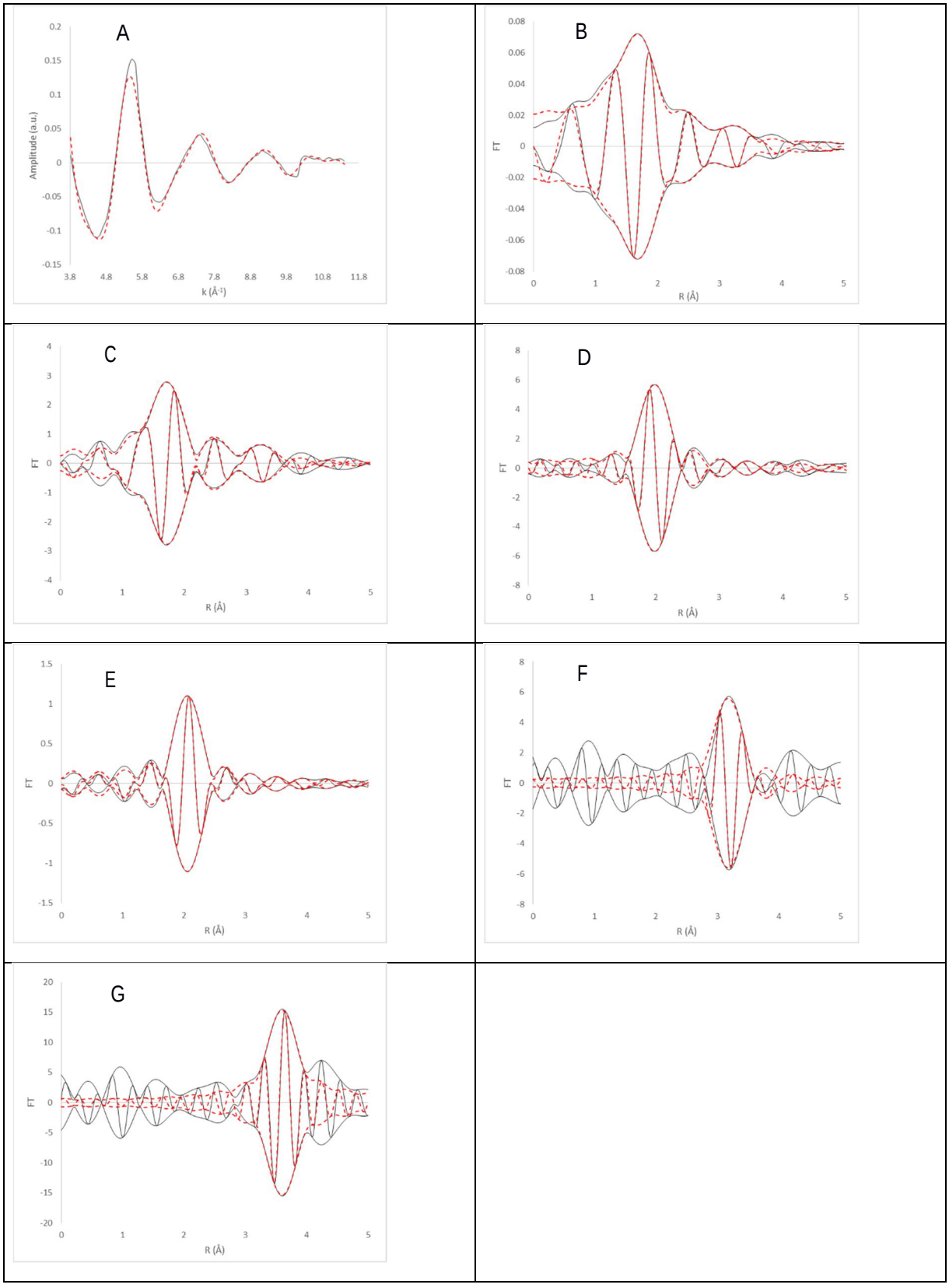

Figure S6. EXAFS Model 1 representing the data characterizing MgO-supported complexes formed by adsorption of $Ir(C_2H_4)_2(acac)$ on MgO treated at 1273 K to give an Ir loading of 1.0 wt%. Spectra were recorded with sample in flowing helium at room temperature. (A) k^1-weighted EXAFS function (solid line) obtained from the data, and the sum of all modeled contributions (dashed line); (B) k^1-weighted imaginary part and magnitude of the Fourier transform of the EXAFS function (solid line), and the sum of all modeled contributions (dashed line); (C) k^3-weighted imaginary part and magnitude of the Fourier transform of the EXAFS function (solid line), and the sum of all modeled contributions (dashed line); (D) k^2-weighted imaginary part and magnitude of the Fourier transform of residual data (solid line) and modeled contribution (dashed line) of the $Ir–O_{support}$ shell; (E) k^1-weighted imaginary part and magnitude of the Fourier transform of residual data (solid line) and modeled contribution (dashed line) of the $Ir–C_{ethylene}$ shell; (F) k^3-weighted imaginary part and magnitude of the Fourier transform of residual data (solid line) and modeled contribution (dashed line) of the $Ir–Mg_{support}$ shell; (G) k^3-weighted imaginary part and magnitude of the Fourier transform of residual data (solid line) and modeled contribution (dashed line) of the $Ir–O_{supportLong}$ shell.

Model 2:

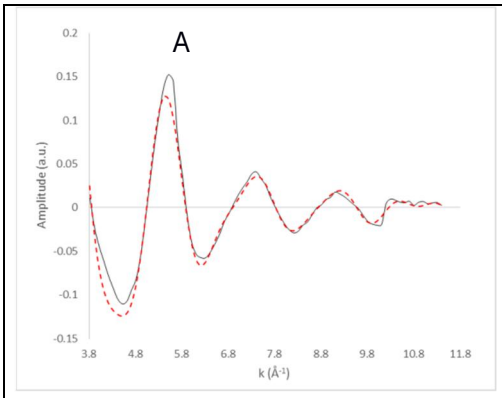

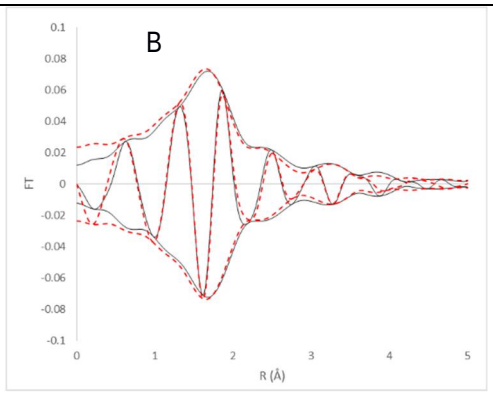

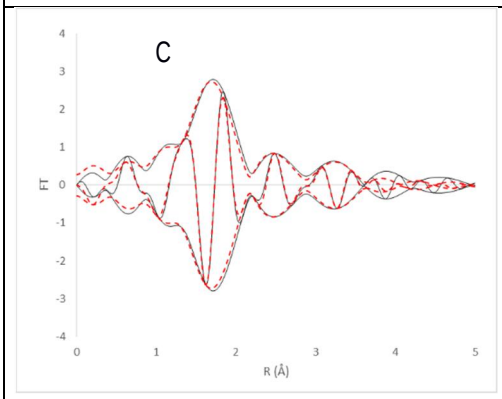

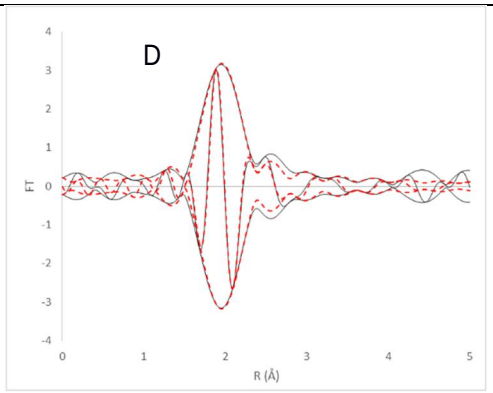

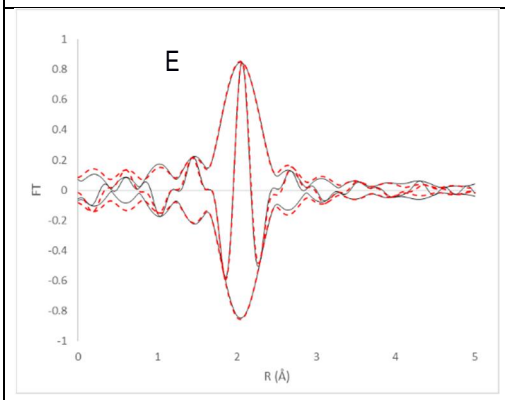

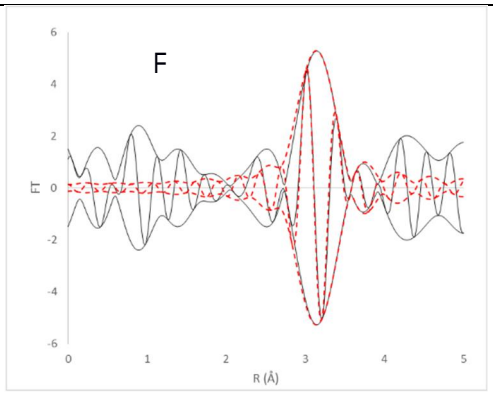

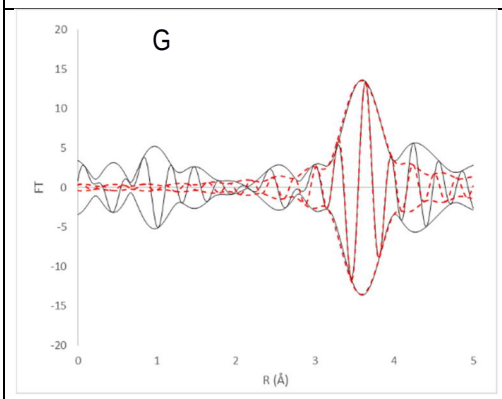

Figure S7. EXAFS Model 2 representing the data characterizing MgO-supported complexes formed by adsorption of $Ir(C_2H_4)_2(acac)$ on MgO treated at 1273 K to give an Ir loading of 1.0 wt%. Spectra were recorded with sample in flowing helium at room temperature. (A) k^1-weighted EXAFS function (solid line) obtained from the data, and the sum of all modeled contributions (dashed line); (B) k^1-weighted imaginary part and magnitude of the Fourier transform of the EXAFS function (solid line), and the sum of all modeled contributions (dashed line); (C) k^3-weighted imaginary part and magnitude of the Fourier transform of the EXAFS function (solid line), and the sum of all modeled contributions (dashed line); (D) k^2-weighted imaginary part and magnitude of the Fourier transform of residual data (solid line) and modeled contribution (dashed line) of the $Ir–O_{support}$ shell; (E) k^1-weighted imaginary part and magnitude of the Fourier transform of residual data (solid line) and modeled contribution (dashed line) of the $Ir–C_{ethylene}$ shell; (F) k^3-weighted imaginary part and magnitude of the Fourier transform of residual data (solid line) and modeled contribution (dashed line) of the $Ir–Mg_{support}$ shell; (G) k^3-weighted imaginary part and magnitude of the Fourier transform of residual data (solid line) and modeled contribution (dashed line) of the $Ir–O_{supportLong}$ shell.

Model 3:

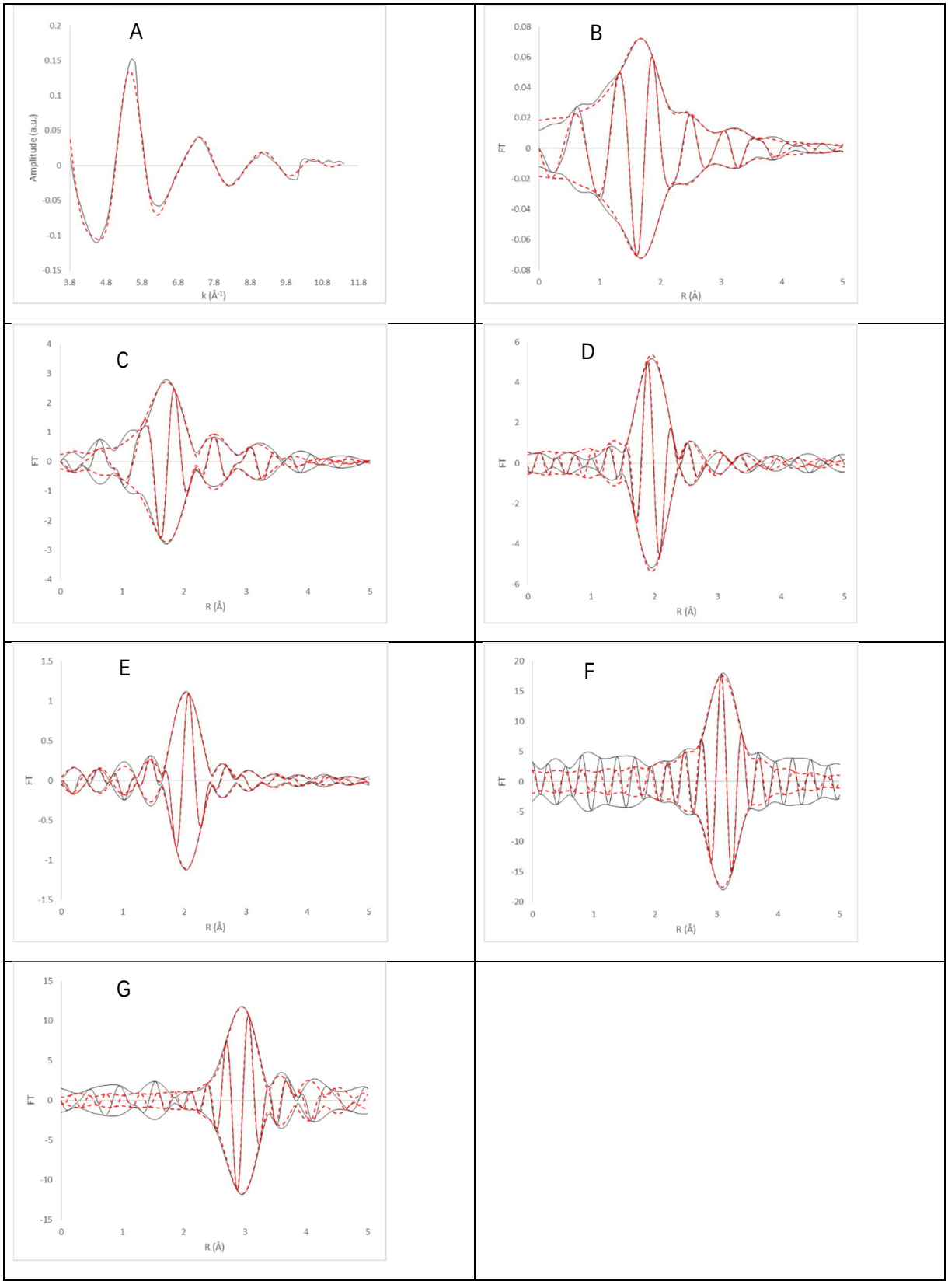

Figure S8. EXAFS Model 1 representing the data characterizing MgO-supported Ir complexes formed by adsorption of $Ir(C_2H_4)_2(acac)$ on MgO treated at 1273 K to give an iridium loading of 1.0 wt%. Spectra were recorded with sample in flowing helium at room temperature. (A) k^1-weighted EXAFS function (solid line) obtained from the data, and the sum of all modeled contributions (dashed line); (B) k^1-weighted imaginary part and magnitude of the Fourier transform of the EXAFS function (solid line), and the sum of all modeled contributions (dashed line); (C) k^3-weighted imaginary part and magnitude of the Fourier transform of the EXAFS function (solid line), and the sum of all modeled contributions (dashed line); (D) k^2-weighted imaginary part and magnitude of the Fourier transform of residual data (solid line) and modeled contribution (dashed line) of the $Ir–O_{support}$ shell; (E) k^1-weighted imaginary part and magnitude of the Fourier transform of residual data (solid line) and modeled contribution (dashed line) of the $Ir–C_{ethylene}$ shell; (F) k^3-weighted imaginary part and magnitude of the Fourier transform of residual data (solid line) and modeled contribution (dashed line) of the $Ir–Mg_{support}$ shell; (G) k^3-weighted imaginary part and magnitude of the Fourier transform of residual data (solid line) and modeled contribution (dashed line) of the Ir–Ir shell.

MgO-supported $Ir(C_2H_4)_2$; as made; 0.1 wt % Ir:

Table S3. EXAFS models representing the data at the Ir L_{III} edge characterizing MgO-supported complexes formed by adsorption of $Ir(C_2H_4)_2(acac)$ on MgO treated at 1273 K to give an Ir loading of 0.1 wt%. The values of *k* ranged from 3.87 to 12.15 Å; Error = 0.00114; *Denotes best-fit model; [a]Notation: *N*, coordination number; *R*, distance between absorber and backscatterer atoms; σ^2, Debye-Waller/disorder term; ΔE_0, inner potential correction.

Model	Shell	N^a	$10^3 \times \sigma^2$ (Å^2)^a	R (Å) ^{a}	ΔE_0 (eV) ^{a}	Goodness of Fit
1*	Ir–C	4.1	1.2	2.02	5.65	2.70
	$Ir–O_{Sup}$	2.9	3.5	1.90	-7.86	
	$Ir–Mg_{Sup}$	4.6	7.3	3.02	-7.72	
	$Ir–Mo_{sul}$	1.5	0.7	3.15	-0.10	
2	Ir–C	4.1	1.2	2.02	5.65	3.14
	$Ir–O_{Sup}$	3.1	3.5	1.89	-7.86	
	$Ir–Mg_{Sup}$	1.9	0.8	3.16	-15.1	
	Ir–Ir	2.3	7.2	2.82	-20.6	
3	Ir–C	2.0	1.0	2.06	-11.8	2.77
	$Ir–O_{Sup}$	1.9	8.9	1.87	12.2	
	$Ir–Mg_{Sup}$	4.0	7.3	3.02	-7.98	
	$Ir–Mg_{SupL}$	1.3	1.1	3.14	0.95	

Model 1:

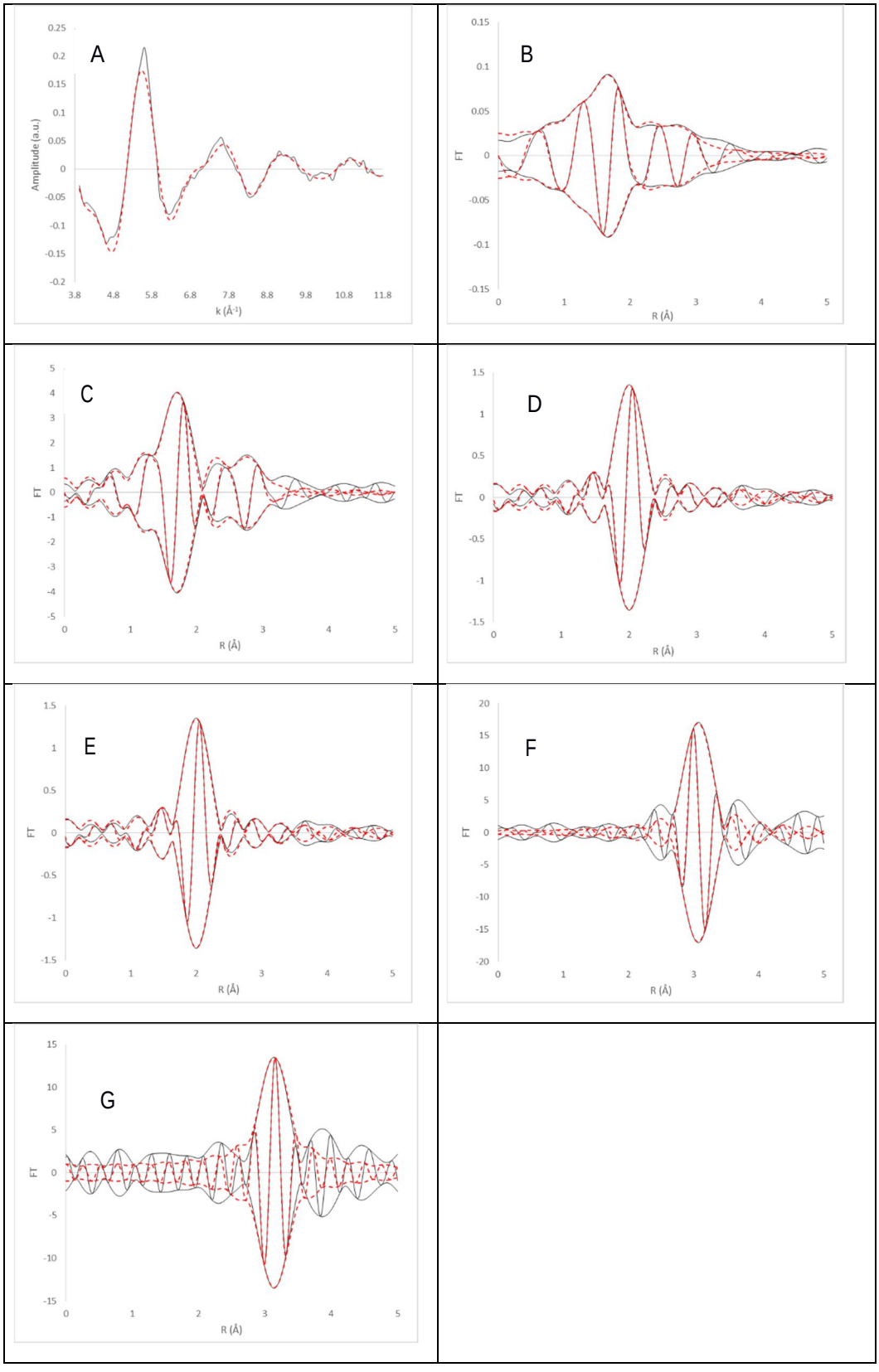

Figure S9. EXAFS data characterizing MgO-supported complexes formed by adsorption of $Ir(C_2H_4)_2(acac)$ on MgO treated at 1273 K to give an Ir loading of 0.1 wt%. Spectra were recorded with sample in flowing helium at room temperature. (A) k^1-weighted EXAFS function (solid line) obtained from the data, and the sum of all modeled contributions (dashed line); (B) k^1-weighted imaginary part and magnitude of the Fourier transform of the EXAFS function (solid line), and the sum of all modeled contributions (dashed line); (C) k^3-weighted imaginary part and magnitude of the Fourier transform of the EXAFS function (solid line), and the sum of all modeled contributions (dashed line); (D) k^2-weighted imaginary part and magnitude of the Fourier transform of residual data (solid line) and modeled contribution (dashed line) of the $Ir–O_{support}$ shell; (E) k^1-weighted imaginary part and magnitude of the Fourier transform of residual data (solid line) and modeled contribution (dashed line) of the $Ir–C_{ethylene}$ shell; (F) k^3-weighted imaginary part and magnitude of the Fourier transform of residual data (solid line) and modeled contribution (dashed line) of the $Ir–Mg_{supportShort}$ shell; (G) k^3-weighted imaginary part and magnitude of the Fourier transform of residual data (solid line) and modeled contribution (dashed line) of the $Ir–Mg_{supportLong}$ shell.

Model 2:

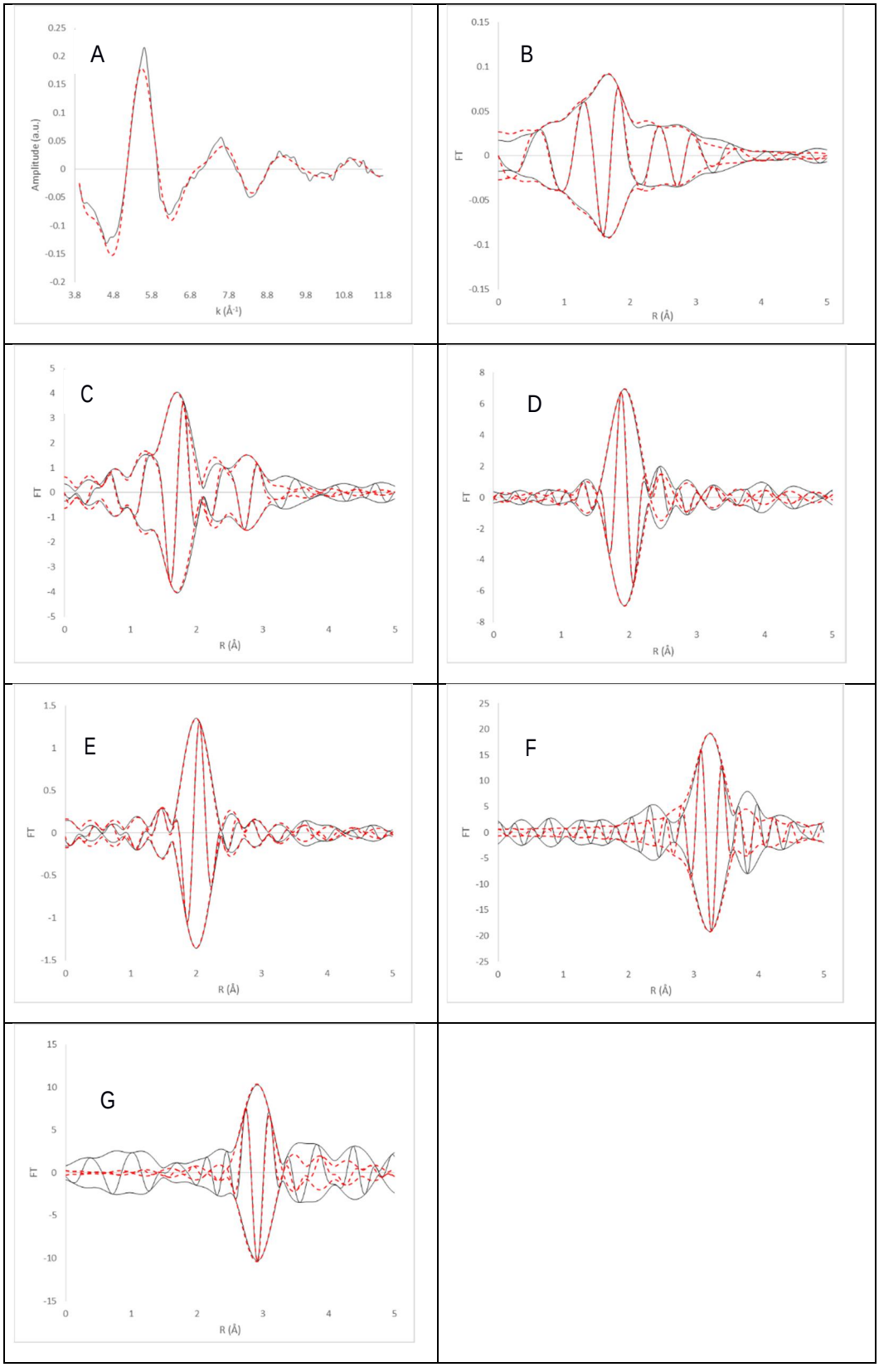

Figure S10. EXAFS data characterizing MgO-supported complexes formed by adsorption of $Ir(C_2H_4)_2(acac)$ on MgO treated at 1273 K to give an Ir loading of 0.1 wt%. Spectra were recorded with sample in flowing helium at room temperature. (A) k^1-weighted EXAFS function (solid line) obtained from the data, and the sum of all modeled contributions (dashed line); (B) k^1-weighted imaginary part and magnitude of the Fourier transform of the EXAFS function (solid line), and the sum of all modeled contributions (dashed line); (C) k^3-weighted imaginary part and magnitude of the Fourier transform of the EXAFS function (solid line), and the sum of all modeled contributions (dashed line); (D) k^2-weighted imaginary part and magnitude of the Fourier transform of residual data (solid line) and modeled contribution (dashed line) of the $Ir–O_{support}$ shell; (E) k^1-weighted imaginary part and magnitude of the Fourier transform of residual data (solid line) and modeled contribution (dashed line) of the $Ir–C_{ethylene}$ shell; (F) k^3-weighted imaginary part and magnitude of the Fourier transform of residual data (solid line) and modeled contribution (dashed line) of the $Ir–Mg_{support}$ shell; (G) k^3-weighted imaginary part and magnitude of the Fourier transform of residual data (solid line) and modeled contribution (dashed line) of the Ir–Ir shell.

Model 3:

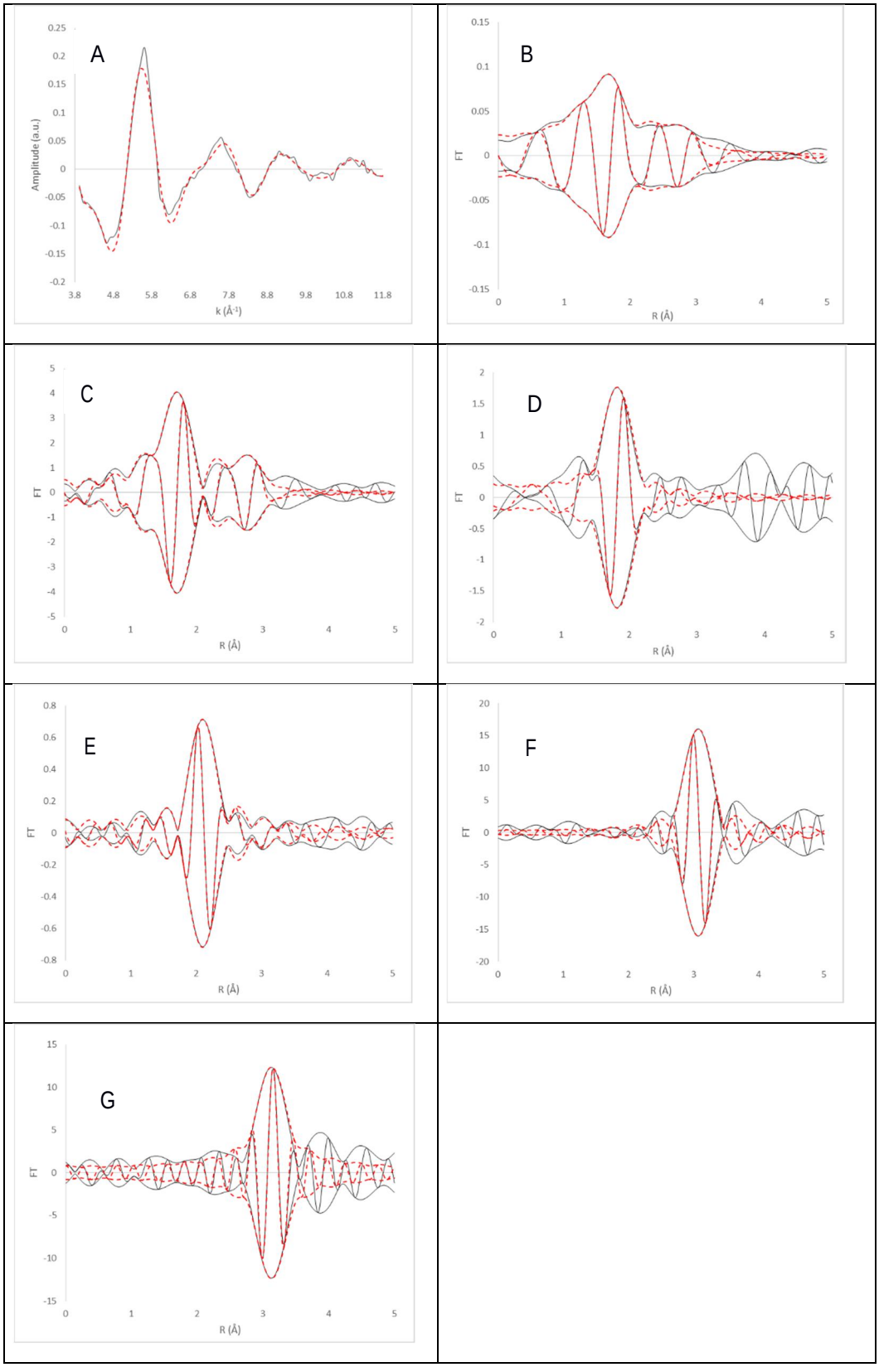

Figure S11. EXAFS data characterizing MgO-supported complexes formed by adsorption of $Ir(C_2H_4)_2(acac)$ on MgO treated at 1273 K to give an Ir loading of 0.1 wt%. Spectra were recorded with the sample in flowing helium at room temperature. (A) k^1-weighted EXAFS function (solid line) obtained from the data, and the sum of all modeled contributions (dashed line); (B) k^1-weighted imaginary part and magnitude of the Fourier transform of the EXAFS function (solid line), and the sum of all modeled contributions (dashed line); (C) k^3-weighted imaginary part and magnitude of the Fourier transform of the EXAFS function (solid line), and the sum of all modeled contributions (dashed line); (D) k^2-weighted imaginary part and magnitude of the Fourier transform of residual data (solid line) and modeled contribution (dashed line) of the $Ir–O_{support}$ shell; (E) k^1-weighted imaginary part and magnitude of the Fourier transform of residual data (solid line) and modeled contribution (dashed line) of the $Ir–C_{ethylene}$ shell; (F) (F) k^3-weighted imaginary part and magnitude of the Fourier transform of residual data (solid line) and modeled contribution (dashed line) of the $Ir–Mg_{supportShort}$ shell; (G) k^3-weighted imaginary part and magnitude of the Fourier transform of residual data (solid line) and modeled contribution (dashed line) of the $Ir–Mg_{supportLong}$ shell.

MgO-supported $Ir(C_2H_4)_2$; as made; 0.05 wt% Ir:

Table S4. EXAFS models representing the data at the Ir L_{III} edge characterizing MgO-supported iridium complexes formed by adsorption of $Ir(C_2H_4)_2(acac)$ on MgO treated at 1273 K to give an iridium loading of 0.05 wt%. The range of *k* was 3.85 to 13.28 Å; error = 0.00132. *Denotes best-fit model.

Model	Shell	N^a	$10^3 \times \sigma^2$ (Å^2)^a	R (Å)^a	ΔE_0 (eV)^a	Goodness of Fit
1*	Ir–C	4.0	3.5	2.03	3.8	2.57
	$Ir–O_{Sup}$	3.0	7.1	1.95	-12.3	
	$Ir–Mg_{Sup}$	1.1	5.4	2.94	8.0	
	$Ir–Mg_{SupLong}$	4.2	13.5	3.14	-14.5	
2	Ir–C	4.0	3.5	2.03	3.8	1.50
	$Ir–O_{Sup}$	3.0	7.1	1.95	-11.5	
	$Ir–Mg_{Sup}$	1.1	6.8	2.96	-5.6	
	$Ir–Mg_{SupLong}$	4.2	12.0	3.08	-6.8	
	$Ir–O_{SupLong}$	4.8	8.5	3.95	9.9	
3	Ir–C	4.0	3.5	2.03	3.8	1.61
	$Ir–O_{Sup}$	3.0	7.1	1.95	-11.8	
	$Ir–Mg_{Sup}$	1.1	6.1	2.94	4.6	
	$Ir–Mg_{SupLong}$	4.2	13.7	3.12	-13.8	
	Ir–Ir	3.9	14.1	3.67	16.3	

[a]Notation: *N*, coordination number; *R*, distance between absorber and backscatterer atoms; σ^2, Debye-Waller/disorder term; ΔE_0, inner potential correction. Subscripts: Sup, refers to an atom identified to be belonging to the support; Long, refers to the long contribution involving an atom in the support.

Model 1:

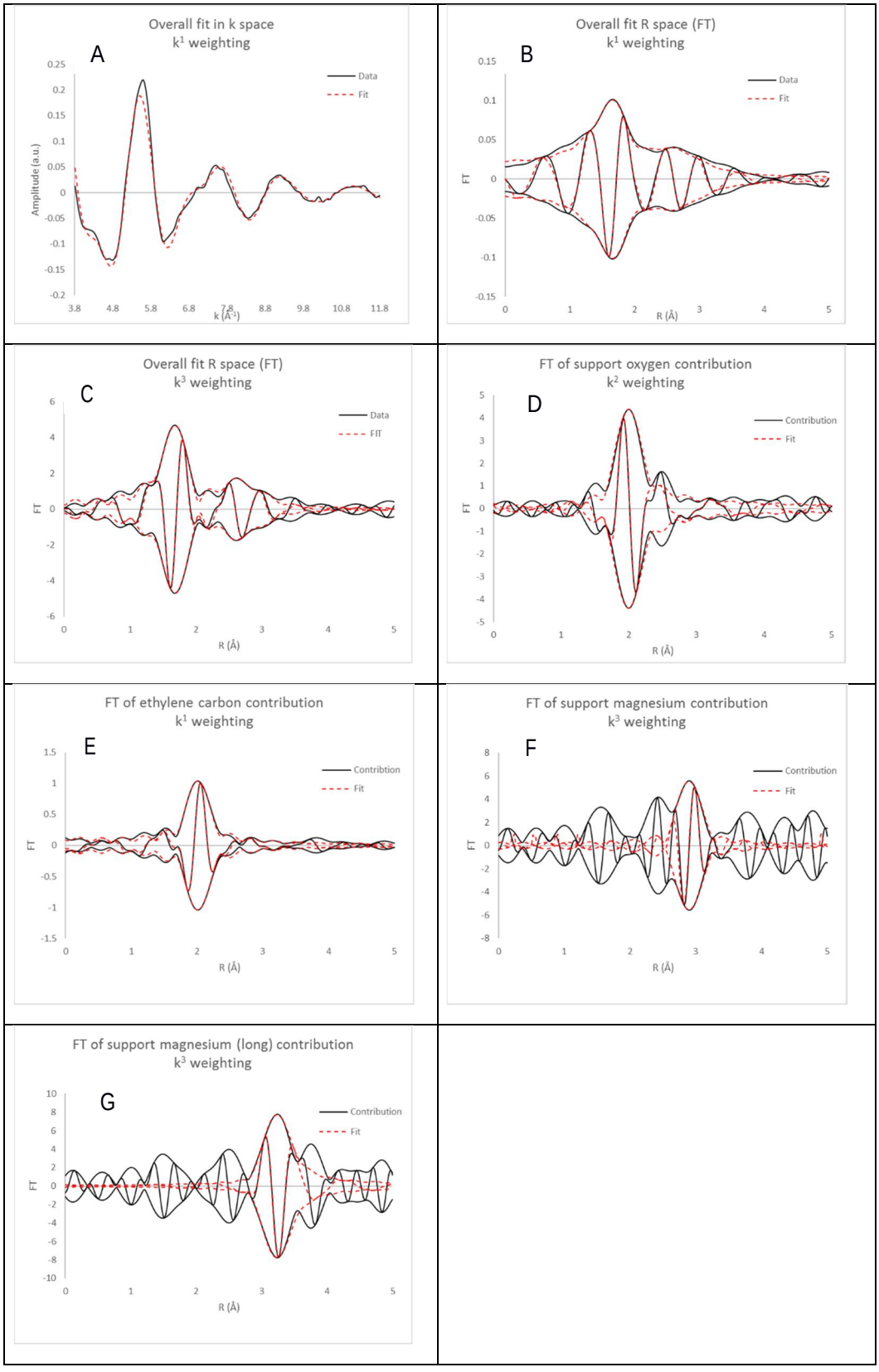
Overall fit in k space
k¹ weighting
A
Data
Fit
Amplitude (a.u.)
k (Å⁻¹)
Overall fit R space (FT)
k¹ weighting
B
Data
Fit
FT
R (Å)
Overall fit R space (FT)
k³ weighting
C
Data
FIT
FT
R (Å)
FT of support oxygen contribution
k² weighting
D
Contribution
Fit
FT
R (Å)
FT of ethylene carbon contribution
k¹ weighting
E
Contribtion
Fit
FT
R (Å)
FT of support magnesium contribution
k³ weighting
F
Contribution
Fit
FT
R (Å)
FT of support magnesium (long) contribution
k³ weighting
G
Contribution
Fit
FT
R (Å)

Figure S12. EXAFS data characterizing MgO-supported complexes formed by adsorption of $Ir(C_2H_4)_2(acac)$ on MgO treated at 1273 K to give an Ir loading of 0.05 wt%. Spectra were recorded with sample in flowing helium at room temperature. (A) k^1-weighted EXAFS function (solid line) obtained from the data, and the sum of all modeled contributions (dashed line); (B) k^1-weighted imaginary part and magnitude of the Fourier transform of the EXAFS function (solid line), and the sum of all modeled contributions (dashed line); (C) k^3-weighted imaginary part and magnitude of the Fourier transform of the EXAFS function (solid line), and the sum of all modeled contributions (dashed line); (D) k^2-weighted imaginary part and magnitude of the Fourier transform of residual data (solid line) and modeled contribution (dashed line) of the $Ir–O_{support}$ shell; (E) k^1-weighted imaginary part and magnitude of the Fourier transform of residual data (solid line) and modeled contribution (dashed line) of the $Ir–C_{ethylene}$ shell; (F) k^3-weighted imaginary part and magnitude of the Fourier transform of residual data (solid line) and modeled contribution (dashed line) of the $Ir–Mg_{supportShort}$ shell; (G) k^3-weighted imaginary part and magnitude of the Fourier transform of residual data (solid line) and modeled contribution (dashed line) of the $Ir–Mg_{supportLong}$ shell.

Model 2:

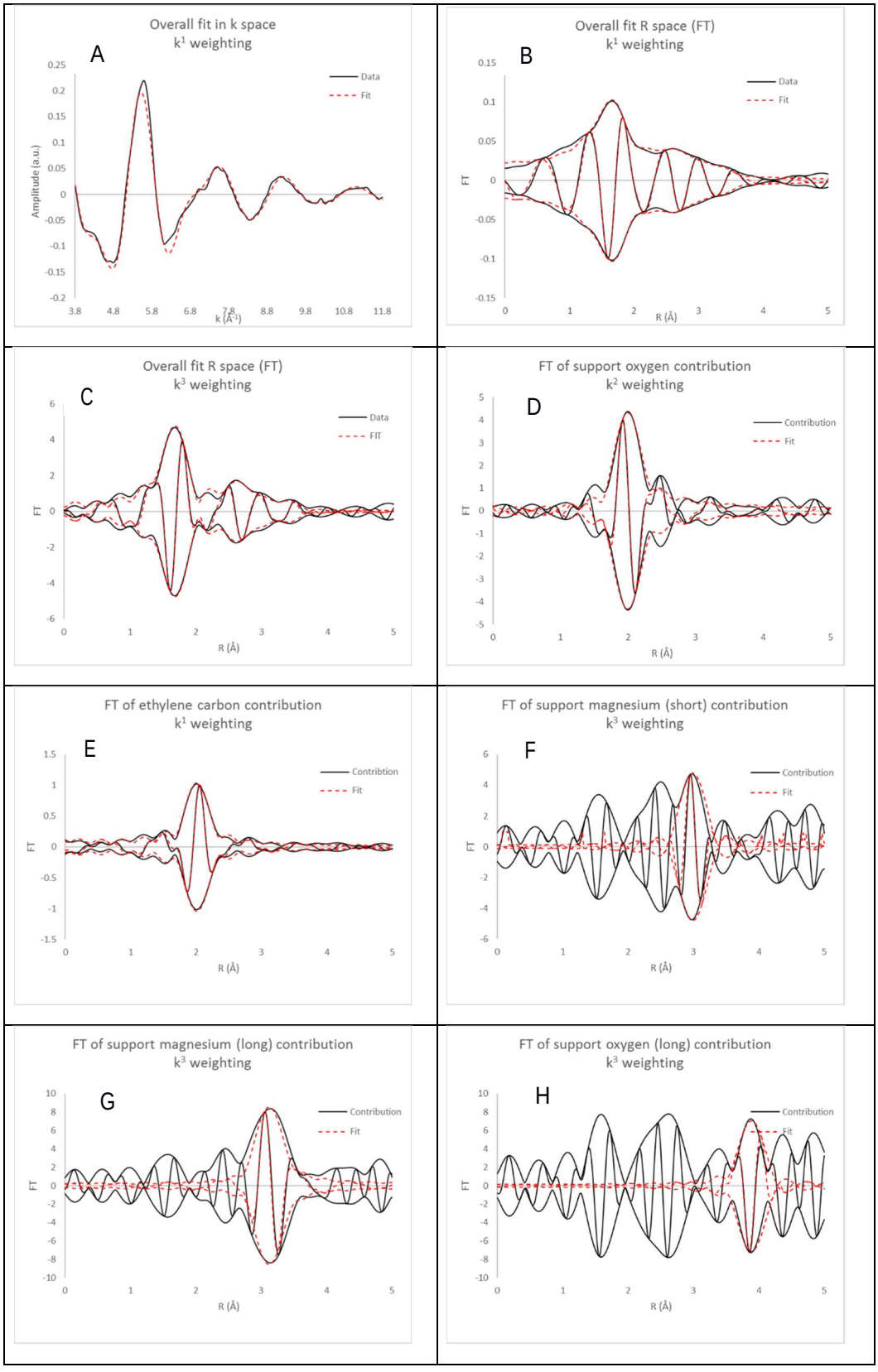
Overall fit in k space
k¹ weighting
A
Data
Fit
Amplitude (a.u.)
k (Å⁻¹)
Overall fit R space (FT)
k¹ weighting
B
Data
Fit
FT
R (Å)
Overall fit R space (FT)
k³ weighting
C
Data
FIT
FT
R (Å)
FT of support oxygen contribution
k² weighting
D
Contribution
Fit
FT
R (Å)
FT of ethylene carbon contribution
k¹ weighting
E
Contribtion
Fit
FT
R (Å)
FT of support magnesium (short) contribution
k³ weighting
F
Contribution
Fit
FT
R (Å)
FT of support magnesium (long) contribution
k³ weighting
G
Contribution
Fit
FT
R (Å)
FT of support oxygen (long) contribution
k³ weighting
H
Contribution
Fit
FT
R (Å)

Figure S13. EXAFS data characterizing MgO-supported complexes formed by adsorption of $Ir(C_2H_4)_2(acac)$ on MgO treated at 1273 K to give an Ir loading of 0.05 wt%. Spectra were recorded with the sample in flowing helium at room temperature. (A) k^1-weighted EXAFS function (solid line) obtained from the data, and the sum of all modeled contributions (dashed line); (B) k^1-weighted imaginary part and magnitude of the Fourier transform of the EXAFS function (solid line), and the sum of all modeled contributions (dashed line); (C) k^3-weighted imaginary part and magnitude of the Fourier transform of the EXAFS function (solid line), and the sum of all modeled contributions (dashed line); (D) k^2-weighted imaginary part and magnitude of the Fourier transform of residual data (solid line) and modeled contribution (dashed line) of the $Ir–O_{supportShort}$ shell; (E) k^1-weighted imaginary part and magnitude of the Fourier transform of residual data (solid line) and modeled contribution (dashed line) of the $Ir–C_{ethylene}$ shell; (F) k^3-weighted imaginary part and magnitude of the Fourier transform of residual data (solid line) and modeled contribution (dashed line) of the $Ir–Mg_{supportShort}$ shell; (G) k^3-weighted imaginary part and magnitude of the Fourier transform of residual data (solid line) and modeled contribution (dashed line) of the $Ir–Mg_{supportLong}$ shell; (H) k^3-weighted imaginary part and magnitude of the Fourier transform of residual data (solid line) and modeled contribution (dashed line) of the $Ir–O_{supportLong}$ shell.

Model 3:

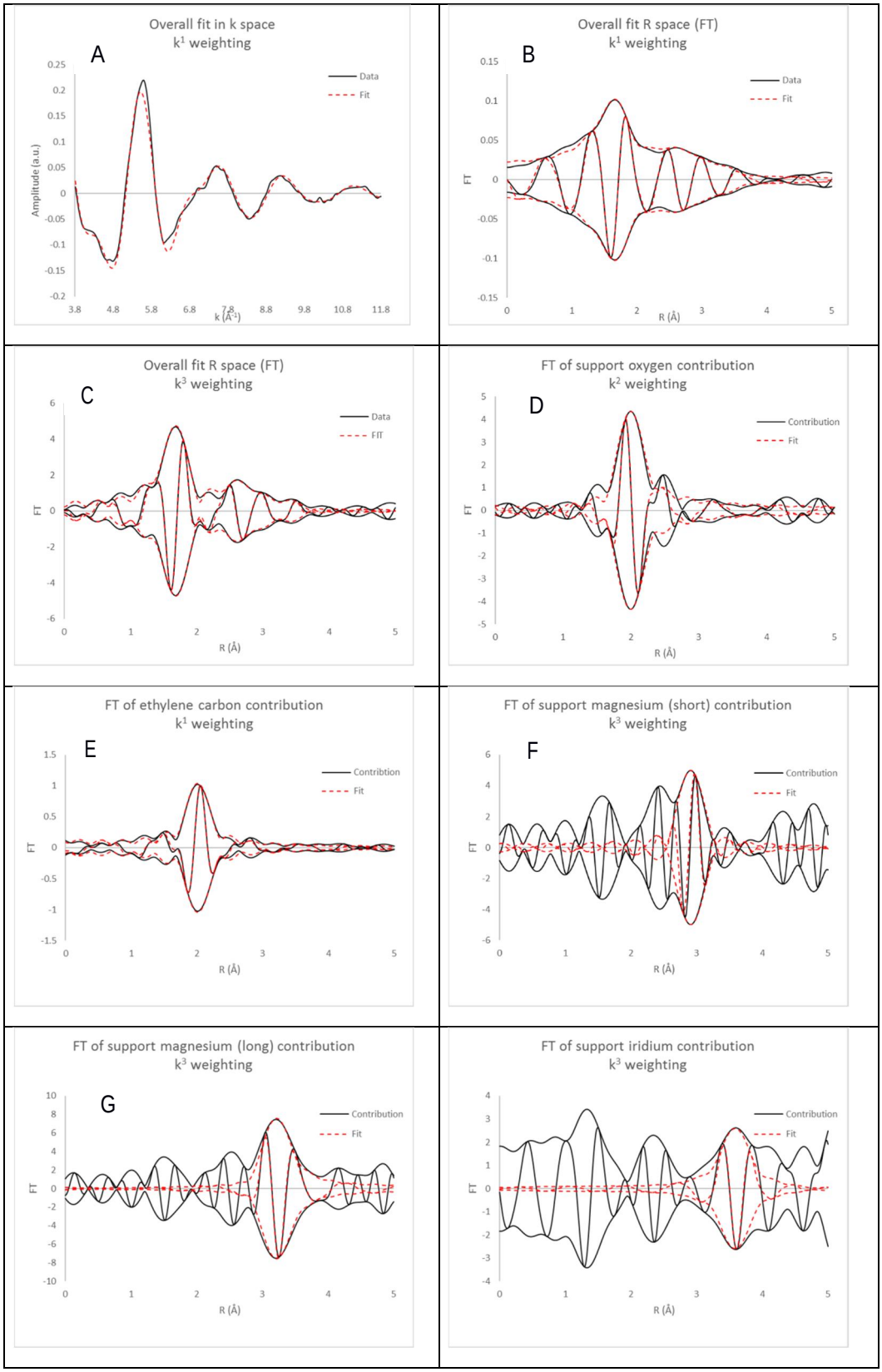
Overall fit in k space
k¹ weighting
A
Data
Fit
Amplitude (a.u.)
k (Å⁻¹)
Overall fit R space (FT)
k¹ weighting
B
Data
Fit
FT
R (Å)
Overall fit R space (FT)
k³ weighting
C
Data
FIT
FT
R (Å)
FT of support oxygen contribution
k² weighting
D
Contribution
Fit
FT
R (Å)
FT of ethylene carbon contribution
k¹ weighting
E
Contribtion
Fit
FT
R (Å)
FT of support magnesium (short) contribution
k³ weighting
F
Contribution
Fit
FT
R (Å)
FT of support magnesium (long) contribution
k³ weighting
G
Contribution
Fit
FT
R (Å)
FT of support iridium contribution
k³ weighting
Contribution
Fit
FT
R (Å)

Figure S14. EXAFS data characterizing MgO-supported complexes formed by adsorption of $Ir(C_2H_4)_2(acac)$ on MgO treated at 1273 K to give an Ir loading of 1.0 wt%. Spectra were recorded with the sample in flowing helium at room temperature. (A) k^1-weighted EXAFS function (solid line) obtained from the data, and the sum of all modeled contributions (dashed line); (B) k^1-weighted imaginary part and magnitude of the Fourier transform of the EXAFS function (solid line), and the sum of all modeled contributions (dashed line); (C) k^3-weighted imaginary part and magnitude of the Fourier transform of the EXAFS function (solid line), and the sum of all modeled contributions (dashed line); (D) k^2-weighted imaginary part and magnitude of the Fourier transform of residual data (solid line) and modeled contribution (dashed line) of the $Ir–O_{support}$ shell; (E) k^1-weighted imaginary part and magnitude of the Fourier transform of residual data (solid line) and modeled contribution (dashed line) of the $Ir–C_{ethylene}$ shell; (F) k^3-weighted imaginary part and magnitude of the Fourier transform of residual data (solid line) and modeled contribution (dashed line) of the $Ir–Mg_{supportShort}$ shell; (G) k^3-weighted imaginary part and magnitude of the Fourier transform of residual data (solid line) and modeled contribution (dashed line) of the $Ir–Mg_{supportLong}$ shell; (H) k^3-weighted imaginary part and magnitude of the Fourier transform of residual data (solid line) and modeled contribution (dashed line) of the Ir–Ir shell.

MgO-supported $Ir(C_2H_4)_2$; as made; 0.01 wt % Ir:

Table S5. EXAFS models representing the data at the Ir L_{III} edge characterizing MgO-supported complexes formed by adsorption of $Ir(C_2H_4)_2(acac)$ on MgO treated at 1273 K to give an Ir loading of 0.01 wt%. The range of k was from 3.85 to 11.58 $Å^{-1}$; Error = 0.0009; *Denotes best-fit model.

Model	Shell	N^a	$10^3 \times \sigma^2$ ($Å^2$)[a]	R (Å)[a]	ΔE_0 (eV)[a]	Goodness of Fit
1*	$Ir–O_{Sup}$	3.0	4.3	1.93	-9.2	7.74
	Ir–C	3.9	2.1	2.02	11.9	
	$Ir–Mg_{Sup}$	2.6	8.5	3.03	-4.9	
2	$Ir–O_{Sup}$	3.0	5.5	1.96	-6.8	9.11
	Ir–C	2.0	0.7	2.02	15.6	
	$Ir–Mg_{Sup}$	2.0	6.2	3.03	-5.0	
3	$Ir–O_{Sup}$	3.9	4.5	1.93	-5.4	3.32
	Ir–C	4.0	1.7	2.02	17.0	
	$Ir–Mg_{Sup}$	2.7	4.5	3.06	-5.9	
	Ir–Ir	2.1	11.0	2.80	-30.5	

[a]Notation: N, coordination number; R, distance between absorber and backscatterer atoms; σ^2, Debye-Waller/disorder term; ΔE_0, inner potential correction. Subscripts: Sup, refers to an atom identified to be belonging to the support.

Model 1:

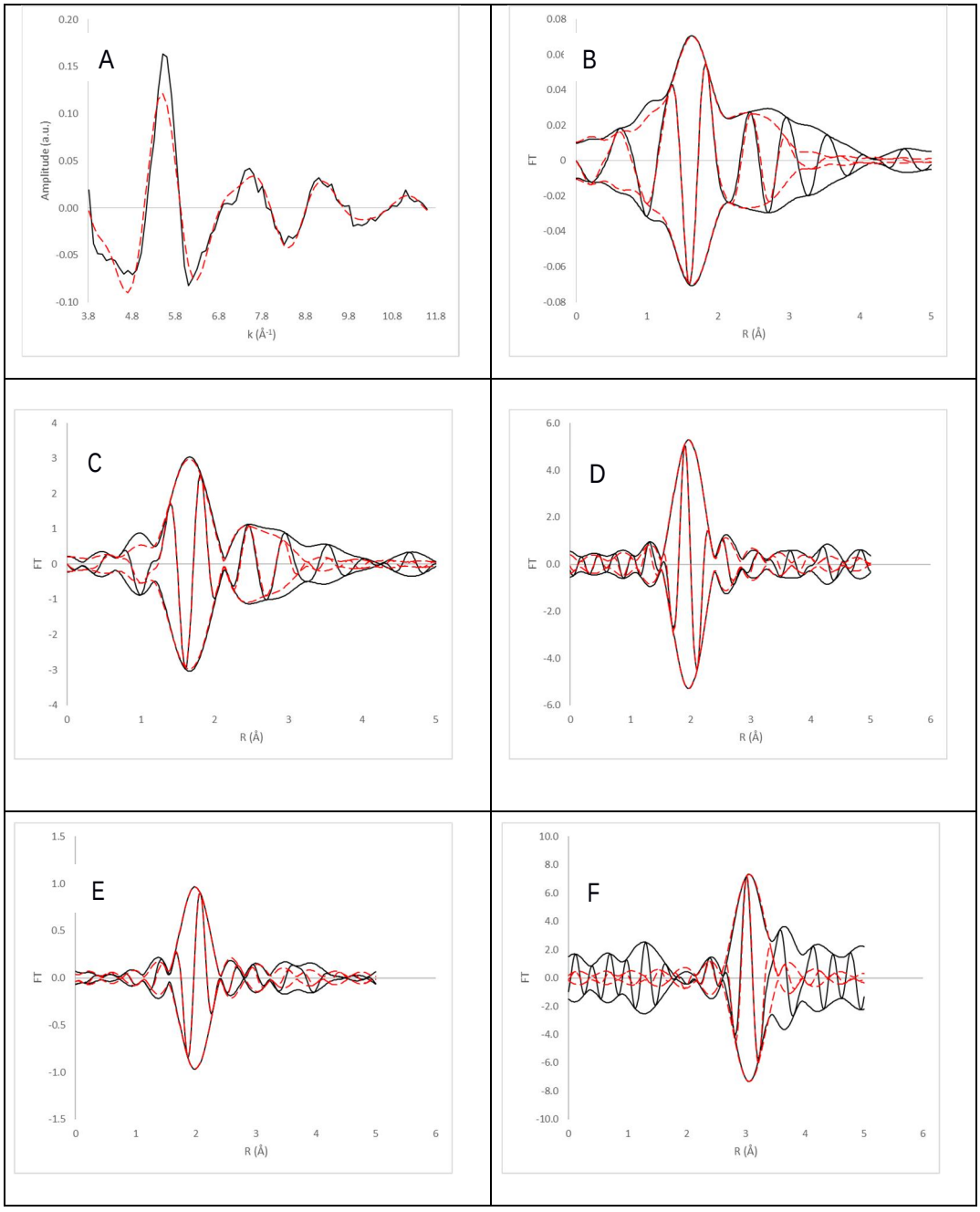

Figure S15. EXAFS Model 1 representing the data characterizing MgO-supported complexes formed by adsorption of $Ir(C_2H_4)_2(acac)$ on MgO treated at 1273 K to give an Ir loading of 0.01 wt%. Spectra were recorded with sample in flowing helium at room temperature. (A) k^1-weighted EXAFS function (solid line) obtained from the data, and the sum of all modeled contributions (dashed line); (B) k^1-weighted imaginary part and magnitude of the Fourier transform of the EXAFS function (solid line), and the sum of all modeled contributions (dashed line); (C) k^3-weighted imaginary part and magnitude of the Fourier transform of the EXAFS function (solid line), and the sum of all modeled contributions (dashed line); (D) k^2-weighted imaginary part and magnitude of the Fourier transform of residual data (solid line) and modeled contribution (dashed line) of the $Ir–O_{support}$ shell; (E) k^1-weighted imaginary part and magnitude of the Fourier transform of residual data (solid line) and modeled contribution (dashed line) of the $Ir–C_{ethylene}$ shell; (F) k^3-weighted imaginary part and magnitude of the Fourier transform of residual data (solid line) and modeled contribution (dashed line) of the $Ir–Mg_{support}$ shell.

Model 2:

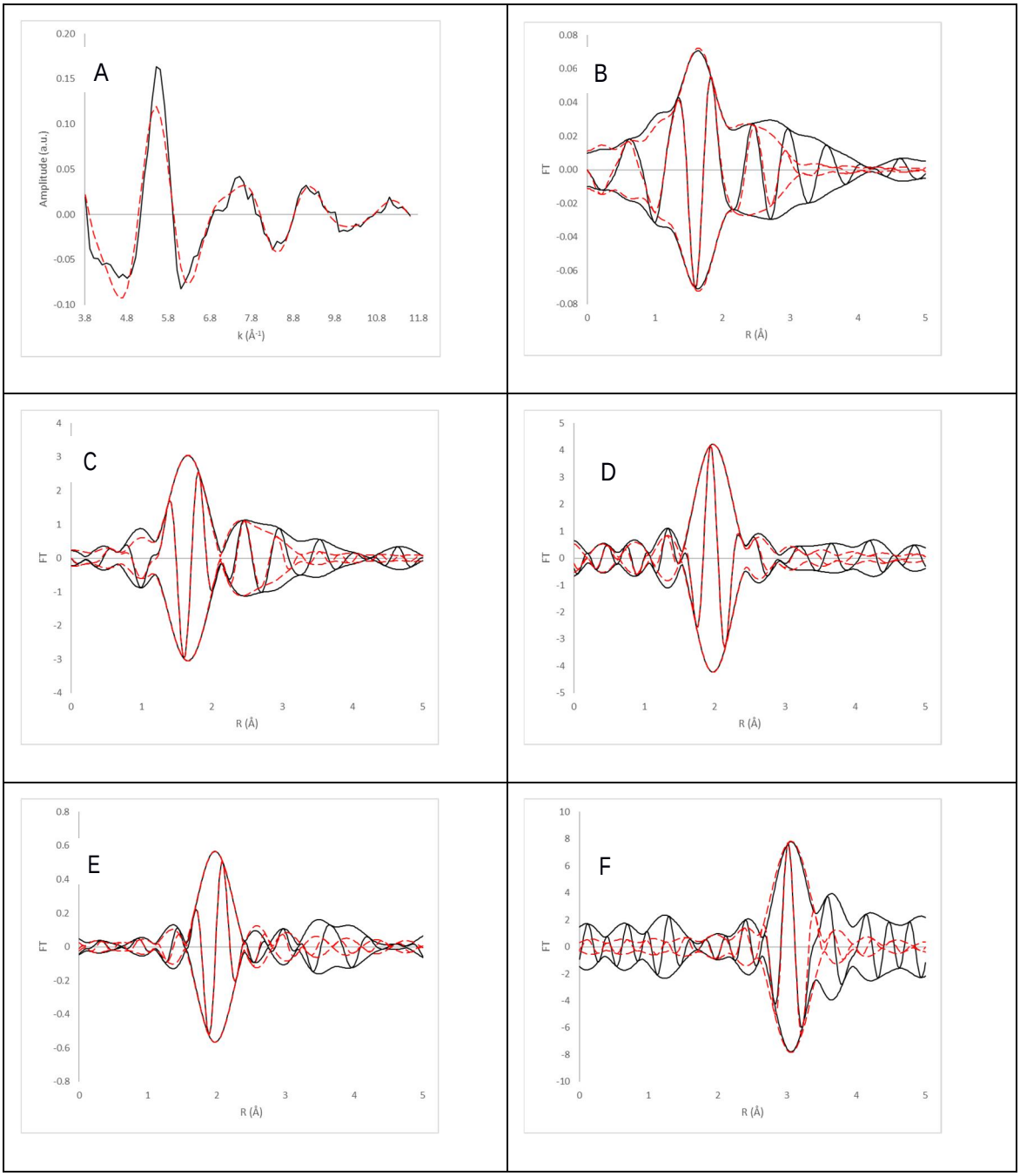

Figure S16. EXAFS Model 2 representing the data characterizing MgO-supported complexes formed by adsorption of $Ir(C_2H_4)_2(acac)$ on MgO treated at 1273 K to give an Ir loading of 0.01 wt%. Spectra were recorded with sample in flowing helium at room temperature. (A) k^1-weighted EXAFS function (solid line) obtained from the data, and the sum of all modeled contributions (dashed line); (B) k^1-weighted imaginary part and magnitude of the Fourier transform of the EXAFS function (solid line), and the sum of all modeled contributions (dashed line); (C) k^3-weighted imaginary part and magnitude of the Fourier transform of the EXAFS function (solid line), and the sum of all modeled contributions (dashed line); (D) k^2-weighted imaginary part and magnitude of the Fourier transform of residual data (solid line) and modeled contribution (dashed line) of the $Ir–O_{support}$ shell; (E) k^1-weighted imaginary part and magnitude of the Fourier transform of residual data (solid line) and modeled contribution (dashed line) of the $Ir–C_{ethylene}$ shell; (F) k^3-weighted imaginary part and magnitude of the Fourier transform of residual data (solid line) and modeled contribution (dashed line) of the $Ir–Mg_{support}$ shell.

Model 3:

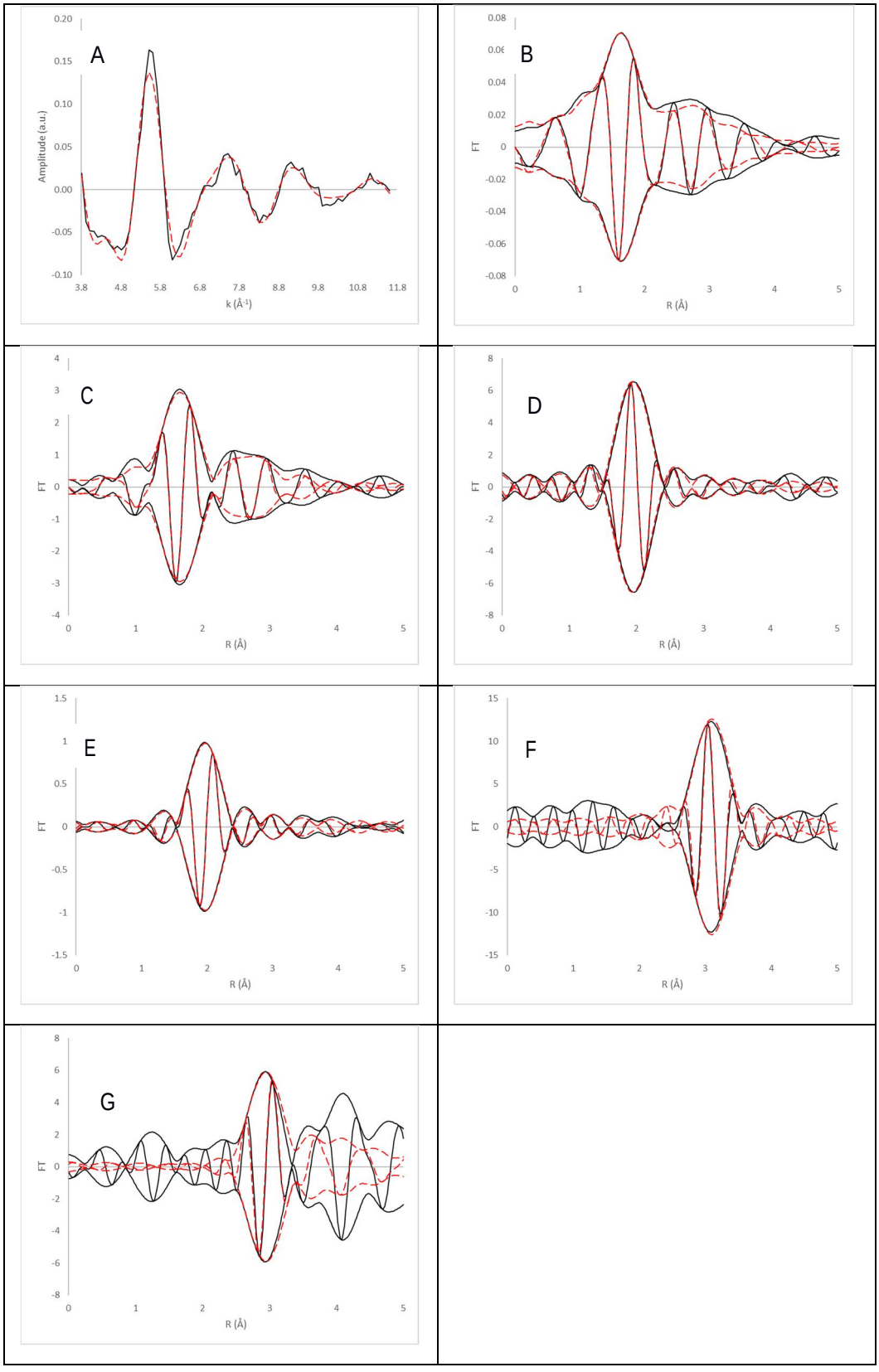

Figure S17. EXAFS Model 1 representing the data characterizing MgO-supported complexes formed by adsorption of $Ir(C_2H_4)_2(acac)$ on MgO treated at 1273 K to give an iridium loading of 0.01 wt%. Spectra were recorded with sample in flowing helium at room temperature. (A) k^1-weighted EXAFS function (solid line) obtained from the data, and the sum of all modeled contributions (dashed line); (B) k^1-weighted imaginary part and magnitude of the Fourier transform of the EXAFS function (solid line), and the sum of all modeled contributions (dashed line); (C) k^3-weighted imaginary part and magnitude of the Fourier transform of the EXAFS function (solid line), and the sum of all modeled contributions (dashed line); (D) k^2-weighted imaginary part and magnitude of the Fourier transform of residual data (solid line) and modeled contribution (dashed line) of the $Ir–O_{support}$ shell; (E) k^1-weighted imaginary part and magnitude of the Fourier transform of residual data (solid line) and modeled contribution (dashed line) of the $Ir–C_{ethylene}$ shell; (F) k^3-weighted imaginary part and magnitude of the Fourier transform of residual data (solid line) and modeled contribution (dashed line) of the $Ir–Mg_{support}$ shell; (G) k^3-weighted imaginary part and magnitude of the Fourier transform of residual data (solid line) and modeled contribution (dashed line) of the Ir–Ir shell.

MgO supported $Ir(C_2H_4)_2$; post H_2 exposure; 1.0 wt % Ir:

EXAFS analysis was not completed for this sample as STEM images showed a range of cluster sizes in the images making the results of the EXAFS analysis less than insightful.

MgO supported $Ir(C_2H_4)_2$; post H_2 exposure; 0.1 wt % Ir:

Initial EXAFS modeling predicted that the iridium had not undergone significant aggregation. However, after investigation of the samples with STEM, it was apparent that the models had to be reworked to account for the cluster formation.

Table S6 EXAFS models representing the data at the Ir L_{III} edge characterizing MgO-supported samples formed by adsorption of $Ir(C_2H_4)_2(acac)$ on MgO treated at 1273 K to give an Ir loading of 0.1 wt% and treated with flowing H_2 at 573 K for 250 min. The range of k was from 4.00 to 12.95 Å; Error = 0.00118; *Denotes best-fit model.

Model	Shell	N^a	$10^3 \times \sigma^2$ (Å^2)^a	R (Å)^a	ΔE_0 (eV)^a	Goodness of Fit
1*	Ir–C	4.2	4.2	2.02	1.08	1.14
	$Ir–O_{Sup}$	3.1	8.3	1.89	-10.58	
	$Ir–Mg_{Sup}$	2.5	5.8	2.82	1.17	
	$Ir– Mg_{SupL}$	2.6	6.3	3.02	-0.84	
2	Ir–C	4.2	3.5	2.00	5.00	1.25
	$Ir–O_{Sup}$	3.0	7.3	1.87	-7.37	
	$Ir–Mg_{Sup}$	3.4	7.5	2.78	35.43	
	Ir–Ir	2.8	5.3	2.97	-0.89	
3	Ir–C	3.1	2.2	2.02	1.82	1.89
	$Ir–O_{Sup}$	3.1	6.9	1.89	-7.13	
	$Ir–Mg_{Sup}$	2.5	6.0	2.83	0.90	
	$Ir– Mg_{SupL}$	2.6	6.0	3.03	-0.42	

[a]Notation: N, coordination number; R, distance between absorber and backscatterer atoms; σ^2, Debye-Waller/disorder term; ΔE_0, inner potential correction. Subscripts: Sup, refers to an atom that is part of the support; L, refers to the long absorber–backscatterer contribution involving such an atom in the support.

Model 1:

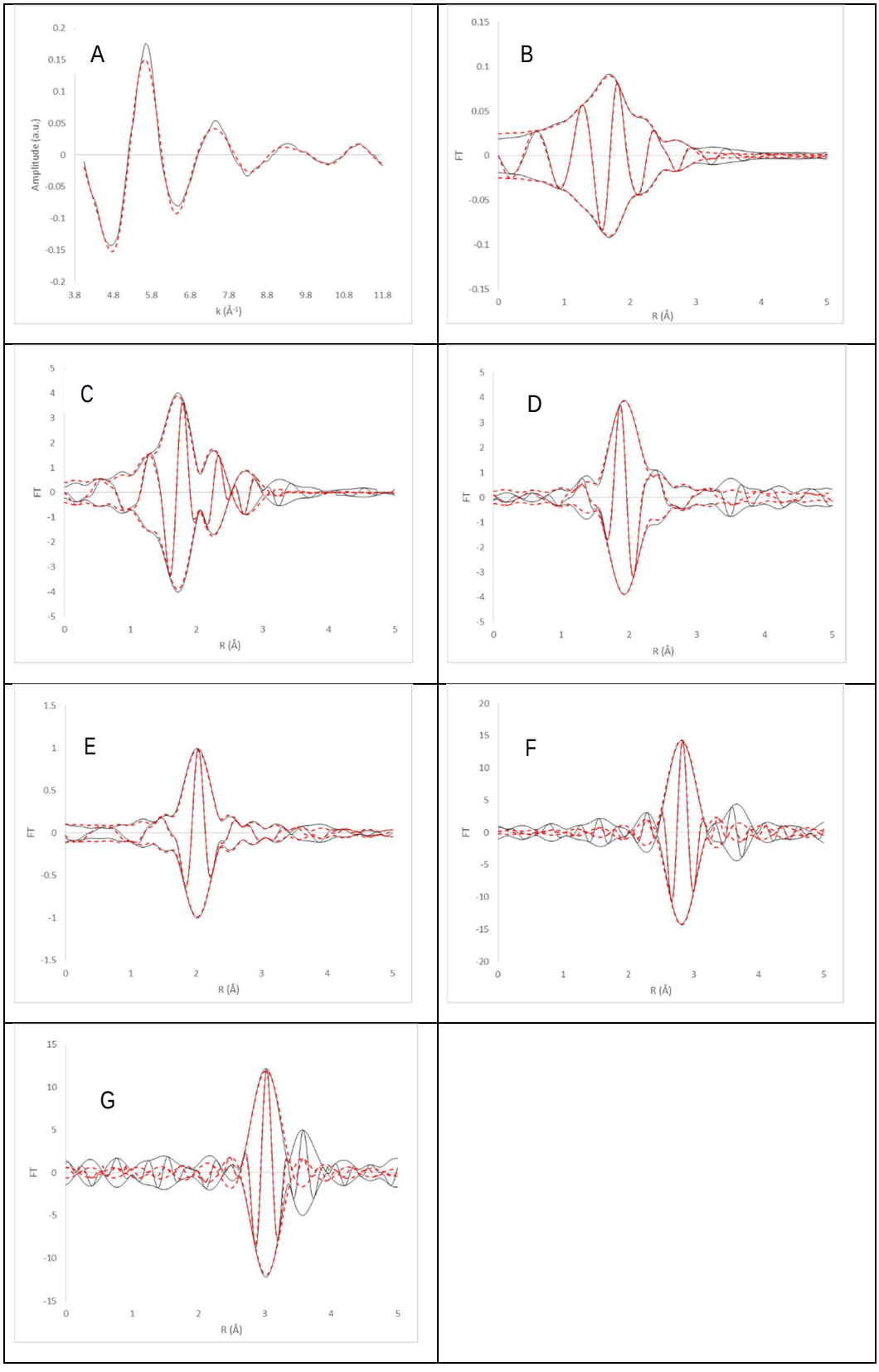

Figure S18. EXAFS data characterizing MgO-supported species formed by adsorption of $Ir(C_2H_4)_2(acac)$ on MgO treated at 1273 K to give an Ir loading of 0.1 wt% and treated in flowing H_2 at 573 K for 250 min. Spectra were recorded with sample in flowing helium at room temperature after sample had been treated in flowing H_2 at 573 K for 232 min. (A) k^1-weighted EXAFS function (solid line) obtained from the data, and the sum of all modeled contributions (dashed line); (B) k^1-weighted imaginary part and magnitude of the Fourier transform of the EXAFS function (solid line), and the sum of all modeled contributions (dashed line); (C) k^3-weighted imaginary part and magnitude of the Fourier transform of the EXAFS function (solid line), and the sum of all modeled contributions (dashed line); (D) k^2-weighted imaginary part and magnitude of the Fourier transform of residual data (solid line) and modeled contribution (dashed line) of the $Ir–O_{support}$ shell; (E) k^1-weighted imaginary part and magnitude of the Fourier transform of residual data (solid line) and modeled contribution (dashed line) of the $Ir–C_{ethylene}$ shell; (F) k^3-weighted imaginary part and magnitude of the Fourier transform of residual data (solid line) and modeled contribution (dashed line) of the $Ir–Mg_{supportShort}$ shell; (G) k^3-weighted imaginary part and magnitude of the Fourier transform of residual data (solid line) and modeled contribution (dashed line) of the $Ir–Mg_{supportLong}$ shell.

Model 2:

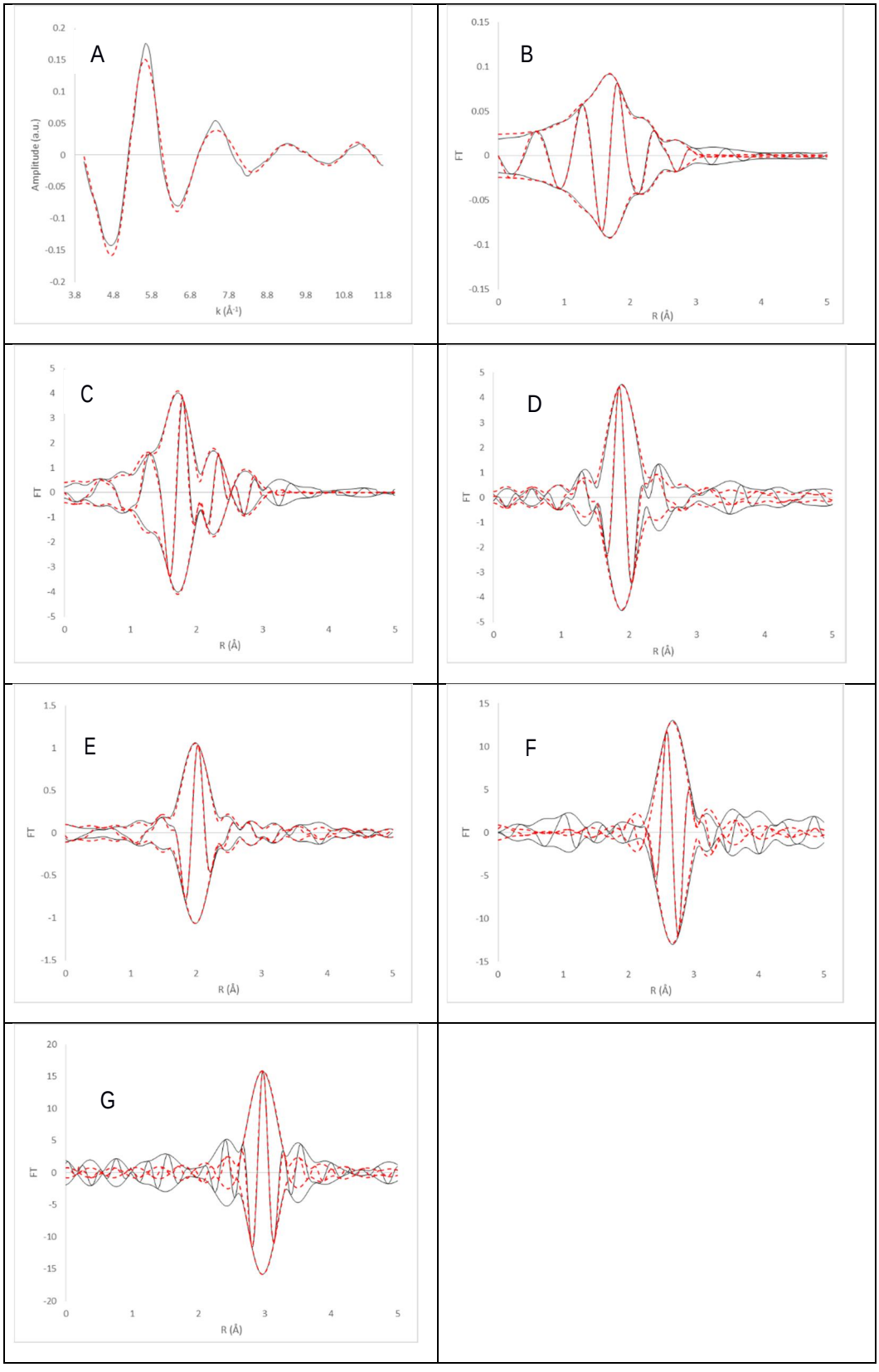

Figure S19. EXAFS data characterizing MgO-supported species formed by adsorption of $Ir(C_2H_4)_2(acac)$ on MgO treated at 1273 K to give an Ir loading of 0.1 wt% and treated in flowing H_2 at 573 K for 250 min. Spectra were recorded with sample in flowing helium at room temperature after sample had been treated in flowing H_2 at 573 K for 232 min. (A) k^1-weighted EXAFS function (solid line) obtained from the data, and the sum of all modeled contributions (dashed line); (B) k^1-weighted imaginary part and magnitude of the Fourier transform of the EXAFS function (solid line), and the sum of all modeled contributions (dashed line); (C) k^3-weighted imaginary part and magnitude of the Fourier transform of the EXAFS function (solid line), and the sum of all modeled contributions (dashed line); (D) k^2-weighted imaginary part and magnitude of the Fourier transform of residual data (solid line) and modeled contribution (dashed line) of the Ir–$O_{support}$ shell; (E) k^1-weighted imaginary part and magnitude of the Fourier transform of residual data (solid line) and modeled contribution (dashed line) of the Ir–$C_{ethylene}$ shell; (F) k^3-weighted imaginary part and magnitude of the Fourier transform of residual data (solid line) and modeled contribution (dashed line) of the Ir–Ir shell; (G) k^3-weighted imaginary part and magnitude of the Fourier transform of residual data (solid line) and modeled contribution (dashed line) of the Ir–$Mg_{support}$ shell.

Model 3:

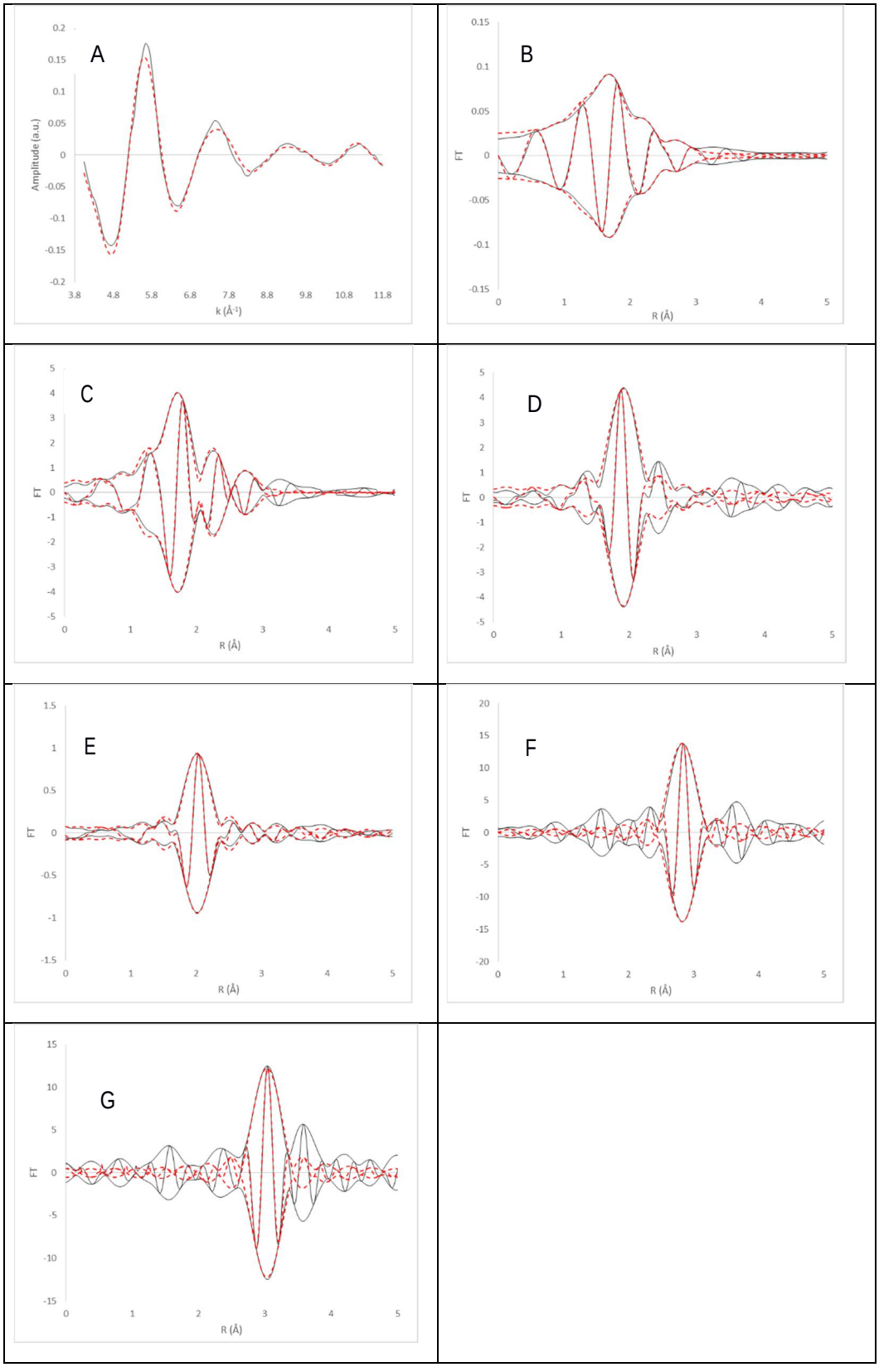

Figure S20. EXAFS data characterizing MgO-supported species formed by adsorption of $Ir(C_2H_4)_2(acac)$ on MgO treated at 1273 K to give an Ir loading of 0.1 wt% ant treated in flowing H_2 at 573 K for 250 min. Spectra were recorded with sample in flowing helium at room temperature after sample had been treated in flowing H_2 at 573 K for 232 min. (A) k^1-weighted EXAFS function (solid line) obtained from the data, and the sum of all modeled contributions (dashed line); (B) k^1-weighted imaginary part and magnitude of the Fourier transform of the EXAFS function (solid line), and the sum of all modeled contributions (dashed line); (C) k^3-weighted imaginary part and magnitude of the Fourier transform of the EXAFS function (solid line), and the sum of all modeled contributions (dashed line); (D) k^2-weighted imaginary part and magnitude of the Fourier transform of residual data (solid line) and modeled contribution (dashed line) of the Ir–$O_{support}$ shell; (E) k^1-weighted imaginary part and magnitude of the Fourier transform of residual data (solid line) and modeled contribution (dashed line) of the Ir–$C_{ethylene}$ shell; (F) k^3-weighted imaginary part and magnitude of the Fourier transform of residual data (solid line) and modeled contribution (dashed line) of the Ir–$Mg_{supportShort}$ shell; (G) k^3-weighted imaginary part and magnitude of the Fourier transform of residual data (solid line) and modeled contribution (dashed line) of the Ir–$Mg_{supportLong}$ shell.

MgO-supported $Ir(C_2H_4)_2$ following exposure to H_2; 0.05 wt % Ir:

Table S7. EXAFS data at the Ir L_{III} edge characterizing MgO-supported species formed by adsorption of $Ir(C_2H_4)_2(acac)$ on MgO treated at 873 K to give an Ir loading of 0.05 wt% and treated with flowing H_2 at 573 K for 250 min; the value of *k* ranged from 4.08 to 13.62 $Å^{-1}$; Error: 0.00163.

Model	Shell	N^a	$10^3 \times \sigma^2$ ($Å^2$)[a]	R (Å)[a]	ΔE_0 (eV)[a]	Goodness of Fit
1*	$Ir–O_{Sup}$	2.8	4.3	2.05	3.1	0.714
	Ir–C	3.8	8.7	1.97	-13.3	
	$Ir–Mg_{Sup}$	2.1	1.4	2.88	-10.3	
	$Ir–Mg_{SupLong}$	3.1	4.0	3.05	-5.1	
	$Ir–O_{SupLong}$	2.1	2.5	3.58	5.1	
2	$Ir–O_{Sup}$	3.0	4.0	2.05	-13.0	6.91
	Ir–C	4.0	7.5	1.97	5.2	
	$Ir–Mg_{Sup}$	2.1	1.3	2.88	-10.0	
	$Ir–Mg_{SupLong}$	3.1	3.8	2.98	-4.9	
	$Ir–O_{SupLong}$	2.1	2.5	3.58	6.6	
3	$Ir–O_{Sup}$	4.0	7.0	1.97	-13.2	0.746
	Ir–C	3.0	3.6	2.06	5.8	
	$Ir–Mg_{Sup}$	1.7	4.6	2.86	-0.4	
	Ir–Ir	1.1	4.8	2.91	-14.7	
	$Ir–O_{SupLong}$	3.0	3.3	3.58	-0.3	

[a]Notation: *N*, coordination number; *R*, distance between absorber and backscatterer atoms; σ^2, Debye-Waller/disorder term; ΔE_0, inner potential correction. Subscripts: Eth, refers to the carbon in the ethylene ligand; Sup, refers to an atom identified on the support; Long refers to the longer of the two Ir–O contributions.

Model 1:

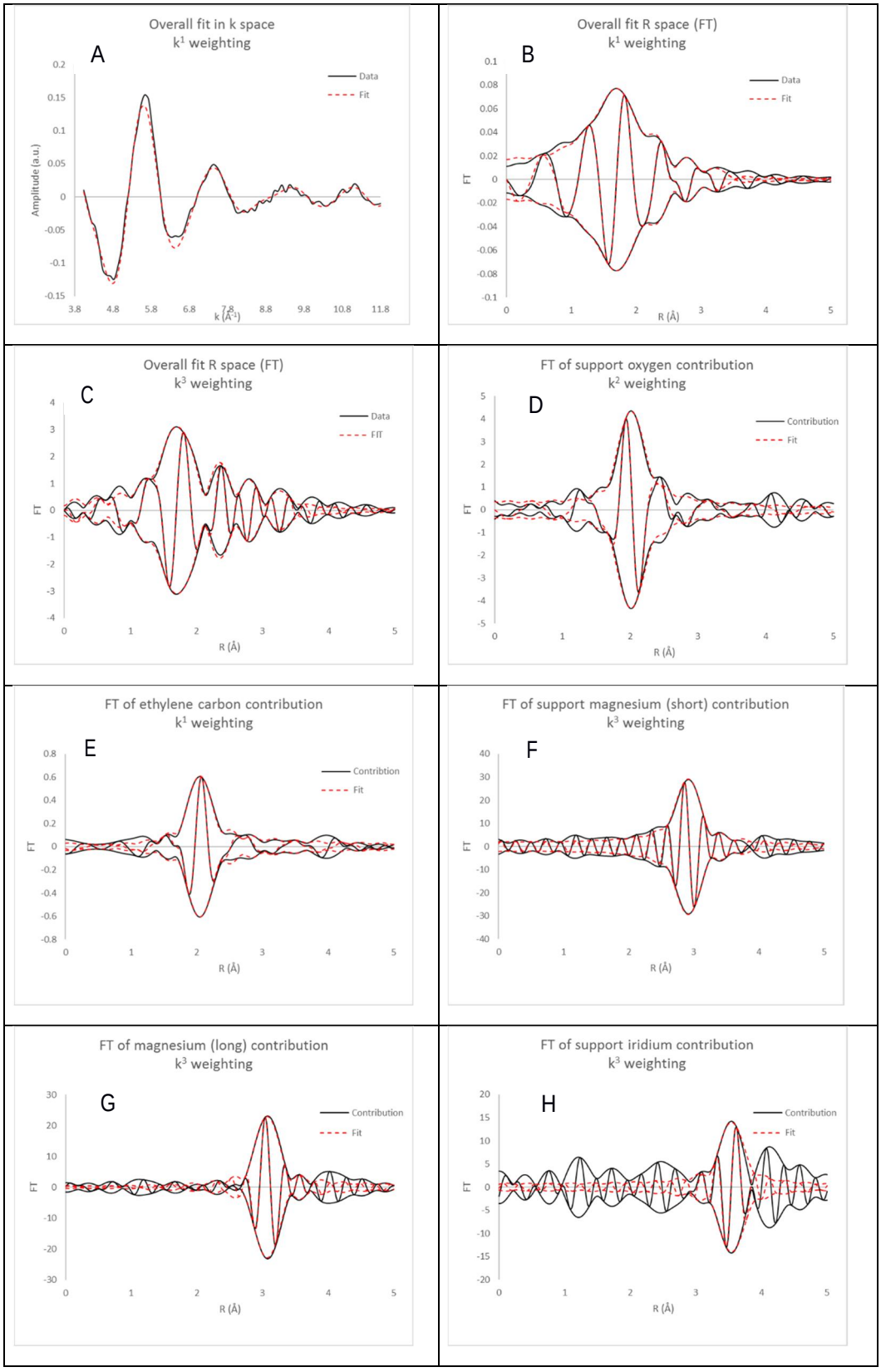
Overall fit in k space
k¹ weighting
A
Data
Fit
Amplitude (a.u.)
k (Å⁻¹)
Overall fit R space (FT)
k¹ weighting
B
Data
Fit
FT
R (Å)
Overall fit R space (FT)
k³ weighting
C
Data
FIT
FT
R (Å)
FT of support oxygen contribution
k² weighting
D
Contribution
Fit
FT
R (Å)
FT of ethylene carbon contribution
k¹ weighting
E
Contribtion
Fit
FT
R (Å)
FT of support magnesium (short) contribution
k³ weighting
F
FT
R (Å)
FT of magnesium (long) contribution
k³ weighting
G
Contribution
Fit
FT
R (Å)
FT of support iridium contribution
k³ weighting
H
Contribution
Fit
FT
R (Å)

Figure S21. EXAFS data characterizing MgO-supported species formed by adsorption of $Ir(C_2H_4)_2(acac)$ on MgO treated at 1273 K to give an Ir loading of 0.05 wt% and treated with flowing H_2 at 573 K for 250 min. Spectra were recorded with sample in flowing helium at room temperature. (A) k^1-weighted EXAFS function (solid line) obtained from the data, and the sum of all modeled contributions (dashed line); (B) k^1-weighted imaginary part and magnitude of the Fourier transform of the EXAFS function (solid line), and the sum of all modeled contributions (dashed line); (C) k^3-weighted imaginary part and magnitude of the Fourier transform of the EXAFS function (solid line), and the sum of all modeled contributions (dashed line); (D) k^2-weighted imaginary part and magnitude of the Fourier transform of residual data (solid line) and modeled contribution (dashed line) of the $Ir–O_{support}$ shell; (E) k^1-weighted imaginary part and magnitude of the Fourier transform of residual data (solid line) and modeled contribution (dashed line) of the $Ir–C_{ethylene}$ shell; (F) k^3-weighted imaginary part and magnitude of the Fourier transform of residual data (solid line) and modeled contribution (dashed line) of the $Ir–Mg_{supportShort}$ shell; (G) k^3-weighted imaginary part and magnitude of the Fourier transform of residual data (solid line) and modeled contribution (dashed line) of the $Ir–Mg_{supportLong}$ shell; (H) k^3-weighted imaginary part and magnitude of the Fourier transform of residual data (solid line) and modeled contribution (dashed line) of the $Ir–O_{supportLong}$ shell.

Model 2:

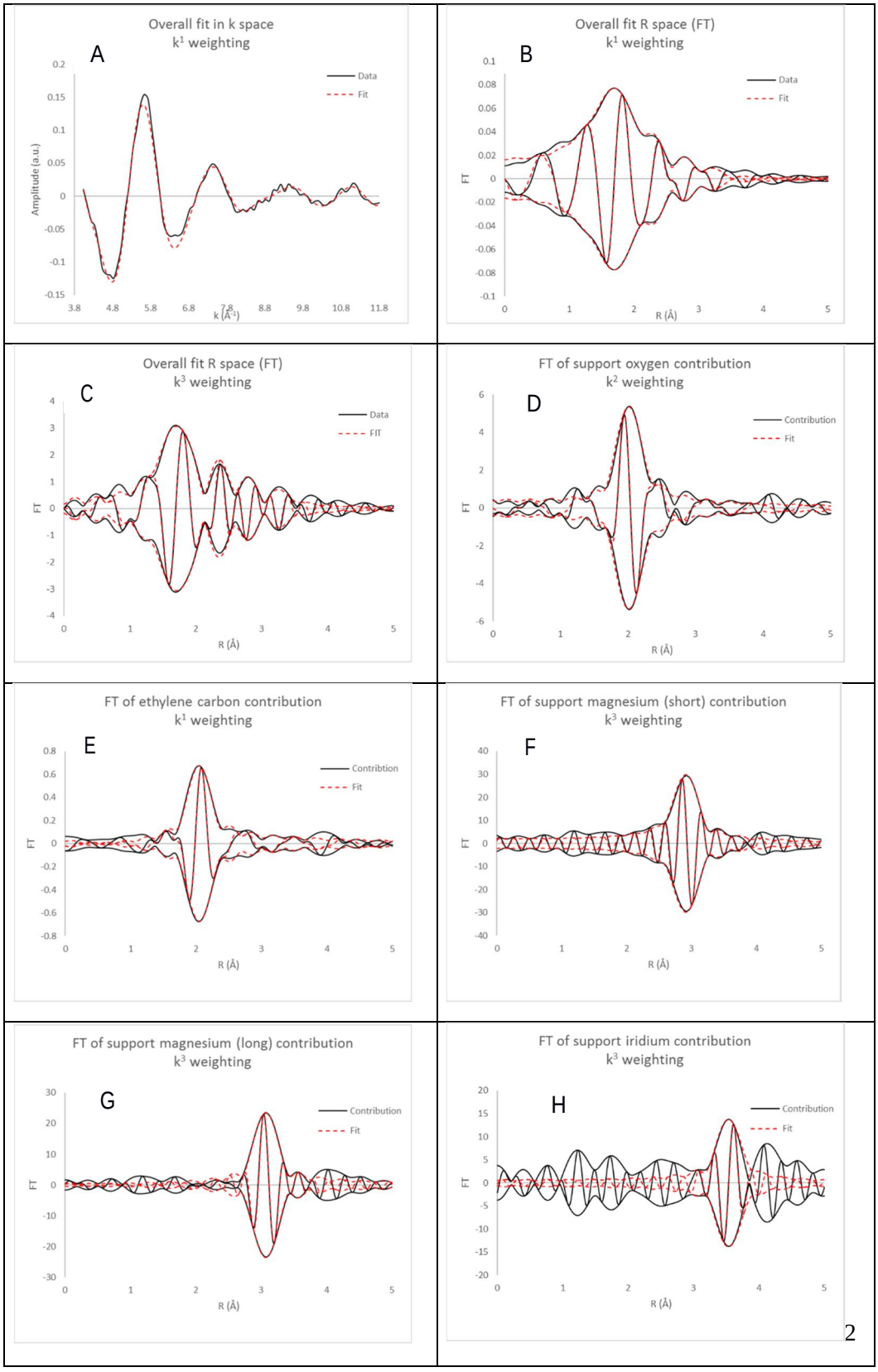
Overall fit in k space
k¹ weighting
A
Data
Fit
Amplitude (a.u.)
k (Å⁻¹)
Overall fit R space (FT)
k¹ weighting
B
Data
Fit
FT
R (Å)
Overall fit R space (FT)
k³ weighting
C
Data
FIT
FT
R (Å)
FT of support oxygen contribution
k² weighting
D
Contribution
Fit
FT
R (Å)
FT of ethylene carbon contribution
k¹ weighting
E
Contribtion
Fit
FT
R (Å)
FT of support magnesium (short) contribution
k³ weighting
F
FT
R (Å)
FT of support magnesium (long) contribution
k³ weighting
G
Contribution
Fit
FT
R (Å)
FT of support iridium contribution
k³ weighting
H
Contribution
Fit
FT
R (Å)

2

Figure S22. EXAFS data characterizing MgO-supported iridium species formed by adsorption of $Ir(C_2H_4)_2(acac)$ on MgO treated at 1273 K to give an Ir loading of 0.05 wt% and treated with flowing H_2 at 573 K for 250 min. Spectra were recorded with sample in flowing helium at room temperature. (A) k^1-weighted EXAFS function (solid line) obtained from the data, and the sum of all modeled contributions (dashed line); (B) k^1-weighted imaginary part and magnitude of the Fourier transform of the EXAFS function (solid line), and the sum of all modeled contributions (dashed line); (C) k^3-weighted imaginary part and magnitude of the Fourier transform of the EXAFS function (solid line), and the sum of all modeled contributions (dashed line); (D) k^2-weighted imaginary part and magnitude of the Fourier transform of residual data (solid line) and modeled contribution (dashed line) of the $Ir–O_{support}$ shell; (E) k^1-weighted imaginary part and magnitude of the Fourier transform of residual data (solid line) and modeled contribution (dashed line) of the $Ir–C_{ethylene}$ shell; (F) k^3-weighted imaginary part and magnitude of the Fourier transform of residual data (solid line) and modeled contribution (dashed line) of the $Ir–Mg_{supportShort}$ shell; (G) k^3-weighted imaginary part and magnitude of the Fourier transform of residual data (solid line) and modeled contribution (dashed line) of the $Ir–Mg_{supportLong}$ shell; (H) k^3-weighted imaginary part and magnitude of the Fourier transform of residual data (solid line) and modeled contribution (dashed line) of the $Ir–O_{supportLong}$ shell.

Model 3:

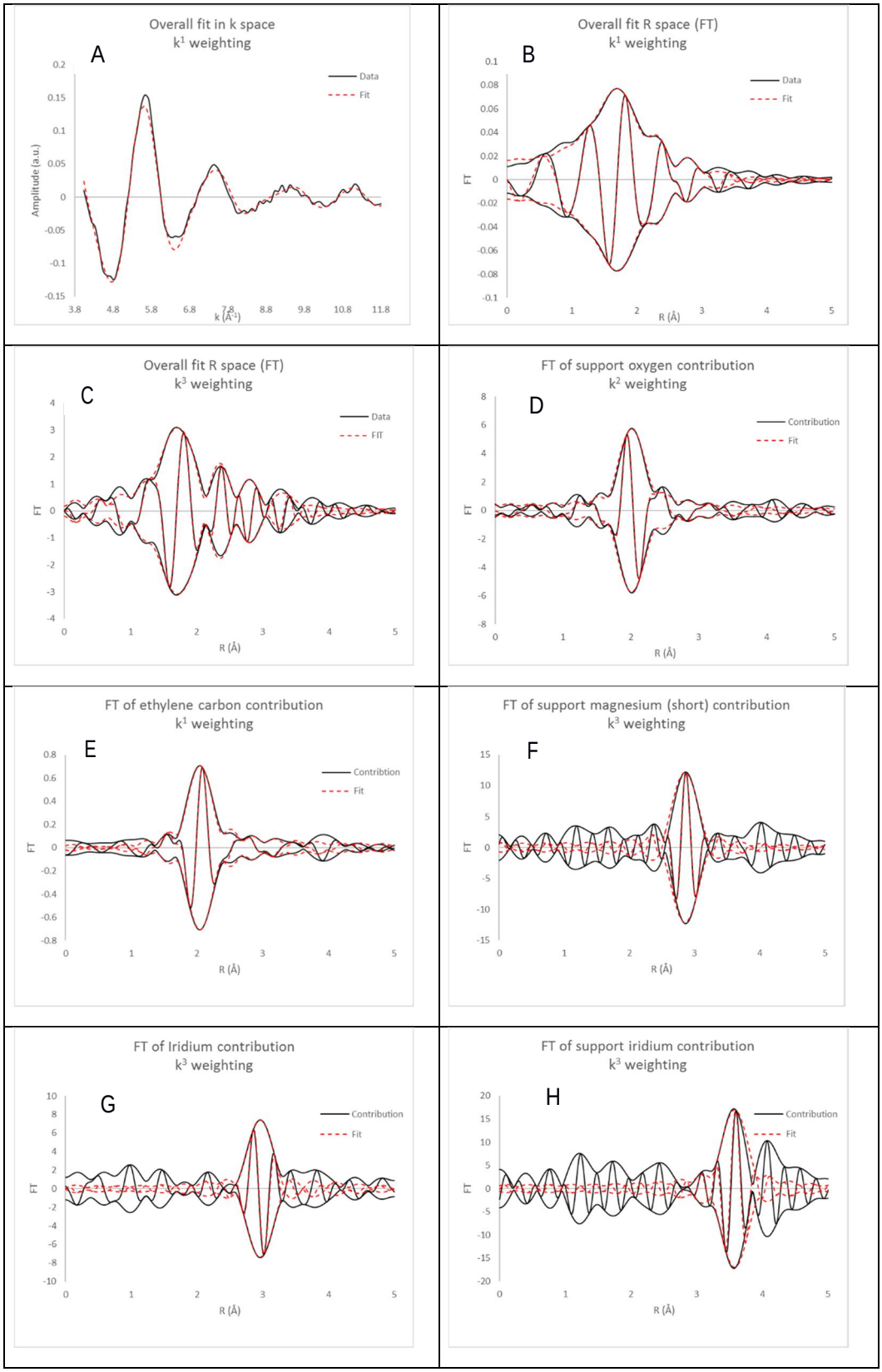
Overall fit in k space
k¹ weighting
A
Data
Fit
Amplitude (a.u.)
k (Å⁻¹)
Overall fit R space (FT)
k¹ weighting
B
Data
Fit
FT
R (Å)
Overall fit R space (FT)
k³ weighting
C
Data
FIT
FT
R (Å)
FT of support oxygen contribution
k² weighting
D
Contribution
Fit
FT
R (Å)
FT of ethylene carbon contribution
k¹ weighting
E
Contribtion
Fit
FT
R (Å)
FT of support magnesium (short) contribution
k³ weighting
F
FT
R (Å)
FT of Iridium contribution
k³ weighting
G
Contribution
Fit
FT
R (Å)
FT of support iridium contribution
k³ weighting
H
Contribution
Fit
FT
R (Å)

Figure S23. EXAFS data characterizing MgO-supported species formed by adsorption of $Ir(C_2H_4)_2(acac)$ on MgO treated at 1273 K to give an Ir loading of 1.0 wt% and treated with flowing H_2 at 573 K for 250 min. Spectra were recorded with sample in flowing helium at room temperature. (A) k^1-weighted EXAFS function (solid line) obtained from the data, and the sum of all modeled contributions (dashed line); (B) k^1-weighted imaginary part and magnitude of the Fourier transform of the EXAFS function (solid line), and the sum of all modeled contributions (dashed line); (C) k^3-weighted imaginary part and magnitude of the Fourier transform of the EXAFS function (solid line), and the sum of all modeled contributions (dashed line); (D) k^2-weighted imaginary part and magnitude of the Fourier transform of residual data (solid line) and modeled contribution (dashed line) of the $Ir–O_{support}$ shell; (E) k^1-weighted imaginary part and magnitude of the Fourier transform of residual data (solid line) and modeled contribution (dashed line) of the $Ir–C_{ethylene}$ shell; (F) k^3-weighted imaginary part and magnitude of the Fourier transform of residual data (solid line) and modeled contribution (dashed line) of the $Ir–Mg_{support}$ shell; (G) k^3-weighted imaginary part and magnitude of the Fourier transform of residual data (solid line) and modeled contribution (dashed line) of the Ir–Ir shell; (H) k^3-weighted imaginary part and magnitude of the Fourier transform of residual data (solid line) and modeled contribution (dashed line) of the $Ir–O_{supportLong}$ shell.

MgO-supported $Ir(C_2H_4)_2$; following exposure to H_2; 0.01 wt % Ir:

Table S8. EXAFS models representing the data at the Ir L_{III} edge characterizing MgO-supported species formed by adsorption of $Ir(C_2H_4)_2$(acac) on MgO treated at 1273 K to give an Ir loading of 0.01 wt% and treated with flowing H_2 at 573 K for 250 min. K from 3.94 to 11.56 $Å^{-1}$; Error = 0.00104; *Denotes best-fit model.

Model	Shell	N^a	$10^3 \times \sigma^2$ ($Å^2$)[a]	R (Å) [a]	ΔE_0 (eV) [a]	Goodness of Fit
1	Ir-O_{Sup}	3.1	2.6	2.03	-13.9	4.88
	Ir-C	2.1	3.4	2.12	10.2	
	Ir-Mg_{Sup}	2.0	7.0	3.12	-14.3	
2*	Ir-O_{Sup}	3.3	2.6	2.01	-17.6	1.70
	Ir-C	4.1	3.8	2.10	3.6	
	Ir-Mg_{Sup}	3.0	10.1	3.13	-14.9	
3	Ir-O_{Sup}	2.0	6.2	2.00	5.0	2.12
	Ir-C	2.0	8.9	2.06	-18.5	
	Ir-Mg_{Sup}	2.0	5.4	3.09	-11.3	
	Ir-Ir	1.0	10.5	2.68	-13.9	

[a]Notation: N, coordination number; R, distance between absorber and backscatterer atoms; σ^2, Debye-Waller/disorder term; ΔE_0, inner potential correction. Subscripts: Sup, refers to an atom that is part of the support.

Model 1:

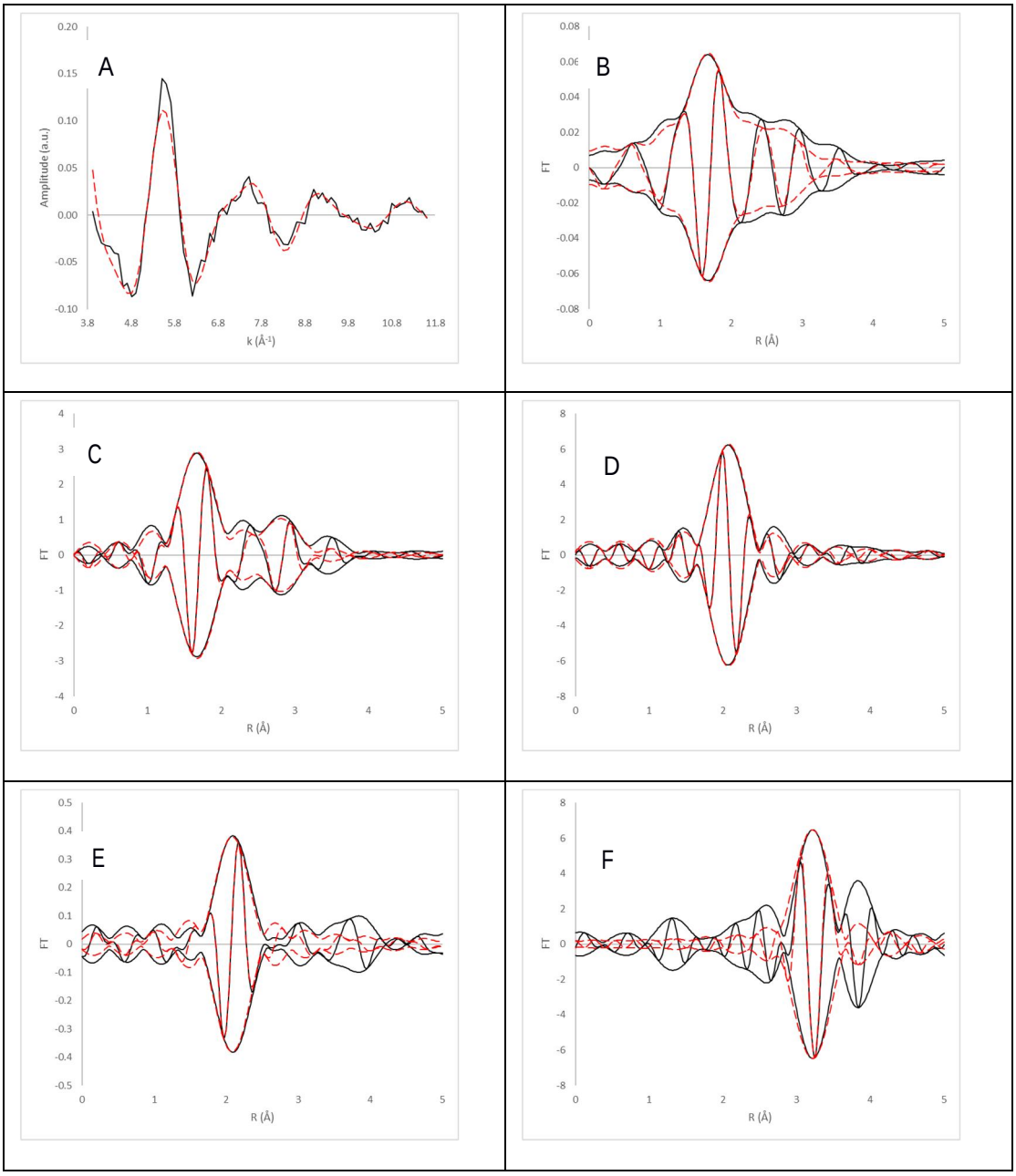

Figure S24. EXAFS Model 1 representing the data characterizing MgO-supported species formed by adsorption of $Ir(C_2H_4)_2(acac)$ on MgO treated at 1273 K to give an Ir loading of 0.01 wt% and treatment with flowing H_2 at 573 K for 250 min. Spectra were recorded with sample in flowing helium at room temperature. (A) k^1-weighted EXAFS function (solid line) obtained from the data, and the sum of all modeled contributions (dashed line); (B) k^1-weighted imaginary part and magnitude of the Fourier transform of the EXAFS function (solid line), and the sum of all modeled contributions (dashed line); (C) k^3-weighted imaginary part and magnitude of the Fourier transform of the EXAFS function (solid line), and the sum of all modeled contributions (dashed line); (D) k^2-weighted imaginary part and magnitude of the Fourier transform of residual data (solid line) and modeled contribution (dashed line) of the $Ir–O_{support}$ shell; (E) k^1-weighted imaginary part and magnitude of the Fourier transform of residual data (solid line) and modeled contribution (dashed line) of the $Ir–C_{ethylene}$ shell; (F) k^3-weighted imaginary part and magnitude of the Fourier transform of residual data (solid line) and modeled contribution (dashed line) of the $Ir–Mg_{support}$ shell.

Model 2:

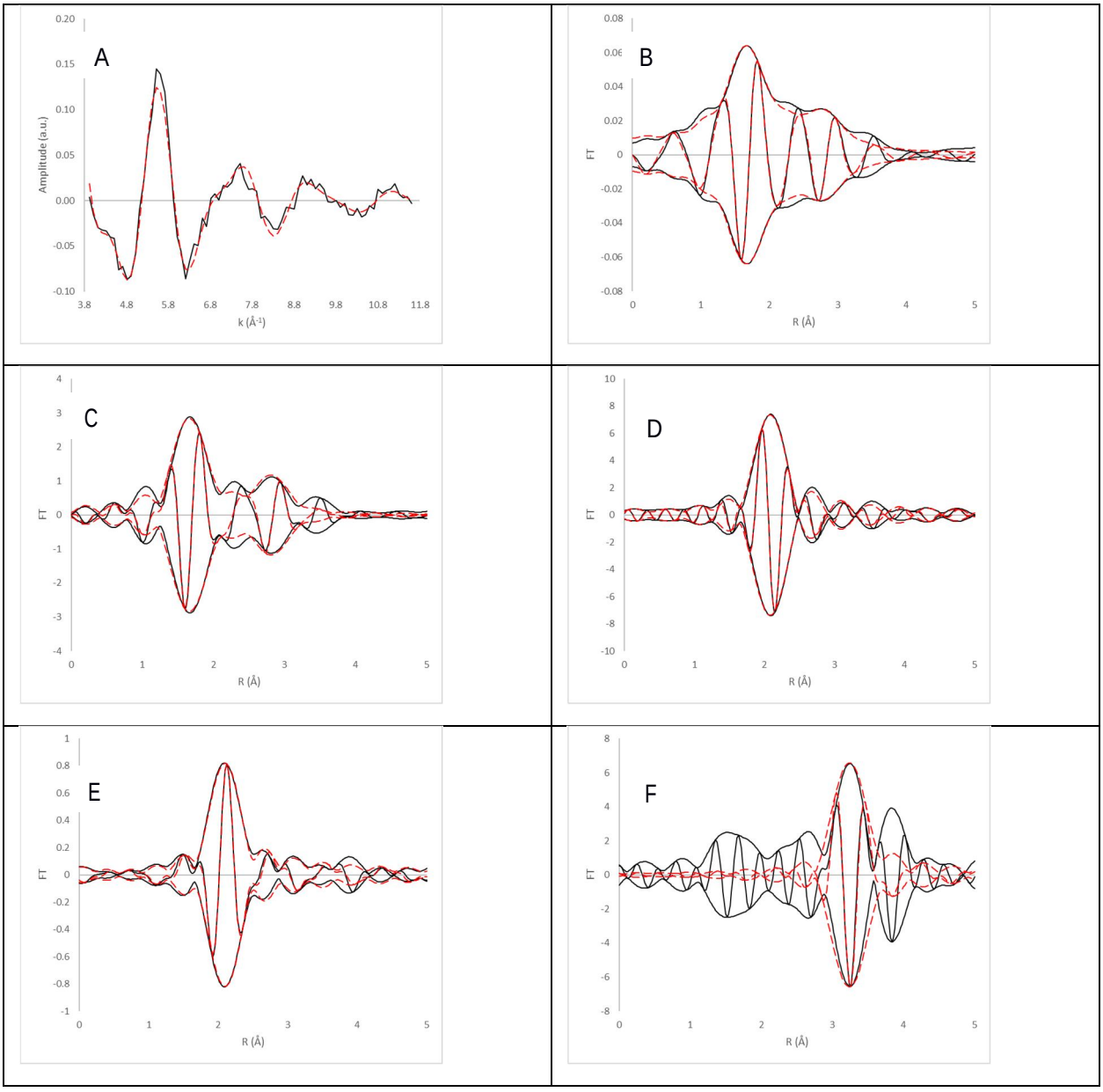

Figure S25. EXAFS Model 2 representing the data characterizing MgO-supported species formed by adsorption of $Ir(C_2H_4)_2(acac)$ on MgO treated at 1273 K to give an Ir loading of 0.01 wt% and treatment with flowing H_2 at 573 K for 250 min. Spectra were recorded with sample in flowing helium at room temperature. (A) k^1-weighted EXAFS function (solid line) obtained from the data, and the sum of all modeled contributions (dashed line); (B) k^1-weighted imaginary part and magnitude of the Fourier transform of the EXAFS function (solid line), and the sum of all modeled contributions (dashed line); (C) k^3-weighted imaginary part and magnitude of the Fourier transform of the EXAFS function (solid line), and the sum of all modeled contributions (dashed line); (D) k^2-weighted imaginary part and magnitude of the Fourier transform of residual data (solid line) and modeled contribution (dashed line) of the $Ir–O_{support}$ shell; (E) k^1-weighted imaginary part and magnitude of the Fourier transform of residual data (solid line) and modeled contribution (dashed line) of the $Ir–C_{ethylene}$ shell; (F) k^3-weighted imaginary part and magnitude of the Fourier transform of residual data (solid line) and modeled contribution (dashed line) of the $Ir–Mg_{support}$ shell.

Model 3:

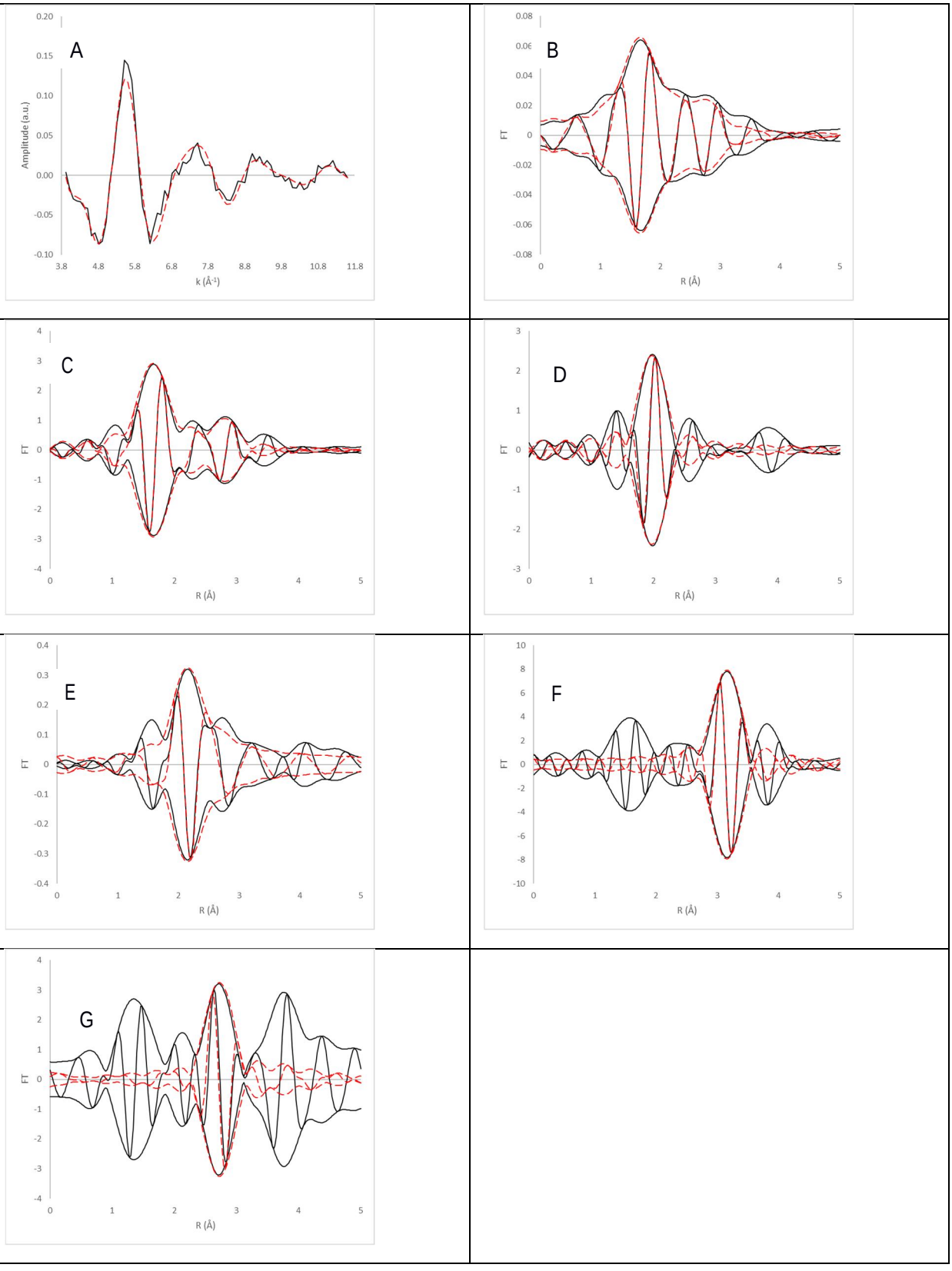

Figure S26. EXAFS Model 3 representing the data characterizing MgO-supported species formed by adsorption of $Ir(C_2H_4)_2(acac)$ on MgO treated at 1273 K to give an Ir loading of 0.01 wt% and treatment with flowing H_2 at 573 K for 250 min. Spectra were recorded with sample in flowing helium at room temperature. (A) k^1-weighted EXAFS function (solid line) obtained from the data, and the sum of all modeled contributions (dashed line); (B) k^1-weighted imaginary part and magnitude of the Fourier transform of the EXAFS function (solid line), and the sum of all modeled contributions (dashed line); (C) k^3-weighted imaginary part and magnitude of the Fourier transform of the EXAFS function (solid line), and the sum of all modeled contributions (dashed line); (D) k^2-weighted imaginary part and magnitude of the Fourier transform of residual data (solid line) and modeled contribution (dashed line) of the $Ir–O_{support}$ shell; (E) k^1-weighted imaginary part and magnitude of the Fourier transform of residual data (solid line) and modeled contribution (dashed line) of the $Ir–C_{ethylene}$ shell; (F) k^3-weighted imaginary part and magnitude of the Fourier transform of residual data (solid line) and modeled contribution (dashed line) of the $Ir–Mg_{support}$ shell; (G) k^3-weighted imaginary part and magnitude of the Fourier transform of residual data (solid line) and modeled contribution (dashed line) of the Ir–Ir shell.

Additional Computational Details and Results

A $(MgO)_{16}$ model that was shown to work well for Os binding to MgO was used to model the defect-free (100) for Ir bridging to two O atoms. The same model minus an Mg was used to model the corner binding site on the (100) surface, $(Mg_{15}O_{16})^{2-}$. A $(MgO)_{25}$ cluster was used to model Ir binding to a single O site. To model a defected (100) surface with loss of an Mg atom, a larger $(Mg_{24}O_{25})^{2-}$ cluster was used. The (110) surface was modeled by a $(MgO)_{20}$ cluster and the (111) surface by a $(Mg_{14}O_{15})^{2-}$ cluster. The model of the (111) surface reconstructed readily to the (100) surface, but we were able to optimize a structure. We examined various formal charge states for the Ir as well.

A natural population analysis (NPA) based on the natural bond orbitals (NBOs)[1,2] was performed by using the NBO6[3,4] code. The orbital energies were calculated at the Douglas-Kroll-Hess second order scalar relativistic level[5,6,7] using polarized double-ζ-DK basis sets.[8,9]

The orbital energies, notably the 2p of the Ir, were calculated at the DKH level. The predicted Ir 2p positions are < 1% too positive, in satisfactory agreement considering the simplicity of the calculation. We predict a blue shift as CO is substituted for C_2H_4, consistent with experiment, but the predicted 2p orbital energy shifts are much smaller than those observed. A natural population analysis (NPA) based on the natural bond orbitals (NBOs) was performed. The L2Ir group charges show very little change on substitution of CO for C_2H_4, consistent with the small changes in the Ir 2p orbital energies. Thus, as shown by the predicted small changes in most cases for the Ir–O bond lengths, the interaction of Ir with the MgO does not change markedly when CO is substituted for C_2H_4.

Table S9. MgO Clusters with 2 CO. scaled ν in cm^{-1} with IR intensity in parentheses in km/mol. Bond distances *R* in Å. NBO charges in e. 2s and 2p Ir orbital energies in eV.

Property	$^1[(MgO)_{16}Ir(I)(CO)_2]^+$ 100 2O bridge	$^2(MgO)_{16}Ir(0)(CO)_2$ 100 2O bridge	$^1[Mg_{15}O_{16}Ir(III)(CO)_2]^+$ 100 corner	$^2Mg_{15}O_{16}Ir(II)(CO)_2$ 100 corner	$^1[Mg_{15}O_{16}Ir(I)(CO)_2]^-$ 100 corner
ν(CO)	asym 2047(1042) sym 2111(894)	asym 2016(933) sym 2086(1011)	asym 2108(827)/ sym 2161(848)/	asym 2028(1110) sym 2094(1094)	asym 1942(1389) sym 2027(1155)
R(Ir-C)	1.850, 1.850	1.844, 1.844	1.911, 1.893	1.868, 1.855	1.830, 1.822
R(C-O)	1.152, 1.152	1.156, 1.156	1.143, 1.144	1.155, 1.154	1.167, 1.169
R(Ir-O)	2.106, 2.106	2.093, 2.093	(1) 1.982, (2) 1.979, (3) 2.024	(1) 2.270, (2) 2.037, (3) 2.082	(1) 3.309, (2) 2.053, (3) 2.092
R(Ir-Mg)	2.723, 2.724	2.762, 2.765	3.023, 3.055	3.052, 3.017	3.386, 2.879, 3.447
NBO Ir	0.14	0.19	1.02	0.76	0.31
NBO CO	0.17	0.14	0.18, 0.22	0.09, 0.14	0.06, 0.01
NBO C	0.62	0.62	0.59, 0.62	0.58, 0.62	0.62, 0.58
NBO O	-0.45	-0.48	-0.41, -0.41	-0.49, -0.48	-0.56, -0.57
2s	-13253.65	-13251.05	-13255.87	-13251.16	-13246.86
2p	-11131.77	-11129.17	-11134.02	-11129.27	-11124.96

Property	$^1[Mg_{24}O_{25}Ir(III)(CO)_2]^+$ 100 Mg defect	$^2Mg_{24}O_{25}Ir(II)(CO)_2$ 100 Mg defect	$^1[Mg_{24}O_{25}Ir(I)(CO)_2]^-$ 100 Mg defect	$^1[(MgO)_{25}Ir(I)(CO)_2]^+$ 100 on O	$^2(MgO)_{25}Ir(0)(CO)_2$ 100 on O
ν(CO)	asym 2078(676) sym 2071(704)	asym 2010(875) sym 2081(902)	asym 1957(1070) sym 2042(873)	asym 2055(944) sym 2113(911)	asym 1959(1150) sym 2017(1275)
R(Ir-C)	1.867, 1.867	1.835, 1.835	1.805, 1.805	1.829, 1.829	1.851, 1.841
R(C-O)	1.147, 1.147	1.156, 1.156	1.166, 1.166	1.152, 1.152	1.165, 1.163
R(Ir-O)	(1) 2.105, (2) 2.078 (3) 4.135	(1) 2.232, (2) 2.308, (3) 3.953	(1) 2.297, (2) 2.622 (3) 4.025	1.920	2.107
R(Ir-Mg)	3.016	3.081	3.128, 3.117	3.328	3.138
NBO Ir	0.99	0.81	0.42	0.24	-0.02
NBO CO	0.24	0.13	0.05	0.18	-0.09, 0.02
NBO C	0.68	0.62	0.60	0.62	0.42, 0.49
NBO O	-0.43	-0.49	-0.55	-0.44	-0.51, -0.51
2s	-13255.40	-13251.89	-13248.36	-13254.46	-13250.09

2p	-11133.58	-11130.05	-11126. 55	-11132.61	-11128.23

Property	$^{1}[(MgO)_{20}Ir(I)(CO)_2]^{+}$ 110	$^{2}(MgO)_{20}Ir(0)(CO)_2$ 110	$^{2}[Mg_{14}O_{15}Ir(0)(CO)_2]^{2-}$ 111	$^{1}[Mg_{14}O_{15}Ir(I)(CO)_2]^{-}$ 111	$^{1}[Mg_{14}O_{15}Ir(III)(CO)_2]^{+}$ 111
ν(CO)	asym 2049(970) sym 2114(954)	asym 1957(1084) sym 2014(1277)	asym 1971(820) sym 2037(1777)	asym 2032(726) sym 2095(1433)	asym 2094(815) sym 2164(810)
R(Ir-C)	1.851, 1.853	1.846, 1.846	1.849, 1.850	1.893, 1.939	1.911, 1.899
R(C-O)	1.152, 1.151	1.165, 1.165	1.163, 1.160	1.155, 1.148	1.141, 1.147
R(Ir-O)	2.089, 2.089	2.174, 2.174	(1) 2.052, (2) 2.078, (3) 2.182	(1) 1.935, (2) 2.021, (3) 1.986	(1) 1.968 (2) 2.010 (3) 1.973
R(Ir-Mg)	3.188	3.037			
NBO Ir	0.13	-0.05	0.72	1.05	1.01
NBO CO	0.17, 0.18	-0.05	0.04, 0.09	0.08, 0.18	0.17, 0.13
NBO C	0.62, 0.63	0.46	0.58, 0.62	0.58, 0.65	0.63, 0.56
NBO O	-0.45, -0.45	-0.51	-0.54, -0.53	-0.50, -0.46	-0.40, -0.43
2s	-13253.62	-13250.51	-13245.99	-13249.85	-13255.65
2p	-11131.76	-11128.67	-11124.12	-11128.00	-11133.78

Table S10. MgO clusters with 2 C_2H_4 ; scaled ν in cm^{-1} with IR intensity in parentheses in km/mol. Bond distances *R* in Å. NBO charges in e. 2s and 2p Ir orbital energies in eV.

Property	$^1[(MgO)_{16}Ir(I)(C_2H_4)_2]^+$ 100 2O bridge	$^2(MgO)_{16}Ir(0)(C_2H_4)_2$ 100 2O bridge	$^1[Mg_{15}O_{16}Ir(III)(C_2H_4)_2]^+$ 100 corner	$^2Mg_{15}O_{16}Ir(II)(C_2H_4)_2$ 100 corner	$^1[Mg_{15}O_{16}Ir(I)(C_2H_4)_2]^-$ 100 corner
ν(C-H)	2971(44) 2971 (7) 2982(1) 2982(23) 3054(1) 3055(2) 3074(11) 3075(39)	2965(37) 2966(17) 2976(13) 2979(20) 3042 (2) 3044(3) 3065(17) 3066(56)	2991 (4) 3002(6) 3009 (3) 3011 (5) 3082(3) 3091(4) 3109(6) 3111(3)	2977(24) 2980(33) 2990(20) 2990(18) 3059(10) 3062(0) 3081(30) 3087(16)	3110(73) 3119(52) 3130(47) 3131(59) 3185(15) 3201(3) 3216(68) 3223(61)
R(Ir-C)	2.111, 2.110, 2.111, 2.110	2.104, 2.103, 2.105, 2.104	2.186, 2.175, 2.162, 2.181	2.110, 2.111, 2.112, 2.119	2.085, 2.082, 2.091, 2.088
R(C-C)	1.413, 1.413	1.416, 1.416	1.392, 1.397	1.418, 1.419	1.427, 1.428
R(C-H)	1.085, 1.088, 1.087, 1.088 1.087, 1.088, 1.085, 1.088	1.086, 1.088, 1.087, 1.088 1.087, 1.088, 1.086, 1.088	1.084, 1.086, 1.087, 1.084 1.084, 1.086, 1.086, 1.088	1.087, 1.086, 1.086,1.086 1.086, 1.087, 1.085, 1.087	1.084, 1.086, 1.087, 1.084 1.084, 1.086, 1.086, 1.088
R(Ir-O)	2.132, 2.131	2.110, 2.113	(1) 1.999, (2) 1.996 (3) 2.027	(1) 2.244, (2) 2.056 (3) 2.098	(1) 3.276 (2) 2.071 (3) 2.104
R(Ir-Mg)	2.699, 2.699	2.738, 2.743	3.041, 3.045	3.048, 2.988	3.350, 2.831, 3.428
NBO Ir	0.54	0.60	1.29	1.16	0.77
NBO C_2H_4	-0.03	-0.07	0.10, 0.03	-0.06, -0.11	-0.16, -0.22
NBO C	-0.41, -0.41	-0.42, -0.42	-0.39, -0.40, -0.44, -0.40	-0.44, -0.42, -0.45, -0.45	-0.44, -0.45, -0.47, -0.46
NBO H	0.21, 0.18, 0.20, 0.20	0.19, 0.20, 0.19, 0.19	0.21, 0.24, 0.21, 0.22 0.21, 0.23, 0.22, 0.21	0.19, 0.20, 0.19, 0.23 0.20, 0.19, 0.19, 0.21	0.17, 0.20, 0.17, 0.19 0.17, 0.18, 0.18, 0.19
2s	-13252.62	-13250.04	-13254.84	-13250.42	-13245.94
2p	-11130.62	-11128.04	-11132.84	-11128.41	-11123.93

Property	$^{1}[Mg_{24}O_{25}Ir(III)(C_2H_4)_2]^{+}$ 100 Mg defect	$^{2}Mg_{24}O_{25}Ir(II)(C_2H_4)_2$ 100 Mg defect	$^{2}(MgO)_{25}Ir(0)(C_2H_4)_2$ 100 on O
ν(C-H)	2985(0) 2987(11) 2993(0) 2995(2) 3083(0) 3090(3) 3101(0) 3109(11)	2974(0) 2976(40) 2983(12) 2985 (4) 3060(0) 3066 (3) 3078(5) 3085(49)	2943(11) 2944(13) 2969(25) 2973 (26) 3036(4) 3039(3) 3054(6) 3057(22)
R(Ir-C)	2.164	2.113	2.085, 2.126, 2.082, 2.125
R(C-C)	1.400	1.425	1.439, 1.440
R(C-H)	1.087, 1.082,1.807, 1.082 1.082, 1.087, 1.082, 1.087	1.084, 1.088, 1.084, 1.088 1.084, 1.088, 1.084, 1.088	1.087, 1.092, 1.086, 1.089 1.087, 1.089, 1.087, 1.092
R(Ir-O)	(1) 2.115 (2) 2.096 (3) 4.179	(1) 2.243 (2) 2.327 (3) 3.901	2.234
R(Ir-Mg)	3.028	3.079	3.140
NBO Ir	1.29	1.18	0.49
NBO C_2H_4	0.06	-0.09	-0.31
NBO C	-0.38, -0.38	-0.43, -0.43	-0.63, -0.49
NBO H	0.19, 0.21, 0.19, 0.21	0.18, 0.20, 0.18, 0.20	0.21, 0.19, 0.20, 0.20
2s	-13254.35	-13251.17	-13249.41
2p	-11132.34	-11129.15	-11127.38

Property	$^{1}[(MgO)_{20}Ir(I)(C_2H_4)_2]^{+}$ 110	$^{2}(MgO)_{20}Ir(0)(C_2H_4)_2$ 110	$^{2}[Mg_{14}O_{15}Ir(0)(C_2H_4)_2]^{2-}$ 111	$^{1}[Mg_{14}O_{15}Ir(I)(C_2H_4)_2]^{-}$ 111	$^{1}[Mg_{14}O_{15}Ir(III)(C_2H_4)_2]^{+}$
ν(C-H)	2954(23) 2961(28) 2970(21) 2976(16) 3057(0) 3060(1) 3075(17) 3080(23)	2899(84) 2900(21) 2941(62) 2941(19) 3012(14) 3014(31) 3056(32) 3056(6)	2848(144) 2954 (20) 2957(64) 2968(58) 3011(34) 3034 (6) 3046 (24) 3056(57)	2909 (86) 2923(34) 2962(92) 2970(61) 3015(73) 3036(10) 3048(27) 3058 (33)	2991(14) 2992(20) (300713) 3033(4) 3073(11) 3084(1) 3105(14) 3127(3)
R(Ir-C)	2.122, 2.120, 2.122, 2.122	2.074, 2.137, 2.074, 2.137	2.111, 2.093, 2.114, 2.129	2.102, 2.097, 2.106, 2.092	2.138, 2.133, 2.155, 2.163
R(C-C)	1.412, 1.412	1.447, 1.447	1.425, 1.416	1.423, 1.426	1.400, 1.398
R(C-H)	1.084, 1.089, 1.085, 1.090 1.084, 1.089, 1.085, 1.091	1.085, 1.096, 1.089, 1.091 1.089, 1.091, 1.085, 1.096	1.088, 1.088, 1.089, 1.088 1.089, 1.088, 1.089, 1.097	1.086, 1.092, 1.088, 1.087 1.089, 1.093, 1.088, 1.088	1.083, 1.085, 1.087, 1.084 1.083, 1.083, 1.087, 1.086
R(Ir-O)	2.099, 2.100	2.199, 2.199	2.033, 2.056, 2.285	2.056, 2.073, 2.302	(1) 2.040 (2) 2.168 (3) 2.009 (4) 2.130
R(Ir-Mg)	3.118	3.013			
NBO Ir	0.54	0.42	1.21	1.09	1.25
NBO C_2H_4	-0.04, -0.05	-0.36, -0.36	-0.19, -0.08	-0.18, -0.12	0.10, 0.09
NBO C	-0.41, -0.42, -0.41, -0.42	-0.51, -0.60, -0.60, -0.51	-0.46, -0.48, -0.46, -0.43	-0.45, -0.47, -0.44, -0.47	-0.35, -0.38, -0.34, -0.42
NBO H	0.19, 0.21, 0.21, 0.18 0.21, 0.19, 0.21, 0.18	0.18, 0.19, 0.16, 0.21 0.21, 0.16, 0.19, 0.18	0.20, 0.18, 0.19, 0.18 0.17, 0.20, 0.17, 0.27	0.20, 0.18, 0.17, 0.19 0.18, 0.19, 0.17, 0.25	0.20, 0.21, 0.20, 0.22 0.22, 0.23, 0.21, 0.20
2s	-13252.86	-13249.46	-13245.09	-13246.88	-13254.02
2p	-11130.88	-11127.50	-11123.08	-11124.87	-11132.03

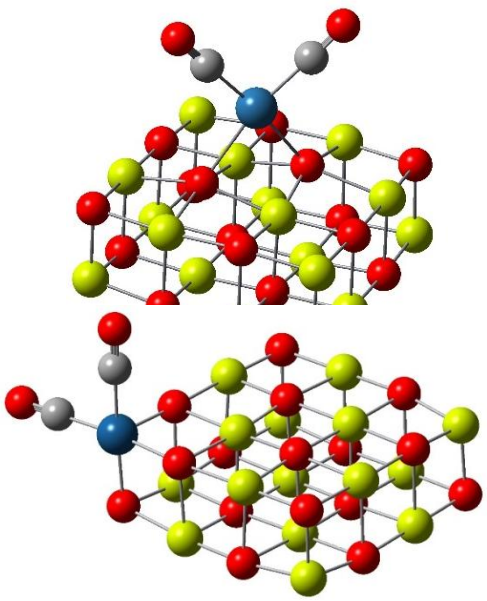

$(MgO)_{25}$ 100 1O onsite

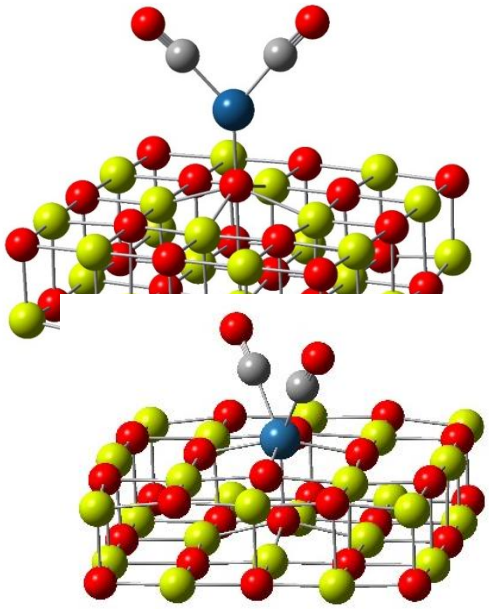

$(MgO)_{16}$ 100 2O bridge

$[Mg_{15}O_{16}]^{2-}$ 100 Edge

$[Mg_{24}O_{25}]^{2-}$ 100 Mg defect

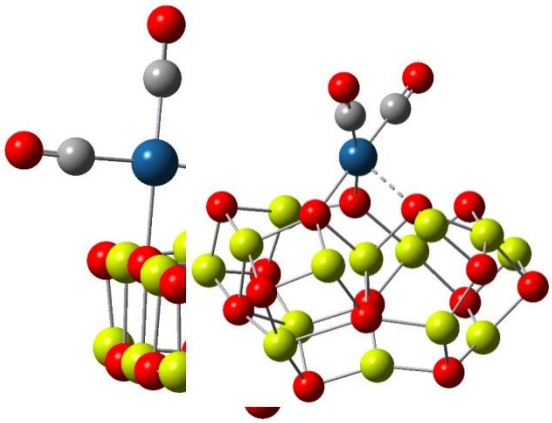

$(MgO)_{20}$ 110

$[Mg_{14}O_{15}]^{2-}$ 111

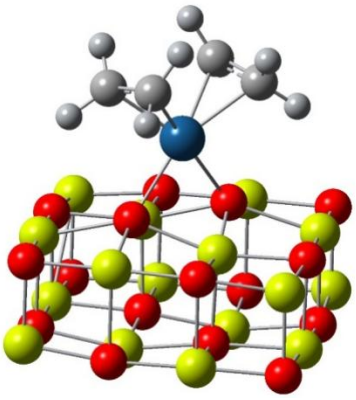

$(MgO)_{16}$ 100 2O bridge

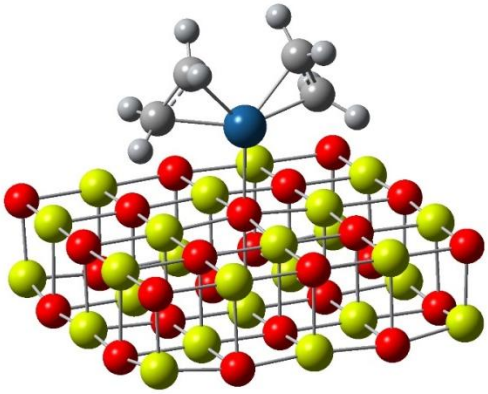

$(MgO)_{25}$ 100 1O onsite

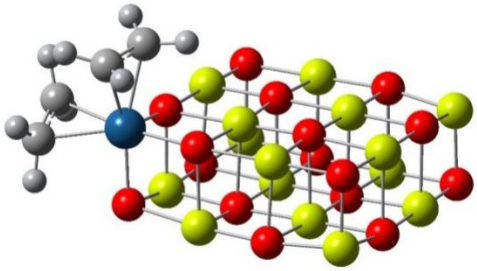

$[Mg_{15}O_{16}]^{2-}$ 100 Edge

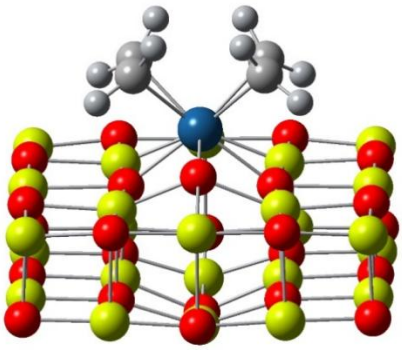

$[Mg_{24}O_{25}]^{2-}$ 100 Mg defect

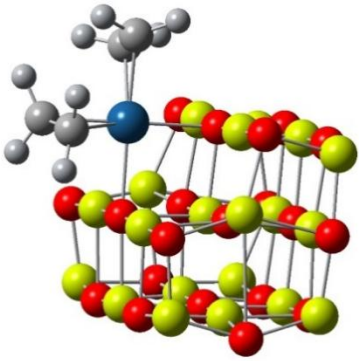

$(MgO)_{20}$ 110

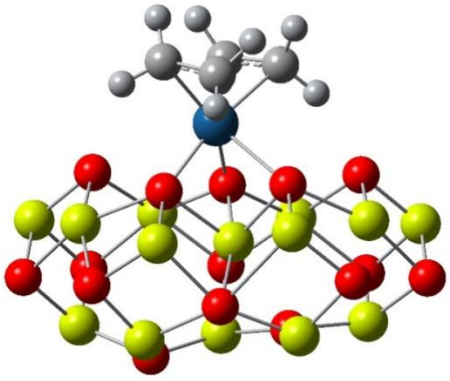

$[Mg_{14}O_{15}]^{2-}$ 111

Figure S27. Optimized molecular structures of cluster models.

Table S11. Cartesian x, y, z coordinates in Å for molecular cluster models.

$^{2}(MgO)_{16}Ir(0)(CO)_{2}$

O	-2.886141	-0.074574	1.474154
O	-0.011030	0.152507	4.118618
MG	-1.471767	-0.057886	0.000000
O	-0.051395	0.735946	1.294419
MG	1.420041	0.267550	2.790515
O	-0.051395	0.735946	-1.294419
MG	1.468189	0.146826	0.000000
O	2.869124	0.329545	1.474829
MG	-2.706130	-2.183909	1.429967
O	-1.306807	-2.092925	2.819926
MG	0.122086	-1.759839	4.080047
O	-1.228326	-2.060189	0.000000
O	1.583213	-1.888608	2.818666
MG	0.176652	-2.501546	-1.404542
O	1.509090	-1.866313	0.000000
MG	2.983512	-1.786072	1.429514
MG	-1.442590	0.065655	2.789838
MG	1.420041	0.267550	-2.790515
O	2.869124	0.329545	-1.474829
MG	4.145114	0.232308	0.000000
O	1.583213	-1.888608	-2.818666
MG	2.983512	-1.786072	-1.429514
O	4.346722	-1.677036	0.000000
O	-2.886141	-0.074574	-1.474154
MG	-1.442590	0.065655	-2.789838
O	-4.069064	-2.265445	0.000000
MG	-2.706130	-2.183909	-1.429967
O	-1.306807	-2.092925	-2.819926
MG	-4.134327	-0.345197	0.000000
O	-0.011030	0.152507	-4.118618
MG	0.122086	-1.759839	-4.080047
MG	0.176652	-2.501546	1.404542
C	-0.257886	3.662343	-1.318210
C	-0.257886	3.662343	1.318210
O	-0.314527	4.455588	2.157368
O	-0.314527	4.455588	-2.157368
IR	-0.167064	2.376199	0.000000

$^{1}[(MgO)_{16}Ir(I)(CO)_{2}]^{+}$

O	-2.888822	0.131859	1.470490
O	0.000428	0.186447	4.110596
MG	-1.516069	0.046656	0.000000
O	0.002356	0.636540	1.291208

MG	1.455574	0.211315	2.811333
O	0.002356	0.636540	-1.291208
MG	1.514643	0.028224	0.000000
O	2.888062	0.104339	1.470775
MG	-2.888921	-1.960453	1.454914
O	-1.449536	-1.964785	2.823055
MG	-0.007424	-1.724291	4.120469
O	-1.381579	-2.024950	0.000000
O	1.430411	-1.979167	2.822780
MG	-0.010557	-2.254261	-1.438117
O	1.362440	-2.039678	0.000000
MG	2.870657	-1.987466	1.455650
MG	-1.455229	0.221782	2.812051
MG	1.455574	0.211315	-2.811333
O	2.888062	0.104339	-1.470775
MG	4.187015	-0.071086	0.000000
O	1.430411	-1.979167	-2.822780
MG	2.870657	-1.987466	-1.455650
O	4.192397	-1.992901	0.000000
O	-2.888822	0.131859	-1.470490
MG	-1.455229	0.221782	-2.812051
O	-4.211395	-1.955696	0.000000
MG	-2.888921	-1.960453	-1.454914
O	-1.449536	-1.964785	-2.823055
MG	-4.189854	-0.034213	0.000000
O	0.000428	0.186447	-4.110596
MG	-0.007424	-1.724291	-4.120469
MG	-0.010557	-2.254261	1.438117
C	0.018402	3.597528	-1.319682
C	0.018402	3.597528	1.319682
O	0.022011	4.385140	2.160456
O	0.022011	4.385140	-2.160456
IR	0.011928	2.300461	0.000000

[1] $[Mg_{15}O_{16}Ir(I)(CO)_2]^-$

O	3.391853	2.576129	-0.911760
O	5.524009	-0.765717	-0.582089
MG	1.600266	1.435525	-1.098983
O	2.780021	-0.228581	-1.005420
MG	3.901811	-1.878102	-0.816404
O	0.008131	0.305846	-1.362079
MG	1.138220	-1.325924	-1.214656
O	2.365751	-3.068515	-1.109667
MG	3.071580	2.528812	1.203397
O	4.230594	0.929648	1.410045
MG	5.142923	-0.761340	1.302742

O 1.426184 1.390269 1.073849
O 3.631940 -1.984459 1.313483
MG -0.408469 0.321094 0.878971
O 0.814877 -1.389654 0.953689
MG 1.979774 -3.046819 0.989210
MG 4.411762 0.901344 -0.711403
MG -1.576625 -0.865468 -1.576303
O -0.497753 -2.541684 -1.557946
MG 0.681434 -4.017787 -1.185911
O -1.957214 -1.012053 0.438400
MG -0.785494 -2.567811 0.576198
O 0.378558 -4.187008 0.704539
O 0.476689 3.148120 -1.231906
MG -1.266988 1.955952 -1.131419
O 2.000946 4.186932 1.087526
MG 0.323450 3.098517 0.935341
O -1.280061 2.086098 0.823669
MG 2.129747 4.061217 -0.829077
O -2.764759 0.676631 -1.577199
MG 2.455334 -0.254657 1.178958
IR -3.750658 0.009525 0.095169
C -5.284954 0.888889 -0.343056
C -4.521103 -0.699515 1.596397
O -6.274551 1.437049 -0.628188
O -4.998678 -1.169594 2.554060

$^{2}Mg_{15}O_{16}Ir(II)(CO)_{2}$
O 2.706634 2.952158 -0.905560
O 5.464189 0.142617 -0.363692
MG 1.286943 1.462455 -1.197933
O 2.714034 0.083108 -0.970408
MG 4.154165 -1.310664 -0.658676
O -0.058029 0.016107 -1.533601
MG 1.375677 -1.361528 -1.253668
O 2.866954 -2.784439 -0.999366
MG 2.276306 2.885508 1.184183
O 3.708522 1.550606 1.488662
MG 5.008286 0.103195 1.501626
O 0.887214 1.411117 0.970650
O 3.777574 -1.410510 1.442768
MG -0.470250 -0.027499 0.663707
O 0.946563 -1.412471 0.912438
MG 2.416458 -2.808559 1.089189
MG 4.075569 1.535907 -0.616020
MG -1.415712 -1.458819 -1.699715
O -0.041701 -2.866570 -1.546854

MG	1.418574	-4.081901	-1.099532
O	-1.835135	-1.529395	0.310086
MG	-0.373169	-2.889337	0.552970
O	1.062193	-4.225094	0.780560
O	-0.218655	2.887258	-1.415700
MG	-1.533177	1.397735	-1.579037
O	0.848213	4.233624	0.942123
MG	-0.519461	2.833524	0.688982
O	-1.881350	1.394054	0.428302
MG	1.180387	4.166869	-0.947440
O	-2.849334	-0.095477	-1.786711
MG	2.307247	0.036102	1.193298
IR	-3.449852	-0.224593	0.154961
C	-4.910152	0.879209	-0.148064
C	-3.944070	-0.532671	1.930336
O	-5.809313	1.574690	-0.345485
O	-4.224844	-0.744063	3.030684

$^{1}[Mg_{15}O_{16}Ir(III)(CO)_{2}]^{+}$

O	2.488940	3.015463	-0.938666
O	5.389140	0.371338	-0.362187
MG	1.190579	1.472198	-1.210674
O	2.645017	0.158055	-0.971752
MG	4.189477	-1.160188	-0.651410
O	-0.118934	-0.055651	-1.538949
MG	1.425752	-1.376908	-1.249163
O	2.954242	-2.692832	-0.974312
MG	2.102862	2.979121	1.159321
O	3.553788	1.689525	1.460650
MG	4.963553	0.323931	1.508634
O	0.722835	1.416196	0.950528
O	3.790998	-1.246879	1.444831
MG	-0.445568	-0.117537	0.618135
O	0.964903	-1.415639	0.921718
MG	2.541121	-2.741893	1.120395
MG	3.960139	1.687879	-0.639689
MG	-1.362542	-1.620806	-1.722045
O	0.054796	-2.933561	-1.492706
MG	1.606756	-4.098366	-1.065458
O	-1.844556	-1.627456	0.299023
MG	-0.241946	-2.980786	0.587104
O	1.248067	-4.210987	0.814795
O	-0.431597	2.807924	-1.405168
MG	-1.588633	1.269247	-1.710841
O	0.604365	4.241638	0.887769
MG	-0.673296	2.805223	0.660365

O	-2.051291	1.172202	0.374212
MG	0.942059	4.196120	-1.002079
O	-2.889936	-0.286438	-1.753736
MG	2.273269	0.110774	1.194577
IR	-3.364918	-0.297639	0.167406
C	-4.807393	0.893940	-0.119576
C	-3.743702	-0.471103	2.032717
O	-5.669994	1.619021	-0.311152
O	-3.935501	-0.596289	3.153208

$^{1}[Mg_{24}O_{25}Ir(I)(CO)_{2}]^{-}$

O	1.557931	2.011897	2.000206
O	1.559945	-2.006324	1.999904
MG	1.578893	1.986168	0.000000
O	2.024693	0.002857	0.000000
MG	1.581927	-1.978959	0.000000
O	1.557931	2.011897	-2.000206
MG	1.542335	0.003432	-1.910029
O	1.559945	-2.006324	-1.999904
MG	-0.593925	2.026861	1.909369
O	-0.668251	-0.000416	1.870929
MG	-0.585538	-2.026054	1.913406
O	-0.522108	2.188215	0.000000
O	-0.524909	-2.180444	0.000000
MG	-0.593925	2.026861	-1.909369
O	-0.668251	-0.000416	-1.870929
MG	-0.585538	-2.026054	-1.913406
MG	1.542335	0.003432	1.910029
MG	1.488537	1.976445	3.988012
O	1.482360	0.002499	4.055446
MG	1.492450	-1.971225	3.988582
O	-0.665516	1.988599	4.000516
MG	-0.583136	0.001041	3.923452
O	-0.660586	-1.987394	4.003089
MG	1.488537	1.976445	-3.988012
O	1.482360	0.002499	-4.055446
MG	1.492450	-1.971225	-3.988582
O	-0.665516	1.988599	-4.000516
MG	-0.583136	0.001041	-3.923452
O	-0.660586	-1.987394	-4.003089
O	1.664713	-4.142906	0.000000
MG	1.566453	-4.023127	-2.001841
O	-0.540422	-4.200526	1.986659
MG	-0.415376	-4.145441	0.000000
O	-0.540422	-4.200526	-1.986659
MG	1.566453	-4.023127	2.001841

O 1.534898 -3.956163 4.018929
MG -0.385011 -3.909713 3.882128
O 1.534898 -3.956163 -4.018929
MG -0.385011 -3.909713 -3.882128
O 1.661879 4.151544 0.000000
MG 1.560582 4.028294 -2.002248
O -0.546640 4.205321 1.986617
MG -0.418199 4.151901 0.000000
O -0.546640 4.205321 -1.986617
MG 1.560582 4.028294 2.002248
O 1.528119 3.960797 4.020070
MG -0.391537 3.911496 3.880724
O 1.528119 3.960797 -4.020070
MG -0.391537 3.911496 -3.880724
C -3.265769 -0.005186 1.287605
C -3.265769 -0.005186 -1.287605
O -4.069695 -0.000042 2.132142
O -4.069695 -0.000042 -2.132142
IR -2.000457 -0.012555 0.000000

$^{2}Mg_{24}O_{25}Ir(II)(CO)_{2}$
O 1.513235 2.010045 1.958615
O 1.513342 -2.009593 1.959004
MG 1.760793 1.991659 0.000000
O 2.085748 0.000210 0.000000
MG 1.757899 -1.991023 0.000000
O 1.513235 2.010045 -1.958615
MG 1.534443 0.000203 -1.908769
O 1.513342 -2.009593 -1.959004
MG -0.590433 2.033205 1.929494
O -0.614855 0.000056 1.846803
MG -0.590108 -2.033200 1.930118
O -0.920470 2.104594 0.000000
O -0.916332 -2.104209 0.000000
MG -0.590433 2.033205 -1.929494
O -0.614855 0.000056 -1.846803
MG -0.590108 -2.033200 -1.930118
MG 1.534443 0.000203 1.908769
MG 1.493501 1.983641 3.973985
O 1.505155 0.000315 4.015603
MG 1.493790 -1.983074 3.974228
O -0.657979 1.969741 3.996300
MG -0.555341 0.000151 3.954800
O -0.657734 -1.969549 3.996702
MG 1.493501 1.983641 -3.973985
O 1.505155 0.000315 -4.015603

MG	1.493790	-1.983074	-3.974228
O	-0.657979	1.969741	-3.996300
MG	-0.555341	0.000151	-3.954800
O	-0.657734	-1.969549	-3.996702
O	1.565777	-4.075690	0.000000
MG	1.498626	-4.044585	-1.995032
O	-0.593052	-4.140877	1.976599
MG	-0.554310	-4.096596	0.000000
O	-0.593052	-4.140877	-1.976599
MG	1.498626	-4.044585	1.995032
O	1.492112	-3.958221	3.984471
MG	-0.427283	-3.904417	3.899049
O	1.492112	-3.958221	-3.984471
MG	-0.427283	-3.904417	-3.899049
O	1.565655	4.075859	0.000000
MG	1.497797	4.045228	-1.994868
O	-0.593477	4.141067	1.976366
MG	-0.555479	4.096421	0.000000
O	-0.593477	4.141067	-1.976366
MG	1.497797	4.045228	1.994868
O	1.491478	3.958756	3.984229
MG	-0.427938	3.904588	3.898791
O	1.491478	3.958756	-3.984229
MG	-0.427938	3.904588	-3.898791
C	-3.142434	-0.001200	1.319409
C	-3.142434	-0.001200	-1.319409
O	-3.940585	-0.001549	2.156044
O	-3.940585	-0.001549	-2.156044
IR	-1.867690	-0.000546	0.000000

$^{1}[Mg_{24}O_{25}Ir(III)(CO)_{2}]^{+}$

O	1.518605	2.014043	1.881589
O	1.518613	-2.014031	1.881587
MG	2.069056	2.045284	0.000000
O	2.328483	0.000007	0.000000
MG	2.069077	-2.045270	0.000000
O	1.518605	2.014043	-1.881589
MG	1.578542	0.000006	-1.840631
O	1.518613	-2.014031	-1.881587
MG	-0.576236	2.034760	1.854899
O	-0.532146	0.000005	1.675444
MG	-0.576227	-2.034753	1.854893
O	-1.352315	2.027964	0.000000
O	-1.352314	-2.027970	0.000000
MG	-0.576236	2.034760	-1.854899
O	-0.532146	0.000005	-1.675444

MG	-0.576227	-2.034753	-1.854893
MG	1.578542	0.000006	1.840631
MG	1.478063	1.978400	3.933959
O	1.481518	0.000005	3.933273
MG	1.478072	-1.978390	3.933955
O	-0.689802	1.936673	3.892413
MG	-0.563509	0.000002	3.907857
O	-0.689796	-1.936670	3.892411
MG	1.478063	1.978400	-3.933959
O	1.481518	0.000005	-3.933273
MG	1.478072	-1.978390	-3.933955
O	-0.689802	1.936673	-3.892413
MG	-0.563509	0.000002	-3.907857
O	-0.689796	-1.936670	-3.892411
O	1.549234	-4.083547	0.000000
MG	1.463516	-4.070183	-1.984317
O	-0.618394	-4.101759	1.932643
MG	-0.604188	-4.148268	0.000000
O	-0.618394	-4.101759	-1.932643
MG	1.463516	-4.070183	1.984317
O	1.426487	-3.934721	3.952534
MG	-0.491740	-3.881318	3.871230
O	1.426487	-3.934721	-3.952534
MG	-0.491740	-3.881318	-3.871230
O	1.549210	4.083560	0.000000
MG	1.463500	4.070194	-1.984319
O	-0.618413	4.101760	1.932645
MG	-0.604204	4.148263	0.000000
O	-0.618413	4.101760	-1.932645
MG	1.463500	4.070194	1.984319
O	1.426471	3.934732	3.952535
MG	-0.491754	3.881324	3.871234
O	1.426471	3.934732	-3.952535
MG	-0.491754	3.881324	-3.871234
C	-3.100224	-0.000038	1.346659
C	-3.100224	-0.000038	-1.346659
O	-3.904483	-0.000075	2.164089
O	-3.904483	-0.000075	-2.164089
IR	-1.806812	-0.000003	0.000000

$^{2}(MgO)_{25}Ir(0)(CO)_{2}$

O	-2.407284	-1.409888	0.288942
O	1.446213	-2.437564	0.408727
MG	-1.965087	0.539303	0.353182
O	0.020441	0.004411	0.679082
MG	2.024690	-0.530270	0.474619

O -1.387687 2.448573 0.365286
MG 0.555684 2.001701 0.467011
O 2.465098 1.419415 0.494462
MG -2.358455 -1.398629 -1.850855
O -0.413373 -1.905835 -1.821441
MG 1.521574 -2.430227 -1.738713
O -1.833129 0.542748 -1.838482
O 2.032204 -0.485021 -1.717651
MG -1.327400 2.486217 -1.782403
O 0.612760 1.960324 -1.740731
MG 2.553991 1.453875 -1.661469
MG -0.503157 -1.992279 0.401675
MG -2.940842 -3.382266 0.232051
O -1.023853 -3.970111 0.313878
MG 0.935461 -4.409918 0.345285
O -2.865609 -3.412718 -1.905430
MG -0.942382 -3.886049 -1.750449
O 0.968298 -4.429565 -1.793173
MG -0.876219 4.420384 0.376749
O 1.081588 3.982214 0.463575
MG 2.999843 3.393991 0.499113
O -0.770553 4.484591 -1.761124
MG 1.132904 3.938085 -1.602100
O 3.061684 3.465489 -1.639871
O 4.005507 -1.052218 0.500301
MG 4.440247 0.906771 0.519878
O 3.535363 -2.936970 -1.700164
MG 4.008280 -1.012104 -1.565135
O 4.552282 0.898876 -1.619768
MG 3.418655 -2.969684 0.439076
O 2.863959 -4.870371 0.380649
MG 2.873252 -4.763990 -1.533701
O 4.899098 2.835588 0.535895
MG 4.880122 2.807769 -1.379792
O -3.941955 1.062719 0.260800
MG -3.359258 2.979914 0.281534
O -4.354975 -0.842496 -1.930122
MG -3.818057 1.064778 -1.794993
O -3.337975 2.994147 -1.862490
MG -4.379711 -0.895041 0.222391
O -4.839403 -2.823330 0.161481
MG -4.695921 -2.754487 -1.748104
O -2.802232 4.882182 0.298834
MG -2.689293 4.816590 -1.613979
MG 0.099672 0.027210 -1.863045
C -1.872377 -0.061828 3.332692

C	0.571872	-0.150562	4.491030
O	-2.911681	-0.124094	3.856007
O	0.948514	-0.212678	5.589789
IR	-0.105019	-0.054711	2.781632

$^{1}[(MgO)_{25}Ir(I)(CO)_{2}]^{+}$

O	-2.376383	-1.434518	0.385534
O	1.454147	-2.386279	0.362027
MG	-2.040776	0.508588	0.321125
O	-0.000047	0.000090	1.008022
MG	2.040759	-0.508568	0.321147
O	-1.454136	2.386290	0.362046
MG	0.489403	2.030878	0.365019
O	2.376402	1.434568	0.385630
MG	-2.434979	-1.478539	-1.795656
O	-0.470634	-1.921412	-1.814250
MG	1.476791	-2.439814	-1.801290
O	-1.924942	0.471704	-1.819068
O	1.924845	-0.471618	-1.818857
MG	-1.476797	2.439920	-1.801114
O	0.470613	1.921517	-1.814283
MG	2.434945	1.478596	-1.795606
MG	-0.489387	-2.030842	0.364931
MG	-2.908772	-3.451824	0.326405
O	-0.972720	-3.987961	0.344916
MG	0.991553	-4.411154	0.316903
O	-2.889254	-3.478806	-1.799356
MG	-0.967435	-3.950563	-1.729381
O	0.953516	-4.424288	-1.812055
MG	-0.991513	4.411236	0.316952
O	0.972754	3.988030	0.344894
MG	2.908802	3.451844	0.326460
O	-0.953547	4.424413	-1.811888
MG	0.967439	3.950643	-1.729343
O	2.889256	3.478849	-1.799343
O	3.997463	-0.982437	0.330915
MG	4.408947	0.980644	0.321877
O	3.480641	-2.891939	-1.819863
MG	3.957193	-0.969473	-1.745830
O	4.420700	0.956253	-1.808337
MG	3.465006	-2.920044	0.307071
O	2.917603	-4.803719	0.290692
MG	2.879575	-4.751083	-1.628622
O	4.793983	2.906173	0.309468
MG	4.747281	2.881027	-1.610559
O	-3.997469	0.982467	0.330844

MG -3.465006 2.920045 0.307210
O -4.420725 -0.956218 -1.808341
MG -3.957215 0.969577 -1.745892
O -3.480650 2.892046 -1.819788
MG -4.408929 -0.980606 0.321832
O -4.793952 -2.906150 0.309488
MG -4.747322 -2.880986 -1.610523
O -2.917606 4.803704 0.290898
MG -2.879626 4.751205 -1.628395
MG -0.000044 0.000050 -2.107673
C -1.188370 -0.115219 4.313313
C 1.188791 0.115463 4.312759
O -1.996439 -0.194794 5.130183
O 1.996766 0.195667 5.129664
IR -0.000036 -0.000307 2.927801

$^{2}(MgO)_{20}Ir(0)(CO)_{2}$
O -1.884647 -0.552750 3.064742
MG -1.980302 -1.889686 1.485445
O -2.006746 -3.368936 0.069830
MG -1.972920 1.074747 1.648799
O -2.024065 -0.344323 0.045621
MG -2.029867 -1.960264 -1.477215
MG -2.103929 1.003438 -1.563993
O -2.008815 -0.526463 -2.986300
MG -3.827512 -0.477077 2.891276
O -4.084094 -1.829791 1.504555
MG -3.952877 -3.069655 0.032602
O -3.907555 1.070264 1.808854
O -4.049519 -2.156982 -1.628225
O -4.065932 0.897712 -1.571241
MG -3.967270 -0.592897 -2.732767
MG 0.062963 -0.536683 2.937562
O 0.032878 -1.950201 1.482919
MG 0.000576 -3.326038 0.000231
O 0.045559 1.047362 1.505348
MG 0.000324 -0.408362 0.000006
O -0.031925 -1.950574 -1.482810
O -0.045407 1.047087 -1.505264
MG -0.062599 -0.537204 -2.937190
O 2.009149 -0.525495 2.986543
MG 2.030725 -1.959190 1.476980
O 2.008047 -3.368252 -0.069277
MG 2.103690 1.004077 1.564425
O 2.024461 -0.343599 -0.045663
MG 1.981051 -1.889226 -1.485612

MG	1.972895	1.075820	-1.648819
O	1.884970	-0.551736	-3.064967
MG	3.967784	-0.591424	2.732935
O	4.050546	-2.155263	1.628149
MG	3.954143	-3.068411	-0.032443
O	4.065721	0.899153	1.571373
MG	4.116189	0.010833	-0.166151
O	4.084588	-1.828907	-1.504747
O	3.907612	1.071271	-1.808754
MG	3.827750	-0.476180	-2.891244
MG	-4.116251	0.009439	0.166234
IR	-0.000513	2.614524	-0.000189
C	0.319428	3.874808	1.310251
C	-0.322474	3.874443	-1.310460
O	0.437336	4.675127	2.148599
O	-0.441782	4.674479	-2.148899

$^{1}[(MgO)_{20}Ir(I)(CO)_{2}]^{+}$

O	1.945441	-0.461899	-2.986212
MG	1.989931	-2.042931	-1.641618
O	2.006920	-3.364924	-0.043347
MG	2.087965	0.950732	-1.546458
O	1.988379	-0.277046	0.097516
MG	2.025308	-1.918827	1.358477
MG	1.928525	0.940850	1.832858
O	1.899200	-0.744065	3.090639
MG	3.950395	-0.560407	-2.768511
O	3.971441	-2.213080	-1.818025
MG	3.975439	-3.072601	-0.128588
O	4.031315	0.884831	-1.532846
O	4.098474	-1.825573	1.365403
O	3.850762	1.007584	1.936420
MG	3.872500	-0.623135	2.904516
MG	-0.000059	-0.461225	-2.957646
O	-0.000131	-1.929161	-1.521944
MG	-0.000310	-3.354634	-0.039881
O	0.000057	1.156210	-1.422172
MG	-0.000145	-0.398576	0.023628
O	-0.000188	-1.992613	1.443503
O	0.000038	1.287336	1.432905
MG	-0.000140	-1.059452	3.173360
O	-1.945593	-0.461436	-2.986088
MG	-1.990185	-2.042204	-1.641246
O	-2.007454	-3.364580	-0.043290
MG	-2.088042	0.951495	-1.546726
O	-1.988649	-0.276696	0.097388

MG	-2.025705	-1.918402	1.358571
MG	-1.928588	0.941463	1.832676
O	-1.899349	-0.743586	3.090399
MG	-3.950609	-0.560145	-2.768454
O	-3.971582	-2.212848	-1.818182
MG	-3.975900	-3.072028	-0.128656
O	-4.031430	0.885237	-1.532908
MG	-4.099388	0.070907	0.227994
O	-4.098818	-1.825098	1.365518
O	-3.850832	1.008109	1.936431
MG	-3.872626	-0.622589	2.904584
MG	4.099247	0.070278	0.227940
IR	0.000323	2.743868	-0.064863
C	0.000557	3.972105	-1.450283
C	0.000769	4.107732	1.189900
O	0.000550	4.720423	-2.326212
O	0.000932	4.945413	1.979466

$^{2}[Mg_{14}O_{15}Ir(0)(CO)_{2}]^{2-}$

O	0.342686	-1.670944	1.878689
O	2.984327	-2.621880	0.953997
MG	0.078888	-0.404476	0.303091
O	-0.385070	-4.119388	0.226382
O	2.839458	0.496353	2.417079
MG	1.150794	1.330086	2.889757
O	4.599989	0.034326	-0.155629
MG	2.951514	1.114615	0.464681
O	0.906857	1.342060	0.890626
O	-2.591604	-1.706031	2.412886
O	-1.632653	0.444335	0.863176
MG	-3.125724	-0.867291	0.658082
O	-2.720137	-2.714568	-0.174378
MG	-1.145181	-0.479830	2.771928
O	3.274000	-1.205908	-2.403429
O	-0.419420	0.694195	-1.535145
O	0.666291	-1.742680	-0.990209
MG	-2.054730	-0.145558	-2.075770
O	-1.993162	-1.998115	-2.803218
MG	1.480909	-0.222656	-2.038678
MG	4.093700	0.474586	-1.945866
O	2.528163	1.427856	-1.521729
O	-3.819022	-0.338145	-1.197087
MG	-3.590488	-2.155767	-1.751288
MG	1.167875	-3.044902	0.451290
MG	3.770449	-1.695465	-0.536568
MG	-0.961653	-2.914386	-1.313602

MG	2.318546	-1.323133	2.245930
MG	-1.579766	-3.072716	1.402326
IR	-0.869333	2.108547	-0.118781
C	-1.544389	3.304608	1.119744
C	-0.165029	3.466283	-1.160939
O	-2.015029	4.087368	1.840037
O	0.251019	4.328569	-1.815857

$^{1}[Mg_{14}O_{15}Ir(I)(CO)_{2}]^{-}$

O	-0.366397	0.028825	2.749487
O	0.759635	-2.154941	0.833274
MG	-0.204290	-0.162763	0.653834
O	-2.077724	-1.201270	0.504570
O	2.399424	-0.786924	2.854015
MG	1.462601	0.793758	2.820842
O	3.859027	-2.503249	0.651150
MG	2.884505	-0.765211	0.838689
O	1.628077	1.096352	0.904379
O	-3.121572	0.849922	2.268539
O	-0.929695	1.839154	0.533479
MG	-3.222461	0.853261	0.195408
O	-4.946280	-0.236909	-0.014416
MG	-1.473263	1.673130	2.381852
O	2.358858	-3.268851	-1.682396
O	0.095252	0.231553	-1.271972
O	-0.581097	-2.289660	-1.839196
MG	-1.861746	-0.805441	-1.901317
O	-3.657355	-1.930791	-1.952917
MG	1.217444	-1.554952	-1.739874
MG	3.881030	-2.172819	-1.267462
O	2.901624	-0.523154	-1.172015
O	-2.964689	0.863496	-1.785480
MG	-4.537252	-0.211888	-1.914895
MG	-0.939964	-2.731544	-0.040855
MG	2.236260	-3.423734	0.211638
MG	-3.981172	-1.874434	-0.079525
MG	0.743120	-1.825161	2.779160
MG	-2.319071	-0.925081	2.454260
IR	0.713306	1.951379	-0.637260
C	1.086934	3.708424	-0.040291
C	2.263673	1.833523	-1.796137
O	1.283325	4.776726	0.352493
O	3.152454	1.970559	-2.509679

$^{1}[Mg_{14}O_{15}Ir(III)(CO)_{2}]^{+}$

O	-0.568004	-1.252586	2.481683

O	-3.515327	0.409609	1.795916
MG	0.270242	-0.134892	-0.913285
O	-1.754519	3.163111	0.637639
O	-2.400605	-2.509371	0.743300
MG	-0.514482	-2.529074	1.034887
O	-5.508175	-1.615263	-0.161288
MG	-3.770142	-2.481940	-0.578460
O	0.758471	-2.078466	-0.357252
O	0.856302	2.117354	2.612069
O	1.564362	0.241401	0.697588
MG	2.118095	2.280019	1.047924
O	0.930119	3.868001	0.441267
MG	0.529148	0.278492	2.430488
O	-4.326292	0.900829	-0.939396
O	2.061493	-0.267596	-1.797043
O	-1.306030	0.921809	-1.010444
MG	2.477781	1.603983	-1.965581
O	1.009385	2.855182	-2.183734
MG	-2.761064	0.147647	-1.949665
MG	-5.272878	-0.670591	-1.813104
O	-3.605598	-1.515515	-2.304036
O	3.301595	2.575778	-0.517185
MG	2.095720	4.012929	-1.029980
MG	-2.836313	1.643082	0.408503
MG	-5.021756	-0.020933	0.750843
MG	-0.468910	2.899248	-0.860949
MG	-2.460168	-1.109486	2.140236
MG	-0.312995	3.456284	1.853577
IR	2.551063	-1.274469	-0.178165
C	2.991618	-2.117902	1.464872
C	3.371745	-2.635943	-1.238621
O	3.240266	-2.600273	2.475338
O	3.827637	-3.444014	-1.902417

$^{2}(MgO)_{16}Ir(0)(C_{2}H_{4})_{2}$

O	3.239563	0.129751	0.037215
O	1.740165	3.750031	0.102908
MG	1.330325	-0.613858	0.010546
O	0.568170	1.195522	0.699740
MG	-0.120135	3.128493	0.166322
O	-0.528838	-1.197016	0.721230
MG	-1.327507	0.613410	0.079844
O	-1.997262	2.551667	0.182373
MG	3.132403	0.104452	-2.079273
O	2.445220	1.957298	-2.065960
MG	1.664394	3.713223	-1.809948

O	1.192140	-0.572581	-2.007193
O	-0.184987	3.172461	-1.990341
MG	-0.659538	-1.267420	-2.482288
O	-1.304115	0.581570	-1.937621
MG	-2.039399	2.497231	-1.933406
MG	2.465315	1.929078	0.087350
MG	-2.454961	-1.928089	0.215503
O	-3.233464	-0.131440	0.211499
MG	-3.764260	1.736719	0.042281
O	-2.554885	-1.947428	-1.939269
MG	-3.244873	-0.097071	-1.906703
O	-3.885493	1.775168	-1.873142
O	2.000603	-2.552938	0.065739
MG	0.123789	-3.127128	0.146046
O	3.772778	-1.768976	-2.086692
MG	1.928992	-2.488654	-2.050118
O	0.072924	-3.164467	-2.009632
MG	3.759314	-1.738324	-0.168756
O	-1.735806	-3.750391	0.180649
MG	-1.760735	-3.705394	-1.736419
MG	0.519699	1.278382	-2.511166
IR	0.065428	-0.004050	2.360942
C	0.181618	-1.575706	3.755985
H	0.499882	-2.495842	3.269782
H	0.744826	-1.329253	4.652822
C	-1.161505	-1.144284	3.634359
H	-1.628580	-0.572651	4.430561
H	-1.855182	-1.741305	3.045524
C	1.371004	1.124479	3.562613
H	1.889053	0.543925	4.320292
H	2.024102	1.725961	2.933637
C	0.038480	1.554666	3.774506
H	-0.310645	2.478376	3.316769
H	-0.466570	1.301277	4.703472

$^{1}[(MgO)_{16}Ir(I)(C_2H_4)_2]^{+}$

O	-2.889883	-1.472570	0.107762
O	-0.003117	-4.124369	0.167609
MG	-1.507535	-0.002154	0.042914
O	0.008798	-1.308532	0.593699
MG	1.446183	-2.808725	0.193062
O	-0.008831	1.306239	0.601636
MG	1.507290	0.002463	0.041964
O	2.890337	-1.471748	0.115180
MG	-2.876943	-1.444793	-1.984699
O	-1.440192	-2.820719	-1.985176

MG	0.000697	-4.121241	-1.744093
O	-1.376839	0.005131	-2.037644
O	1.441636	-2.822455	-1.980893
MG	-0.001733	1.441034	-2.233505
O	1.375657	0.004276	-2.038645
MG	2.877065	-1.450004	-1.979395
MG	-1.449825	-2.809729	0.183915
MG	1.449803	2.809115	0.196104
O	2.889279	1.472812	0.112566
MG	4.183144	0.002202	-0.060956
O	1.438937	2.829738	-1.974120
MG	2.875665	1.453860	-1.980621
O	4.203704	0.002309	-1.982113
O	-2.890372	1.471903	0.123339
MG	-1.446371	2.808460	0.205567
O	-4.204750	0.007399	-1.980150
MG	-2.878020	1.459418	-1.971768
O	-1.442294	2.831371	-1.967389
MG	-4.183598	-0.000416	-0.058960
O	0.003290	4.124149	0.185539
MG	-0.001280	4.129257	-1.726392
MG	0.000689	-1.430777	-2.238854
IR	0.000701	-0.005729	2.281395
C	-0.744270	1.313004	3.750890
H	-1.521952	1.949506	3.333979
H	-1.030033	0.815152	4.673971
C	0.617400	1.599145	3.505780
H	1.377964	1.329990	4.231911
H	0.863897	2.466649	2.896452
C	-0.614851	-1.617058	3.497753
H	-1.375384	-1.351967	4.225435
H	-0.860965	-2.481836	2.884380
C	0.746704	-1.331440	3.744149
H	1.524863	-1.965461	3.324347
H	1.032095	-0.837888	4.669665

$^{1}[Mg_{15}O_{16}Ir(I)(C_{2}H_{4})_{2}]^{-}$

O	3.398081	2.561245	-0.964834
O	5.538682	-0.773376	-0.621730
MG	1.603678	1.414572	-1.117938
O	2.788669	-0.246242	-1.017588
MG	3.911154	-1.892544	-0.819329
O	0.014798	0.277617	-1.337586
MG	1.139593	-1.348135	-1.185539
O	2.375747	-3.089312	-1.078541
MG	3.097768	2.540007	1.153005

O	4.263579	0.944146	1.366595
MG	5.178464	-0.746243	1.267079
O	1.454103	1.398538	1.059669
O	3.673530	-1.973081	1.312887
MG	-0.385326	0.318471	0.893438
O	0.854216	-1.387045	0.981522
MG	2.015390	-3.041075	1.021703
MG	4.420537	0.889623	-0.756806
MG	-1.587055	-0.882045	-1.516874
O	-0.497590	-2.568212	-1.499447
MG	0.688591	-4.036289	-1.125068
O	-1.927938	-1.023698	0.507005
MG	-0.756896	-2.569242	0.635156
O	0.411692	-4.188194	0.771852
O	0.480584	3.125428	-1.265925
MG	-1.262035	1.927483	-1.142831
O	2.022032	4.195478	1.026589
MG	0.343728	3.098420	0.899163
O	-1.261197	2.084148	0.815838
MG	2.135535	4.044462	-0.888612
O	-2.757870	0.673731	-1.599159
MG	2.488964	-0.243510	1.170825
IR	-3.711587	0.023574	0.120302
C	-4.715001	-1.283052	1.408438
H	-5.788844	-1.374775	1.248093
H	-4.195681	-2.239972	1.469695
C	-4.202731	-0.168832	2.140273
H	-3.292847	-0.290055	2.726245
H	-4.882438	0.589543	2.524434
C	-5.097603	1.564909	-0.102412
H	-5.633254	1.835628	0.806379
H	-4.634600	2.404039	-0.618593
C	-5.505641	0.425011	-0.857301
H	-5.329286	0.421554	-1.931303
H	-6.359040	-0.166253	-0.527872

$^{2}Mg_{15}O_{16}Ir(II)(C_{2}H_{4})_{2}$

O	2.797393	2.900785	-0.926888
O	5.495957	0.031369	-0.401344
MG	1.342905	1.439815	-1.208561
O	2.741567	0.030077	-0.986276
MG	4.150116	-1.394405	-0.680708
O	-0.034661	0.024282	-1.520479
MG	1.360332	-1.381237	-1.249620
O	2.825734	-2.840877	-1.007131
MG	2.376131	2.847823	1.164275

O	3.788689	1.484892	1.463127
MG	5.053953	0.006295	1.467281
O	0.961688	1.404570	0.969322
O	3.794637	-1.481235	1.423872
MG	-0.433809	-0.002416	0.678531
O	0.962467	-1.417233	0.921871
MG	2.396319	-2.847547	1.084990
MG	4.136151	1.455898	-0.642901
MG	-1.447216	-1.401175	-1.644036
O	-0.097933	-2.853972	-1.518603
MG	1.339740	-4.098223	-1.086760
O	-1.825398	-1.472477	0.374112
MG	-0.398608	-2.859955	0.583446
O	1.006569	-4.232540	0.800104
O	-0.130343	2.898715	-1.427625
MG	-1.482562	1.438252	-1.567889
O	0.971507	4.223337	0.927126
MG	-0.426638	2.843279	0.680274
O	-1.814978	1.436604	0.430006
MG	1.294380	4.144701	-0.963577
O	-2.840388	0.003465	-1.770248
MG	2.350646	-0.001632	1.180981
IR	-3.417560	-0.117664	0.199273
C	-4.357596	-1.117186	1.804666
H	-5.440823	-1.036620	1.818759
H	-3.966783	-2.130027	1.856177
C	-3.571674	-0.050559	2.311734
H	-2.602875	-0.271859	2.753158
H	-4.045806	0.849750	2.689496
C	-4.750777	1.506602	-0.000268
H	-5.110202	1.898843	0.947049
H	-4.319708	2.252172	-0.663152
C	-5.334625	0.339935	-0.555097
H	-5.285405	0.190088	-1.629345
H	-6.150380	-0.156769	-0.038655

$^{1}[Mg_{15}O_{16}Ir(III)(C_{2}H_{4})_{2}]^{+}$

O	2.619162	2.960331	-0.942882
O	5.436475	0.229272	-0.365966
MG	1.273302	1.452865	-1.223884
O	2.689012	0.096753	-0.973428
MG	4.188440	-1.265579	-0.653606
O	-0.074686	-0.036268	-1.546621
MG	1.418044	-1.398029	-1.252898
O	2.905640	-2.763200	-0.975662
MG	2.218749	2.925935	1.154963

O	3.642402	1.603719	1.458978
MG	5.007732	0.195571	1.504837
O	0.811099	1.410765	0.940261
O	3.792395	-1.341838	1.443282
MG	-0.413138	-0.081078	0.607490
O	0.963412	-1.421666	0.924556
MG	2.492802	-2.794712	1.119827
MG	4.047203	1.589425	-0.641554
MG	-1.383950	-1.548383	-1.701168
O	-0.006567	-2.913951	-1.485439
MG	1.509332	-4.121196	-1.060012
O	-1.847727	-1.555464	0.321433
MG	-0.294171	-2.940824	0.592106
O	1.153884	-4.224872	0.822665
O	-0.302920	2.836002	-1.427186
MG	-1.516273	1.330211	-1.701757
O	0.752427	4.230744	0.881955
MG	-0.561757	2.821329	0.641449
O	-1.962728	1.248825	0.346870
MG	1.102040	4.178282	-1.005914
O	-2.862138	-0.158545	-1.741520
MG	2.313571	0.062505	1.186523
IR	-3.341641	-0.191045	0.195518
C	-4.347352	-0.934212	1.959397
H	-5.367434	-0.570249	2.037827
H	-4.225631	-2.014747	1.941200
C	-3.282272	-0.131031	2.374902
H	-2.353128	-0.601539	2.681296
H	-3.454400	0.872590	2.746556
C	-4.680151	1.536892	0.223535
H	-5.031604	1.734933	1.231603
H	-4.163049	2.360865	-0.255493
C	-5.255901	0.528559	-0.545059
H	-5.145899	0.532588	-1.623678
H	-6.054697	-0.085966	-0.138032

$^{2}Mg_{24}O_{25}Ir(II)(C_{2}H_{4})_{2}$

O	2.010443	-1.978459	-1.534575
O	-2.011522	-1.977664	-1.534271
MG	1.974595	-0.000282	-1.635400
O	-0.000153	-0.000042	-2.049374
MG	-1.974751	0.000342	-1.634445
O	2.010965	1.977753	-1.534421
MG	0.000121	1.914186	-1.564341
O	-2.010529	1.978573	-1.534177
MG	2.013469	-1.942711	0.565926

O -0.000313 -1.856338 0.592146
MG -2.014180 -1.942125 0.566494
O 2.054062 -0.000237 0.758710
O -2.054091 0.000447 0.758793
MG 2.013840 1.942339 0.566121
O 0.000335 1.856647 0.591825
MG -2.012997 1.942999 0.566578
MG -0.000455 -1.914151 -1.564354
MG 1.983961 -3.986818 -1.508861
O -0.000905 -4.033687 -1.515119
MG -1.985653 -3.985811 -1.508472
O 1.963106 -4.012056 0.659071
MG -0.000705 -3.960823 0.536743
O -1.964522 -4.011083 0.659619
MG 1.985536 3.986062 -1.509355
O 0.000679 4.033962 -1.515555
MG -1.984289 3.987041 -1.508901
O 1.964695 4.011259 0.659068
MG 0.000762 3.960930 0.536162
O -1.963075 4.012298 0.659232
O -4.087334 0.000835 -1.538087
MG -4.034850 1.993958 -1.508179
O -4.116592 -1.978112 0.613751
MG -4.075418 0.001082 0.538802
O -4.115873 1.979892 0.613490
MG -4.035792 -1.992238 -1.507810
O -3.964271 -3.985970 -1.488513
MG -3.898387 -3.897461 0.428641
O -3.962764 3.987520 -1.489080
MG -3.896740 3.898841 0.428025
O 4.086919 -0.000743 -1.539081
MG 4.035484 1.992476 -1.508722
O 4.115841 -1.979562 0.613051
MG 4.075391 -0.000374 0.538098
O 4.116838 1.978321 0.612563
MG 4.034634 -1.993773 -1.508458
O 3.962558 -3.987410 -1.489208
MG 3.896917 -3.898808 0.427977
O 3.963988 3.986065 -1.489690
MG 3.898216 3.897510 0.427441
IR 0.000204 -0.000474 1.851370
C -0.712403 -1.425836 3.238806
H -1.247389 -0.997361 4.078617
H -1.221972 -2.277238 2.792126
C 0.712880 -1.426236 3.238484
H 1.221713 -2.277981 2.791621

H	1.248500	-0.998111	4.078056
C	0.713123	1.425354	3.238576
H	1.248387	0.997016	4.078271
H	1.222391	2.276872	2.791807
C	-0.712089	1.425495	3.238522
H	-1.221219	2.277042	2.791627
H	-1.247540	0.997254	4.078152

$^{1}[Mg_{24}O_{25}Ir(III)(C_2H_4)_2]^{+}$

O	-2.011972	1.885565	-1.541389
O	2.011859	1.885685	-1.541386
MG	-2.041210	0.000130	-2.087820
O	0.000009	0.000231	-2.342900
MG	2.041227	0.000256	-2.087798
O	-2.011823	-1.885379	-1.541741
MG	0.000074	-1.834230	-1.580816
O	2.011960	-1.885261	-1.541708
MG	-2.024837	1.843089	0.543001
O	-0.000051	1.674806	0.544438
MG	2.024735	1.843167	0.542955
O	-2.021654	-0.000179	1.281465
O	2.021646	-0.000081	1.281475
MG	-2.024705	-1.843330	0.542677
O	0.000049	-1.674963	0.544128
MG	2.024802	-1.843254	0.542762
MG	-0.000061	1.834543	-1.580455
MG	-1.975290	3.936643	-1.488514
O	-0.000111	3.930121	-1.483785
MG	1.975072	3.936767	-1.488482
O	-1.937931	3.888181	0.688681
MG	-0.000117	3.878456	0.561127
O	1.937691	3.888299	0.688711
MG	-1.975081	-3.936448	-1.489300
O	0.000122	-3.929832	-1.484621
MG	1.975320	-3.936325	-1.489300
O	-1.937708	-3.888472	0.687868
MG	0.000113	-3.878559	0.560305
O	1.937936	-3.888361	0.687876
O	4.077648	0.000278	-1.572101
MG	4.067129	-1.984519	-1.482682
O	4.100173	1.931562	0.599422
MG	4.125735	0.000050	0.583868
O	4.100261	-1.931466	0.599160
MG	4.067066	1.985073	-1.482392
O	3.931138	3.955725	-1.439710
MG	3.877687	3.864997	0.478064

O	3.931402	-3.955173	-1.440516
MG	3.877948	-3.864940	0.477241
O	-4.077635	0.000039	-1.572139
MG	-4.067023	-1.984757	-1.482732
O	-4.100296	1.931340	0.599401
MG	-4.125738	-0.000171	0.583835
O	-4.100145	-1.931682	0.599110
MG	-4.067151	1.984831	-1.482414
O	-3.931361	3.955502	-1.439763
MG	-3.877925	3.864799	0.478005
O	-3.931161	-3.955392	-1.440530
MG	-3.877718	-3.865133	0.477232
IR	-0.000006	-0.000170	1.835662
C	0.699953	1.471967	3.259239
H	1.259823	1.002870	4.057889
H	1.225589	2.285827	2.766522
C	-0.699998	1.471897	3.259368
H	-1.225798	2.285717	2.766767
H	-1.259661	1.002751	4.058134
C	-0.699988	-1.472570	3.259015
H	-1.259865	-1.003616	4.057743
H	-1.225593	-2.286387	2.766198
C	0.699962	-1.472447	3.259119
H	1.225789	-2.286172	2.766389
H	1.259621	-1.003401	4.057948

$^{2}(MgO)_{25}Ir(0)(C_{2}H_{4})_{2}$

O	2.006160	2.016217	0.433396
O	-1.996545	2.027979	0.433356
MG	2.052646	0.015179	0.422933
O	-0.000572	0.006262	0.575917
MG	-2.050605	0.027571	0.419230
O	2.001114	-1.988881	0.348277
MG	-0.004563	-2.040124	0.379628
O	-2.010102	-1.978726	0.347643
MG	2.012223	2.069440	-1.721312
O	0.006628	2.072969	-1.734980
MG	-1.999844	2.079216	-1.723331
O	2.010676	0.058585	-1.772704
O	-2.007533	0.069423	-1.772320
MG	2.003469	-1.951279	-1.801725
O	-0.003947	-1.948027	-1.815029
MG	-2.010290	-1.941296	-1.802129
MG	0.005110	2.055799	0.502402
MG	2.013576	4.043430	0.447720
O	0.010492	4.121965	0.490277

MG	-1.993757	4.054510	0.443550
O	1.996875	4.151097	-1.683641
MG	0.011501	4.104481	-1.580508
O	-1.973398	4.159277	-1.686759
MG	1.996354	-4.020732	0.275833
O	-0.009660	-4.096124	0.301253
MG	-2.015162	-4.009765	0.275483
O	1.977848	-4.031779	-1.861509
MG	-0.009045	-3.989774	-1.761111
O	-1.995481	-4.023164	-1.862332
O	-4.117080	0.028752	0.377619
MG	-4.042941	-1.974274	0.298508
O	-4.079492	2.062802	-1.742443
MG	-4.043721	0.072509	-1.686068
O	-4.088539	-1.913623	-1.826106
MG	-4.027241	2.031385	0.399824
O	-3.978594	4.014679	0.431765
MG	-3.907074	3.988065	-1.486724
O	-4.001413	-3.958088	0.257796
MG	-3.927456	-3.853775	-1.656050
O	4.118288	0.007610	0.381482
MG	4.033577	-1.994163	0.301604
O	4.091007	2.042455	-1.737719
MG	4.046504	0.052508	-1.684100
O	4.083424	-1.933969	-1.822644
MG	4.037809	2.010476	0.403848
O	3.998433	3.993242	0.437781
MG	3.928646	3.968502	-1.481116
O	3.982206	-3.978450	0.260498
MG	3.910935	-3.872936	-1.653406
MG	0.001603	0.064526	-1.781814
IR	-0.002970	-0.224583	2.798378
C	-2.050663	0.201503	3.181192
H	-2.293467	1.260993	3.169272
H	-2.777671	-0.418478	2.651934
C	-1.407462	-0.376329	4.332036
H	-1.629363	-1.409212	4.595316
H	-1.207435	0.257202	5.191503
C	2.047642	0.184641	3.174049
H	2.759512	-0.479345	2.678646
H	2.315025	1.236587	3.113073
C	1.385645	-0.325852	4.346818
H	1.186621	0.354301	5.170487
H	1.591080	-1.346515	4.665058

$^{2}(MgO)_{20}Ir(0)(C_{2}H_{4})_{2}$

O	1.880947	-0.575753	-3.083271
MG	1.975649	-1.886559	-1.488204
O	2.014657	-3.366552	-0.079941
MG	1.944730	1.073096	-1.672333
O	2.021879	-0.335830	-0.054860
MG	2.033957	-1.973085	1.480761
MG	2.091391	0.992617	1.569341
O	2.022438	-0.547689	2.991567
MG	3.816186	-0.469170	-2.901637
O	4.092352	-1.803652	-1.502238
MG	3.960119	-3.055897	-0.040429
O	3.879652	1.093772	-1.833889
O	4.054694	-2.176441	1.635314
O	4.059930	0.898844	1.562029
MG	3.973974	-0.599925	2.717329
MG	-0.071464	-0.554285	-2.942787
O	-0.037495	-1.960470	-1.482638
MG	0.000242	-3.322910	-0.000170
O	-0.049457	1.021354	-1.557652
MG	0.000179	-0.390722	0.000014
O	0.037901	-1.960855	1.482441
O	0.049526	1.021192	1.557941
MG	0.071569	-0.554422	2.942881
O	-2.022360	-0.547581	-2.991605
MG	-2.033642	-1.973151	-1.481018
O	-2.014087	-3.366993	0.079251
MG	-2.091450	0.992531	-1.569197
O	-2.021714	-0.336223	0.054785
MG	-1.975251	-1.887260	1.487969
MG	-1.944770	1.072503	1.672029
O	-1.880679	-0.576536	3.083111
MG	-3.973950	-0.599870	-2.717198
O	-4.054282	-2.176659	-1.635534
MG	-3.959581	-3.056314	0.040049
O	-4.060035	0.898644	-1.561639
MG	-4.098876	0.035287	0.187330
O	-4.091892	-1.804529	1.502154
O	-3.879693	1.092883	1.834135
MG	-3.815778	-0.470068	2.901739
MG	4.098759	0.036071	-0.187165
IR	-0.000195	2.572327	0.000094
C	-0.129570	4.017286	1.482233
H	-0.496571	4.981678	1.134093
H	-0.602506	3.699687	2.412407
C	1.269862	3.694827	1.301573
H	1.771788	3.215844	2.149961

H	1.928747	4.383575	0.782950
C	0.127818	4.017471	-1.481920
H	0.494086	4.982159	-1.133817
H	0.600855	3.700336	-2.412204
C	-1.271403	3.693968	-1.301178
H	-1.773061	3.215019	-2.149758
H	-1.930729	4.382195	-0.782426

$^{1}[(MgO)_{20}Ir(I)(C_2H_4)_2]^{+}$

O	1.962964	-0.506016	-3.036418
MG	2.085187	-1.873906	-1.472583
O	2.125021	-3.322732	-0.026426
MG	2.005076	1.026494	-1.655371
O	2.020548	-0.281210	-0.006643
MG	2.095382	-1.905410	1.467381
MG	2.031086	0.997186	1.649892
O	1.980807	-0.524596	3.029230
MG	3.939763	-0.403315	-2.841330
O	4.139226	-1.782554	-1.497451
MG	4.079343	-2.996805	-0.011956
O	3.922940	1.115725	-1.701839
O	4.129085	-1.888490	1.543140
O	3.956420	1.054686	1.668667
MG	3.964645	-0.457547	2.818228
MG	0.026016	-0.630393	-3.008870
O	0.070201	-1.947770	-1.484913
MG	0.116173	-3.357444	-0.009617
O	-0.018587	1.147744	-1.461904
MG	0.033254	-0.422156	0.000591
O	0.083484	-1.959395	1.475607
O	-0.001311	1.148748	1.466169
MG	0.049701	-0.670257	3.020576
O	-1.911136	-0.608340	-3.022860
MG	-1.940935	-2.016511	-1.486973
O	-1.888910	-3.437359	0.007188
MG	-2.056284	0.893019	-1.631494
O	-1.964587	-0.395282	0.013816
MG	-1.933893	-1.994112	1.456386
MG	-2.016214	0.903461	1.669100
O	-1.889074	-0.643163	3.038397
MG	-3.897161	-0.670595	-2.813808
O	-3.967523	-2.137294	-1.575219
MG	-3.859801	-3.224383	-0.012092
O	-3.984805	0.827253	-1.650790
MG	-4.087699	-0.162913	0.051958
O	-3.993564	-2.019684	1.478603

O	-3.937697	0.882971	1.726679
MG	-3.868730	-0.649580	2.843881
MG	4.127786	0.063677	-0.033891
IR	-0.123836	2.648442	0.001202
C	-0.936882	3.957257	1.460721
H	-1.509480	4.773024	1.032336
H	-1.466057	3.433216	2.257223
C	0.473233	4.019631	1.506157
H	0.987136	3.515638	2.323795
H	1.001327	4.884613	1.120302
C	0.447144	4.084485	-1.450307
H	0.854762	4.993768	-1.021443
H	1.074174	3.651406	-2.228799
C	-0.950267	3.888087	-1.510388
H	-1.351054	3.315561	-2.347570
H	-1.635159	4.637903	-1.129842

$^{2}[Mg_{14}O_{15}Ir(0)(C_{2}H_{4})_{2}]^{2-}$

O	0.149598	-0.888574	2.648558
O	1.593157	-1.954166	0.421956
MG	0.305451	-0.270877	0.651425
O	-1.374762	-3.107229	0.608598
O	3.000281	-0.177383	2.566185
MG	1.481620	0.914770	2.866167
O	4.676826	-1.022737	0.104519
MG	3.214985	0.375953	0.570138
O	1.372814	1.377941	0.981392
O	-2.738728	-0.788721	2.601779
O	-1.359163	0.971510	1.040809
MG	-3.102704	-0.116599	0.673578
O	-4.374070	-1.666217	0.154773
MG	-1.364388	0.504387	2.927751
O	3.266207	-2.157117	-2.166924
O	0.006718	0.308622	-1.217476
O	0.088025	-2.084959	-2.228746
MG	-1.477158	-0.879334	-2.052353
O	-2.968253	-2.374227	-2.251442
MG	1.617503	-0.820406	-1.991558
MG	4.367743	-0.628599	-1.757065
O	2.992616	0.624049	-1.486075
O	-2.980194	0.349579	-1.329810
MG	-4.204792	-1.039859	-1.658544
MG	0.179240	-2.948790	-0.561651
MG	3.398973	-2.425899	-0.258666
MG	-3.022983	-2.944745	-0.401622
MG	1.964716	-1.804822	2.418728

MG	-1.406660	-2.123315	2.270573
IR	-0.343460	2.107880	-0.338622
C	-0.024556	2.956658	-2.248019
H	-0.133709	2.155069	-2.974851
H	-0.624979	3.843665	-2.444228
C	1.172726	3.050667	-1.498676
H	1.462791	4.018255	-1.091870
H	1.961049	2.295680	-1.608701
C	-1.656540	3.667510	0.133665
H	-1.857263	4.354919	-0.685636
H	-2.542017	3.235485	0.594369
C	-0.464536	3.811032	0.902046
H	-0.455342	3.491448	1.942597
H	0.246223	4.598146	0.660554

$^{1}[Mg_{14}O_{15}Ir(I)(C_{2}H_{4})_{2}]^{-}$

O	0.002722	-0.973713	2.689878
O	1.506352	-2.390180	0.600463
MG	0.254044	-0.288489	0.662241
O	-1.550707	-3.096350	0.661937
O	2.956329	-0.309369	2.653898
MG	1.579148	0.960943	2.901925
O	4.567778	-1.280517	0.185844
MG	3.257691	0.259175	0.592817
O	1.448116	1.278814	1.017236
O	-2.863114	-0.571196	2.578547
O	-1.306103	1.070843	1.039488
MG	-3.157825	0.060917	0.610049
O	-4.419815	-1.473285	0.128661
MG	-1.412844	0.612476	2.889828
O	3.178794	-2.232509	-2.190606
O	0.072141	0.278353	-1.187127
O	0.055743	-2.096083	-2.154581
MG	-1.485343	-0.827815	-2.058937
O	-2.993296	-2.285614	-2.231628
MG	1.604250	-0.852808	-2.033852
MG	4.379773	-0.796929	-1.703475
O	3.042358	0.491135	-1.398921
O	-2.929919	0.438875	-1.363783
MG	-4.218116	-0.893567	-1.713735
MG	-0.011496	-3.041002	-0.544422
MG	3.253657	-2.586211	-0.315674
MG	-3.167796	-2.843558	-0.398597
MG	1.770853	-1.768088	2.419775
MG	-1.678604	-2.020431	2.246751
IR	-0.194890	2.136144	-0.349010

C	-0.033224	2.831973	-2.314856
H	-0.161022	1.990329	-2.991716
H	-0.658506	3.692048	-2.546562
C	1.213254	3.013654	-1.646658
H	1.512423	4.024863	-1.373060
H	2.018492	2.285286	-1.771138
C	-1.369346	3.808417	0.123111
H	-1.519168	4.511858	-0.692851
H	-2.284210	3.456205	0.593362
C	-0.160619	3.844702	0.874105
H	-0.161346	3.503205	1.911237
H	0.611707	4.571654	0.639522

$^{1}[Mg_{14}O_{15}Ir(III)(C_{2}H_{4})_{2}]^{+}$

O	-0.815072	-2.653952	2.622010
O	-2.235727	-0.552671	1.417989
MG	-0.622661	-1.186585	-0.155490
O	-1.634127	3.711049	0.845654
O	-1.751362	-2.986353	-0.052058
MG	-0.001540	-3.398279	1.030483
O	-4.515323	-1.410157	-0.416465
MG	-3.054737	-2.337362	-1.296307
O	0.971926	-2.573710	-0.388799
O	-0.209234	1.275756	3.019814
O	0.768461	-0.571540	1.181594
MG	1.226199	1.260162	1.676601
O	1.124321	3.250255	1.403817
MG	-0.626745	-0.599482	2.662120
O	-4.025502	1.450576	-0.547422
O	0.437380	-0.169316	-1.563717
O	-0.989926	2.202962	-1.573204
MG	1.015094	1.741695	-1.524986
O	1.548825	3.610682	-1.374050
MG	-1.237242	0.462719	-2.410525
MG	-4.315295	0.009451	-1.771981
O	-2.665854	-0.778838	-2.444401
O	2.367292	1.192517	-0.057049
MG	2.584975	3.145419	0.126752
MG	-2.530391	2.605550	-0.417952
MG	-3.898446	0.035428	0.753156
MG	-0.039583	3.870618	-0.277109
MG	-2.460003	-2.462449	1.677643
MG	-0.638645	3.014581	2.346877
IR	2.078310	-0.897833	-0.348271
C	3.550318	-0.641445	-1.911617
H	3.355944	0.291733	-2.432004

H	4.561678	-0.734388	-1.525325
C	2.786327	-1.781280	-2.181416
H	3.168505	-2.777755	-1.999617
H	1.933639	-1.723622	-2.847186
C	3.615708	-0.915865	1.129589
H	4.444262	-0.289110	0.819244
H	3.166723	-0.677633	2.090377
C	3.455528	-2.211685	0.625156
H	2.890762	-2.945051	1.187927
H	4.180928	-2.625065	-0.067935

References

[1] Weinhold, F. In *Encyclopedia of Computational Chemistry*,Schleyer, P. V. R., Ed.; Wiley: Chichester, U.K., 1998; Vol. 3, pp 1792−1811.

[2] Weinhold, F.; Landis, C. R. *Valency and Bonding: A Natural Bond Orbital Donor-Acceptor Perspective*, Cambridge University Press Cambridge, U.K., 2003.

[3] Glendening, E. D.; Badenhoop, J. K.; Reed, A. E.; Carpenter, J. E.; Bohmann, J. A.; Morales, C. M.; Landis, C. R.; Weinhold, F. *NBO 6.0*. Theoretical Chemistry Institute, University of Wisconsin, Madison: Madison, WI, 2013.

[4] Glendening, E. D.; Landis, C. R.; Weinhold, F. NBO 6.0: Natural Bond Orbital Analysis Program. *J. Comput. Chem.* 2013, *34*, 1429-1437

[5] Douglas, M.; Kroll, M. N. Quantum Electrodynamical Corrections to the Fine Structure of Helium. *Ann. Phys.* 1974, *82*, 89−155.

[6] Jansen, G.; Hess, B. A. Revision of the Douglas-Kroll Transformation. *Phys. Rev. A* 1989, *39*, 6016-6017.

[7] Wolf, A.; Reiher, M.; Hess, B. A. The Generalized Douglas-Kroll Transformation. *J. Chem. Phys.* 2002, *117*, 9215−9226.

[8] de Jong, W. A.; Harrison, R. J.; Dixon, D. A. Parallel Douglas-Kroll Energy and Gradients in NWChem: Estimating Scalar Relativistic Effects Using Douglas-Kroll Contracted Basis Sets. *J. Chem. Phys.* 2001, *114*, 48−53.

[9] Pantazis, D. A.; Chen, X.-Y.; Landis, C. R.; Neese, F. All-Electron Scalar Relativistic Basis Sets for Third-Row Transition Metal Atoms. *J. Chem. Theory Comput.* 2008, *4*, 908-919.